EXAMINATION OF THE CYTOPROTECTIVE ROLE OF SIRTUIN-1 IN THE RENAL MEDULLA

By

WENJUAN HE

Dissertation

Submitted to the Faculty of the

Graduate School of Vanderbilt University

in partial fulfillment of the requirements

for the degree of

DOCTOR OF PHILOSOPHY

in

Molecular Physiology & Biophysics

August, 2010

Nashville, Tennessee

Approved:

Professor Roland W. Stein

Professor Eric Delpire

Professor Roy Zent

Professor Ann W. Richmond

Professor Owen P. McGuinness

ACKNOWLEDGEMENTS

This dissertation would not have been finished without the help of so many people in so many ways. First of all, I would like to thank my mentors, Dr. Chuan-Ming Hao and Dr. Matthew D. Breyer, who have guided me through these years of the doctoral program. Dr. Hao is an outstanding advisor and a nice person. His office door was always open to me, whenever I had literally any questions. I owe him deep gratitude for supporting me, encouraging me and assuring me with his expertise and insight. Dr. Breyer is a brilliant scientist. I wish I could spend more time with him and learn more from him. He is also a very dedicated scientist, who saves every minute to think about scientific questions. I remember when I came to the lab on the first day, he said that he wanted me to wake up every morning and think about how to study the renal medullary interstitial cells deep inside the kidney. I am afraid that I did do good enough. But when I look up to Dr. Breyer as a role model, I know exactly how I can do better.

I am also grateful to my co-advisor Dr. Owen P. McGuinness and my thesis committee members, Dr. Roland W. Stein, Dr. Eric Delpire, Dr. Roy Zent and Dr. Ann W. Richmond. Their comments and constructive criticisms at different stages of my research were thought-provoking. I especially want to thank Dr. Zent and Dr. Delpire for their continuous encouragement whenever I questioned myself. Dr. Zent has also spent long time for carefully reading and commenting on countless revisions of my manuscript. I greatly appreciate it.

Teamwork is essential to my thesis work. I am so grateful to my dear lab colleagues. Linda S. Davis has helped me with all the immunohistochemistry studies. Yingying Wang maintained the mouse lines for me. Dr. Li You helped me with unilateral ureteral obstruction (UUO) surgeries. Dr. Ming-Zhi Zhang in Dr. Raymond C. Harris Lab and Dr. Hai-Chun Yang in Dr. Agnes B. Fogo Lab also contributed to my first author paper on SIRT1. We had joint lab meetings with Dr. Richard M. Breyer lab every other week. The questions and comments I got from the members of Dr. Richard Breyer lab have enriched my ideas in so many ways.

I am lucky to have two "anti-oxidants" in my life that have kept me away from all the stresses though this lengthy process of PhD, my husband Lei Zhu and my lovely siberian husky Tundra. Words cannot adequately express my gratitude to Lei for his unconditional understanding, patience, humor and love through each and every step of this incredible journey. Lei is also a biological scientist majoring in neuroscience. He graduated from Vanderbilt University in 2007 and now is working as a postdoc fellow. I wish him a very successful scientific career!

I can’t forget to express appreciation to my parents, the first to show me the joys of learning and the first to believe in me and to encourage me to pursue my dreams. I am fortunate to have such a wonderful family actively involved in my life.

Things always seem less painful and more manageable if you have friends with you. I am so lucky that I am surrounded by so many compassionate, intelligent, interested friends, friends from University of Science and Technology of China

where I completed my undergraduate study, friends that I met here at Vanderbilt University, girls in Great Nashville Chinese Dancing Group that I did a lot of performance with, and many others. Their support and help are greatly appreciated.

TABLE OF CONTENTS

Page

LIST OF TABLES

Table Page

LIST OF FIGURES

CHAPTER I

GENERAL INTRODUCTION

Renal Medulla Overview

Structure of Renal Medulla Mammalian kidneys are paired retroperitoneal organs located in the posterior part of the abdomen on each side of the vertebral column. The functional unit of the kidney is the nephron. Each human kidney contains about 10^6 nephrons. The essential components of the nephron are the glomerulus (including Bowman's capsule), the proximal tubule, the thin limbs, the distal tubule, and the collecting ducts (Figure 1). The straight portion of the proximal tubule, the thin limb segments and the straight portion of the distal tubule is also called loop of henle. There are two main populations of nephrons in the kidney: those originating from superficial and midcortical glomeruli which possess a short loop of henle (the cortical nephrons) and those originating from juxtamedullary glomeruli located near the corticomedullary boundary with a long loop of henle (juxtamedullary nephrons). (1)

The kidney can be divided into two major regions: an outer region called the cortex which contains glomeruli, and an inner region called the medulla (Figure 1). On the basis of the specific segments of the nephron located at various levels

in the medulla, the medulla is further divided into an outer zone and an inner zone, with the outer zone subdivided into an outer and an inner stripe.

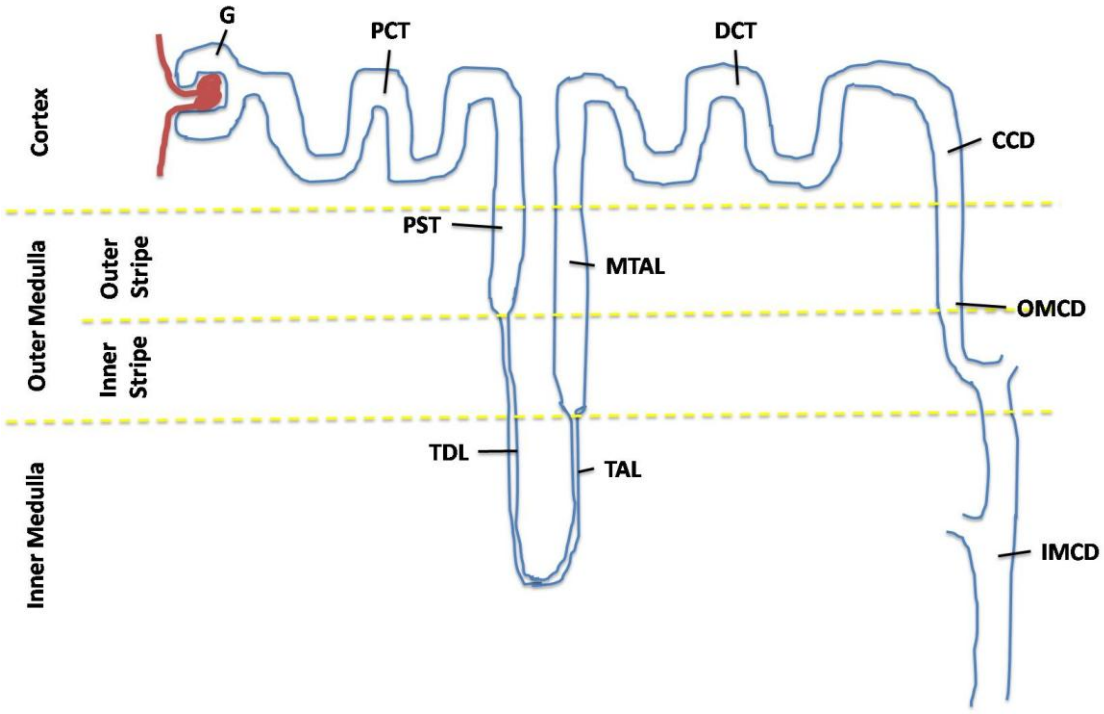

Figure 1. Diagram illustrating kidney structure. G= glomerulus; PCT=proximal convoluted tubule; PST=proximal straight tubule; TDL=thin descending limb of loop of henle; TAL=thin ascending limb of loop of henle; MTAL=medullary thick ascending limb; DCT=distal convoluted tubule; CCD=cortical collecting duct; OMCD=outer medullary collecting duct; IMCD=initial inner medullary collecting duct.

Between renal tubules and vessels, interstitial cells and a loose, flocculent extracellular matrix constitute the renal interstitium. The amount of interstitial tissue in the cortex is limited, and the tubules and capillaries are often directly opposed to each other. However, in the medulla, the interstitium volume gradually increases, from 10% to 20% in the outer medulla to approximately 30% to 40% at the papillary tip of the inner medulla in both rats and rabbits.

Two types of cortical interstitial cells are identified: one that express ecto-5'-nucleotidase, thus resembling a fibroblast (type 1 cortical interstitial cells) and another mononuclear or macrophage or dendritic cell-like (type 2 cortical interstitial cells). Type 1 cortical interstitial cells are the predominant form and also indicated as the site of erythropoietin production in the kidney (2). Type 2 interstitial cells are believed to represent bone marrow-derived cells. In the renal medulla, three types of interstitial cells have been described (3). In the medulla, type 1 interstitial cells are characterized by predominant lipid-containing-droplets. They may resemble type 1 cells in the cortex, however, type 1 medullary interstitial cells do not express erythropoietin or ecto-5'-nucleotidase (4). They are present throughout the inner medulla and are also found in the inner stripe of the outer medulla. Type 2 medullary interstitial cells are virtually identical to the type 2 cells in the cortex. Type 3 medullary interstitial cells are pericytes that are adjacent to vasa recta. Type 2 and type 3 interstitial cells are free of lipid containing droplets and are especially abundant in the outer medulla.

Type 1 medullary interstitial cells have long cytoplasmic projections and are often arranged in rows with their long axis perpendicular to that of renal tubules

and vessels, thus resembling the rungs of a ladder (Figure 2). Often a single interstitial cell can be in direct contact with several vessels and tubules. Specialized cell junctions connecting interstitial cells and tubular and vascular cells in the renal medulla have been reported (5) (6), suggesting potential regulatory roles of type 1 medullary interstitial cells modulating the function of adjacent tubules and vessels. The number and size of the lipid droplets in the type 1 interstitial cells vary considerably depending on the species and the physiological state of the animal (7) (8), such as sodium and water intake. However, controversial data exist concerning how the lipid droplets are related to the diuretic state of an animal. The exact nature of these lipid droplets in type 1 renal medullary interstitial cells remain largely unknown. The predominant type 1 renal medullary interstitial cells (RMICs) are the subject of the present studies.

Figure 2. Light micrograph of the renal medullary interstitium from a normal rat. The lipid containing type 1 medullary interstitial cells bridge the interstitial space between the adjacent thin limbs of henle (TL) and vasa recta (VR). (magnification x830). (Modified from Barry M. Brenner, The Kidney, 8th ed., 2008).

The Medullary Interstitial Environment The division of the kidney into cortical and medullary regions and the further subdivision of the medulla into outer and inner zones are of considerable importance in relating renal structure to its ability to concentrate urine. According to the countercurrent theory of urine concentration, the maximal urine concentration should be directly related to the length of the countercurrent multiplier system, which is comprised by the loop of Henle in a mammalian kidney (9). Although this relationship between the ability to concentrate urine and the length of the loop of Henle seems to be more complex than originally proposed (10), all evidence obtained so far support that the renal ability of concentrating urine is intimately linked to the structure of the renal medulla including the specific transport properties and the unique architecture of the tubular and vascular structures there, which allow countercurrent multiplication (tubular structures) and countercurrent exchange (vascular structures) systems respectively.

The renal medullary interstitium exhibits many unique features not seen in any other organ or tissue of the body including 1-2 molar concentrations of sodium and urea, widely fluctuating tonicity, low blood flow, hypoxia, high concentrations of ammonia and pH changes. These features of renal medulla uniquely stress the cells residing in the medulla through hypertonicity, hypoxia and oxidative stress.

To concentrate urine, the loop of Henle acts as a countercurrent multiplier system, which creates a progressively increasing osmolar concentration (predominantly NaCl and urea) in the renal interstitium from the outer medulla to

the papillary tip of the renal medulla (Figure 3). The formation of the hyperosmotic medullary interstitium promotes water absorption in more distal nephron segments (ie. inner medullary collecting duct). Depending on the hydration status and resultant vasopressin levels, the mammalian kidney produces a urine of widely varying osmolarity. In situations of water depletion, the osmolarities in the papillary tip of renal inner medulla may be several times higher than that of systemic circulation (in humans ~1,200mosm in mice ~5,000mosm versus ~300mosm), which would cause otherwise deadly consequences in other tissues. (11).

Besides high osmotic stress, renal medullary cells are also physiologically subjected to low blood supply and oxygen tension. The renal medulla receives less than 5% of the renal blood flow. In addition, the renal medullary circulation must satisfy the conflicting demands of preserving the cortico-medullary gradients of NaCl and urea, while delivering oxygen and nutrients to the medulla. This is achieved by countercurrent arrangement of the vasa recta organized in a hairpin form to minimize the wash-out of medullary solutes. However, the relatively low flow rates within the vasa recta and the oxygen consumption by tubular epithelium, in particular the medullary thick ascending limb, result in low medullary oxygen tension (12). It has been reported that the partial pressure of oxygen is of the order of 10 - 20 mm Hg in the inner and outer medulla, respectively, compared with ~50 mm Hg in the cortex (13). The pro-hypoxic potentially injurious environment in the renal medulla is supported by human diseased conditions. For instance, in sickle cell anemia, hypoxia sickling of the

red blood cells induces papillary necrosis and loss of urine concentrating capacity in these patients.

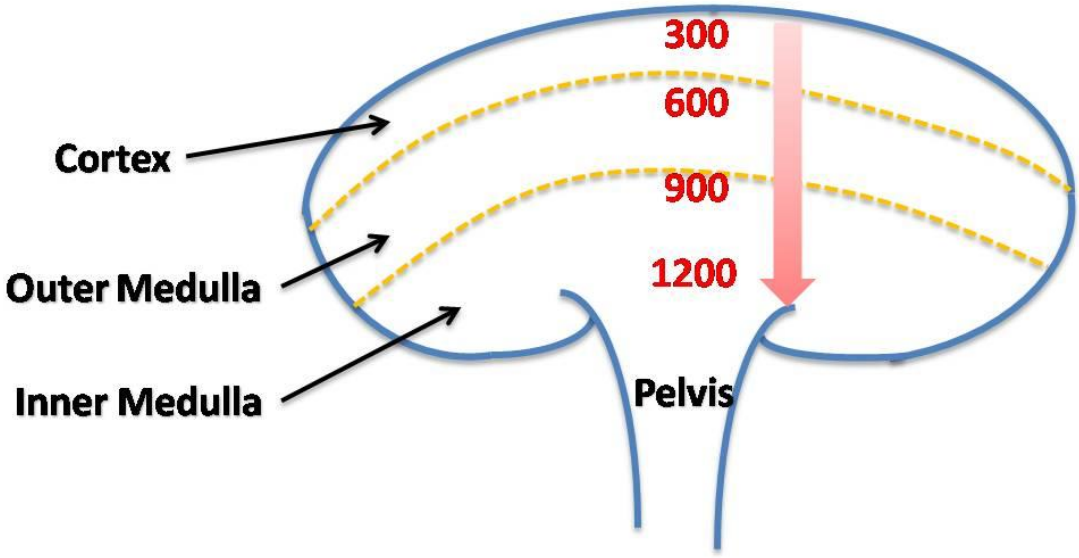

Figure 3. The osmotic gradient in the human kidney. The osmolarity in the interstitium increases from 300 mOsm in the cortex to 1,200 mOsm at the papillary tip of inner medulla.

Hypertonicity and hypoxia are also known to contribute to increased generation of reactive oxygen species (ROS). Although low levels of ROS are indispensible in biological processes such as intracellular signaling, immunity and defense against microorganisms (14-15), excessive ROS can cause oxidative stress, induce lipid, protein and nucleic acid modifications, DNA damage, and ultimately lead to cell dysfunction and death (16) (Figure 4). Under normal conditions there are significant amounts of ROS in the renal medulla (17) (18) (11). Immunohistochemistry staining for markers of oxidative modifications, nitrosylated tyrosine and 4-hydroxynonenal, shows higher levels of both markers in the renal medulla as compared to the renal cortex (Figure 5). The inner medullary interstitium appears to have the highest staining, consistent with the physiological increasing tonicity and hypoxia towards the papillary tip.

Taken together, the renal medulla is characterized by excess oxidative stress that results from rapidly changing interstitial tonicity, high osmotic stress, low blood flow, and low oxygen tension (18-20). Aging and diseased conditions such as the metabolic syndrome may further increase oxidative stress in the kidney and are associated with impaired renal function (21-22). Given that the renal medulla is an essential functional component of the kidney, strategies to maintain robust anti-oxidant mechanisms in the renal medulla is of paramount importance.

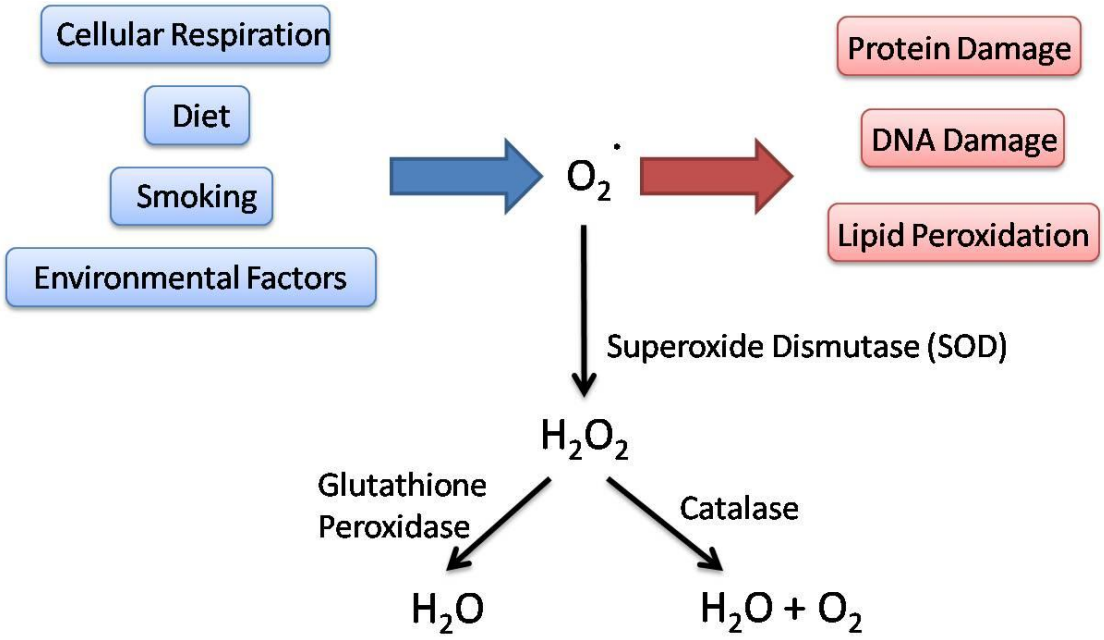

Figure 4. Overview of generation and antioxidant enzymatic detoxification of ROS.

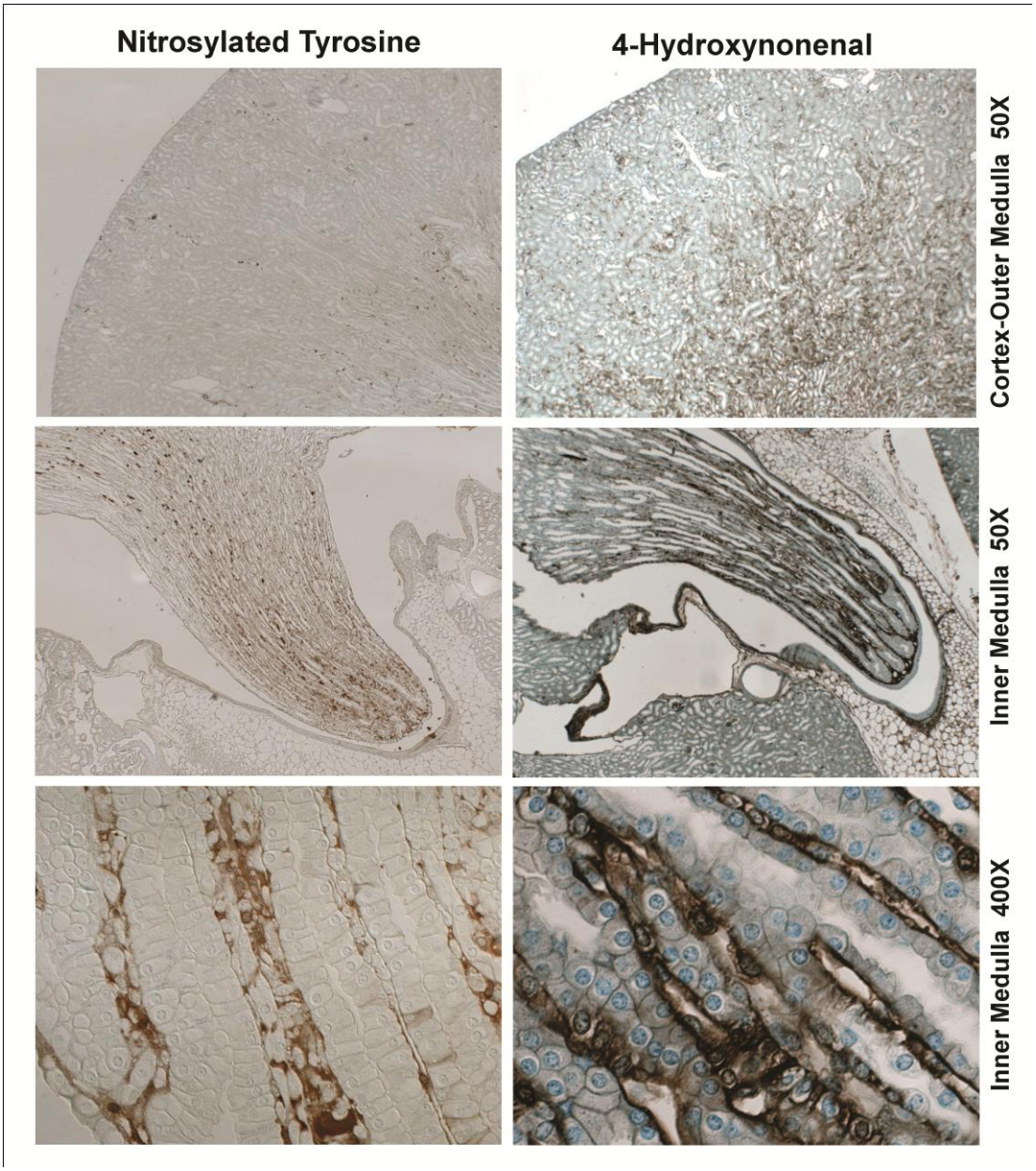

Figure 5. Markers of oxidative stress in the mouse kidney. Immunohistochemistry using oxidative stress markers anti-nitrosylated tyrosine antibody (left panels) and anti-4-hydroxynonenal antibody (right panels). Panels at the bottom show high magnification pictures of the renal inner medulla.

Anti-Stress Mechanisms in Renal Medulla The mechanisms allowing renal medullary cells to not only survive but also to function normally in this harsh environment are only partially characterized. A substantial body of evidence indicate important roles of the enhanced medullary expression and action of immediate-early genes (Fos and Jun), DNA damage inducible genes (GADDs), genes involved in cell cycle control and apoptosis (p53), heat shock proteins, and cyclooxygenase-1 and -2 (COX1 and COX2) and their derived prostaglandins (23) (11). Among them, the cytoprotective activity of COX2 in renal medulla is of note.

Cyclooxygenase is a key enzyme mediating the initial and committed step in the metabolism of arachidonic acid to the prostanoids (Figure 6) (24). COX catalyzes the conversion of arachidonic acid to PGH_2. PGH_2 is then converted to five bioactive prostanoids via distinct prostanoid synthases, including PGE_2, PGI_2, $PGF_{2\alpha}$, PGD_2, and TxB_2. The prostanoids interact with a group of G protein-coupled receptors that mediate their diverse physiological effects. Since prostanoids are rapidly metabolically degraded, their actions are usually limited to the immediate vicinity of their synthetic sites.

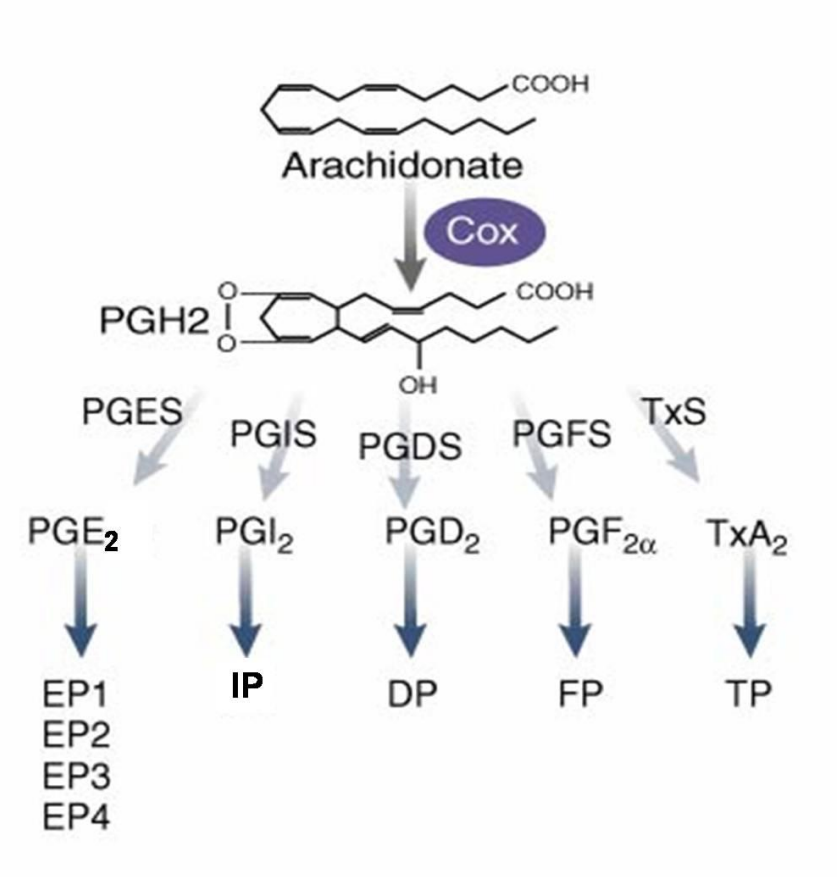

Figure 6. Cyclooxygenase (COX) pathway of arachidonic acid metabolism. COX first converts arachidonic acid to PGH_2 through cyclooxygenase and peroxidase activity. PGH_2 is subsequently metabolized to five major bioactive prostanoids—PGE_2, PGI_2, PGD_2, $PGF_{2\alpha}$, and TxA_2—through their respective synthases, PGES, PGIS, PGDS, PGFS, and TxS. These prostanoids act on their specific receptors to exert their distinct biological effects: E-prostanoid receptors 1–4 (EP1–4), I-prostanoid receptor (IP), D-prostanoid receptor (DP), F-prostanoid receptor (FP), and T-prostanoid receptor (TP).

There are two isoforms of COX, designated COX1 and COX2, which differ in many important respects. COX2 represents an inducible and dynamically regulated form of PGH2 synthase, which is induced by physiological and pathophysiological stressors and plays important roles in the cellular response to stress. COX1 appears to be constitutively expressed in most tissues and plays a constitutive house-keeping role responsible for maintaining basal physiological function. The kidney expresses both COX1 and COX2 in distinct cellular compartments. COX1 is predominantly expressed in the collecting duct. In contrast, COX2 is expressed in cortical thick ascending limb and macula densa of renal cortex. In renal medulla, COX2 is mainly expressed in interstitial cells, where it functions as a key survival factor protecting against hypertonicity induced apoptosis in cell culture, as well as in vivo in water-deprived animals (24) (25) (19). This cytoprotective role of COX2 in the renal medulla is also supported by clinical studies showing that inhibition of COX2 by nonsteroidal anti-inflammatory drugs (NSAIDs) is associated with necrosis of the renal medulla and papilla in patients, especially after dehydration (26) (27) (28), in which renal medullary cells are exposed to an extreme hyperosmotic environment. The NSAID blockage of the protective effects of COX2 severely impairs cellular tolerance to this stress.

The protective activity of COX2 in renal medulla is likely to be mediated through several mechanisms. COX2-derived prostacyclin (PGI2) may promote renal medullary interstitial cell viability through activating the prostacyclin responsive nuclear transcription factor peroxisome proliferator-activated receptor

PPARδ (29). Another study has shown that osmolyte accumulation, which is essential for cells to survive in the hypertonic environment of renal medulla, is dependent on COX2 activity (30). Moreover, renal medullary interstitial cells are in direct contact with vasa recta, suggesting an important role for these cells in maintaining an adequate blood supply to the renal medulla. COX2 derived PGE2 may activate EP2 or EP4 receptor on vasa recta to modulate renal medullary vascular tone (31) (32). Disruption of the blood supply to the renal medulla by COX2 inhibition may therefore partially contribute to NSAID-associated papillary necrosis.

Renal Medulla in the Regulation of Blood Pressure The kidneys are essential organs that are responsible for maintaining body electrolyte/fluid balance and normal blood pressure. Renal dysfunction has long been a recognized feature of essential hypertension (33). Originally, studies focused on the renal cortex, which is the site of glomerular filtration. Reduction of glomerular filtration and the morphological changes within cortical structures such as glomerulosclerosis have been well documented in patients with chronic hypertension. The involvement of the renal medulla in the regulation of blood pressure was proposed in the 1960s when Dr. Eric Muirhead reported that the medullary interstitial cells produced an anti-hypertensive substance, then designated as medullipin (34). Later studies suggested that the chemical nature of this blood pressure lowering substance might contain a product of arachidonic acid metabolism (35). Chemical ablation of renal medullary interstitial cells (RMICs) with bromoethylamine (BEA) leads to

systemic hypertension (36), supporting an indispensible role of these cells in the maintenance of blood pressure. In the mid-1980s Dr. Allen W. Cowley's group demonstrated a relationship between a reduction of renal medullary blood flow and experimental hypertension (37), and described the physiological role of renal medullary blood flow in the phenomena of pressure-natriuresis and diuresis.

COX-derived prostaglandins have been shown to play an important role in modulating sodium homeostasis and maintaining systemic blood pressure (38) (24). Clinical studies show that inhibition of cyclooxygenase in patients chronically ingesting NSAIDs or COX2 inhibitors is associated with the development of new cases of hypertension in the general population (39) (40). Importantly, animal studies show that a high sodium diet markedly increases renal medullary COX2 expression (41) (42), which may protect against sodium retention since inhibition of COX activity by intramedullary infusion of COX inhibitors causes sodium sensitive hypertension (43) (44). COX2 inhibition has also been reported to reduce renal medullary blood flow (45), and a reduction of renal medullary blood flow is known to cause sodium retention and hypertension based on pressure-natriuresis and diuresis theory.

The mechanisms underlying COX-derived prostaglandin modulation of sodium homeostasis and blood pressure maintenance have been partially elucidated. COX2 derived PGE2 or PGI2 and their corresponding EP2 and EP4 receptors or the IP receptor likely contribute to control of medullary blood flow via their vasodilator actions (31) (32). EP2 or IP receptor deficiency is associated with sodium sensitive hypertension (46) (47). Intramedullary infusion of PGE2 or EP2

agonist promotes renal sodium excretion in the setting of sodium loading (42). EP1 and EP3 receptors located in the thick limb and collecting ducts may also directly mediate sodium and water reabsorption through tubular epithelial cells (48-49). These studies support the role for COX-prostaglandin signaling in modulating sodium homeostasis and blood pressure.

In addition to impairing cell viability, reactive oxygen species (ROS) may also alter renal medullary blood flow through either vasodilation or vasoconstriction, and impact renal pressure-natriuresis, body sodium homeostasis and systemic blood pressure (33). The expression of both ROS-generating enzyme NADPH oxidase and ROS-removing enzymes SOD and catalase have been reported in the kidney (50) (51-52), consistent with physiological control of ROS level. Evidence suggests that increased oxidative stress in the renal medulla causes hypertension. Inhibition of anti-oxidant enzymes by intramedullary infusion of specific inhibitors reduces renal medullary blood flow and raises blood pressure in rats (53) (18). Furthermore, aging increases oxidative stress in the kidney and is associated with reduced renal function as well as increased incidence of hypertension (18). All the above observations suggest that maintaining strong anti-oxidant mechanisms in the kidney is of great importance to normal renal function and the regulation of blood pressure.

Sirtuin-1 (SIRT1) Overview

Yeast Sir2 Gene and Its Homologues in Mammals Sir2 was originally identified in the yeast. Yeast Sir2 protein (silent information regulator 2) and its highly conserved homologues are nicotinamide adenine dinucleotide (NAD)+-dependent histone/protein deacetylases (54-55). This catalytic reaction removes an acetyl group from the lysine side chains of a protein substrate, consumes NAD+ as a co-substrate, and generates nicotinamide (NAM) and 2'-*O*-acetyl-ADP-ribose (56) (57) (Figure 7). As the intracellular level of NAD+ and its ratio to its reduced form NADH are dependent on cellular oxygen metabolism and redox state, Sir2 proteins function as molecular sensors of cellular energy balance (58) (59). As a co-substrate, increased NAD+ level is associated with increased deacetylase activity of Sir2. The product NAM, on the other hand, can inhibit Sir2 enzymatic activity. Recently the NAD+ salvage pathway, which mediates the conversion of NAM back to NAD+, has been suggested to play a critical role in the cellular regulation of Sir2 activity (59). In addition to its deacetylase activity, Sir2 also has a mono-ADP-ribosyl transferase activity, which transfers ADP-ribose to substrate proteins.

Sir2 homologues in mammals are called sirtuins. To date, seven sirtuin family members have been identified, SIRT1-7. SIRT1, SIRT5 and SIRT6 are primarily histone/protein deacetylases, whereas SIRT2 and SIRT3 have both deacetylase and mono-ADP-ribosyl transferase activities (60). SIRT4, on the other hand, is the only identified to have an exclusive mono-ADP-ribosyl transferase activity (61)

(62). Besides different catalytic functions and substrates, mammalian sirtuins also differ in regard to their subcellular localizations (63). SIRT1, SIRT6 and SIRT7 are mainly found in the nucleus, whereas SIRT2 is located in the cytoplasm, and SIRT3, 4 and 5 are located in the mitochondria. Among the mammalian sirtuins, SIRT1 is the most extensively studied.

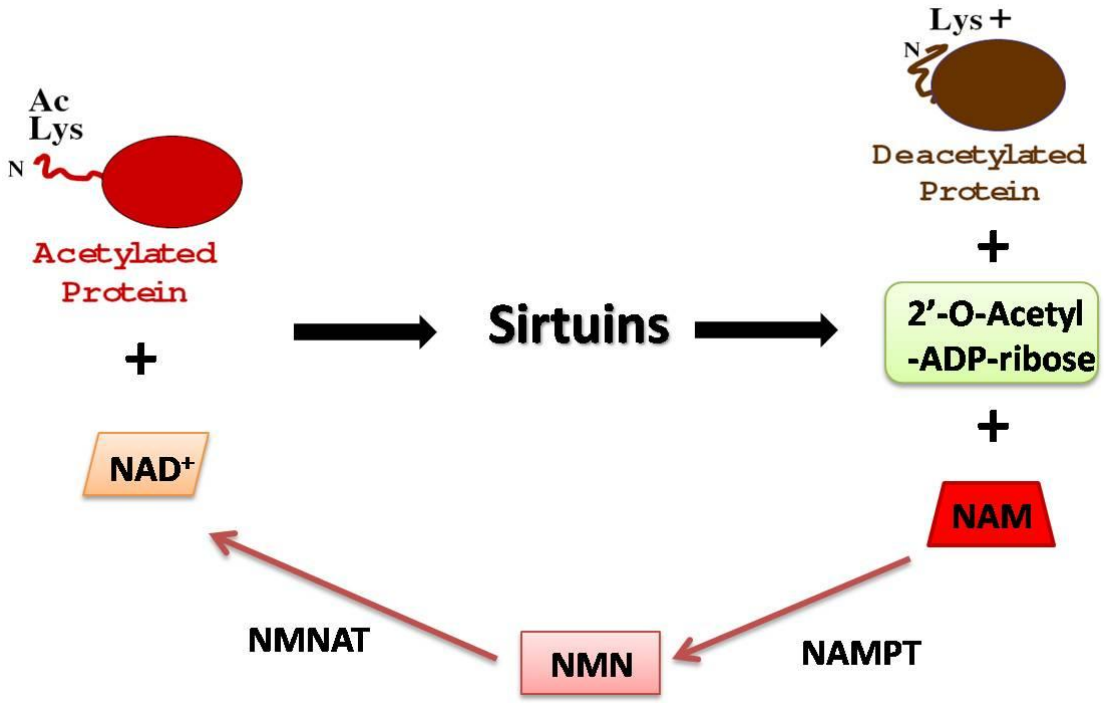

Figure 7. Sirtuins catalyse a unique deacetylation reaction in which NAD is consumed as a co-substrate. During the reaction process, the substrate protein is deacetylated and NAD is cleaved to nicotinamide (NAM) and 2'-O-acetyl-ADP-ribose. NAM can be converted to nicotinamide mononucleotide (NMN) via nicotinamide phosphoribosyltransferase (NAMPT), followed by the conversion of NMN to NAD+ by NMN adenylyltransferase (NMNAT) in the NAD+ salvage pathway.

SIRT1 and Caloric Restriction Caloric restriction (CR) promotes health, reduces the incidence of obesity, diabetes, cancer, neurodegenerative diseases, and increases the lifespan of a wide range of organisms (64-66)). The underlying mechanisms mediating lifespan extension and beneficial health effects of caloric restriction include an important function of Sir2 gene, which was first demonstrated in yeast (67). Later studies have demonstrated an essential role for Sir2 homologues in mediating the beneficial effects of CR in worms, flies, as well as mammals (68).

Mammalian SIRT1 is required and sufficient for the induction of a caloric restriction phenotype in rodents (69). Caloric restriction increases SIRT1 expression levels in several rodent and human tissues such as white adipose, liver, skeletal muscle, brain and kidney (70) (69). SIRT1-overexpressing transgenic mice exhibit a caloric restriction-like phenotype including lower body weight, reduction of fat mass, lower levels of total blood cholesterol, improved glucose homeostasis, increased metabolic rate, higher oxygen consumption, improved physical ability and delayed reproduction (71). In contrast, SIRT1-deficient mice have been shown to be unable to adapt to conditions of caloric restriction (72). These studies are consistent with an essential role for SIRT1 in mediating the beneficial effects of caloric restriction in mammals.

Pleiotropic Effects of SIRT1 Activity In addition to deacetylating histones, SIRT1 has been shown to deacetylate multiple transcriptional factors or co-

factors including p53, FOXO, NFκB, PPARγ and PGC-1α (73) (69) (Figure 8). Through this post-translational protein modulation, alters transcriptional activity or protein stability by SIRT1 exerts pleiotropic effects on the cellular stress response, inflammation, energy expenditure and cellular metabolism in multiple tissues and organs, in a tissue specific manner. Enhanced cell survival during stress conditions (e.g. oxidative stress or genotoxic stress) has been reported to be mediated through the interaction of SIRT1 with FOXO proteins and p53 (73). SIRT1 is anti-inflammatory as it represses the transcriptional activity of nuclear factor κB (NFκB) through deacetylation of its p65 subunit (74). By deacetylating nuclear receptor co-repressor (NCOR), SIRT1 blocks the activity of peroxisome proliferator-activated receptor-γ (PPAR-γ) and regulates fat mobilization from white adipose tissues (69, 75). SIRT1 directly modulates insulin secretion from pancreatic β-cells via deacetylating and repressing the transcription of uncoupling protein 2 (UCP2) (76-77). SIRT1 is also known to regulate insulin signaling through deacetylation of the insulin receptor substrate 2 (IRS2) and repression of protein tyrosine phosphatase 1B (PTP1B) (78). Furthermore, cellular metabolic function controlled by mitochondrial number and function is modulated by SIRT1 via deacetylation of PPAR-γ co-activator 1α (PGC1α) (75).

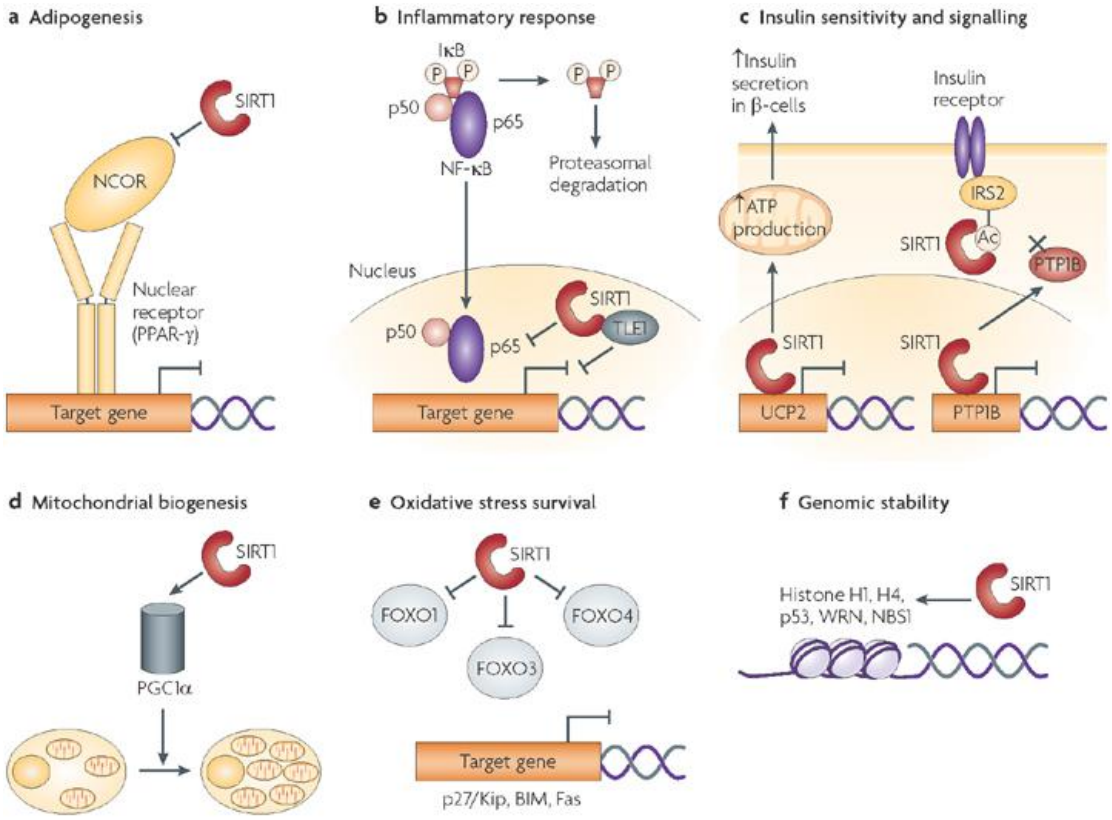

Figure 8. SIRT1 affects major cellular pathways by deacetylation of diverse substrate proteins. (Modified from Philip D. Lambert et al, Nature Reviews Drug Discovery, October 2008. Reprint permission from Macmillan Publishers Ltd).

Although no studies to date have shown a link between SIRT1 activity and human diseases or aging, a wealth of animal model data strongly support the pharmacological potential of SIRT1 activation as a strategy to treat or prevent metabolism or age related diseases (Figure 9). For instance, it has been reported that activation of SIRT1 by resveratrol, a naturally produced SIRT1 activator, improves metabolic syndrome in rodent models of obesity and type 2 diabetes (79) (80). Resveratrol improves insulin sensitivity, lowers glucose levels and extends lifespan of mice on a high fat diet. Newly developed specific and potent small molecule SIRT1 activators designated SRT compounds have also been shown to ameliorate the metabolic effects of type 2 diabetes in several rodent models (81). Moreover, transgenic mice overexpressing SIRT1 exhibit reduced lipid-induced inflammation, improved glucose tolerance and are protected from hepatic steatosis as compared with wild type mice (82). Overexpression of SIRT1 specifically in pancreatic β-cells (BESTO mice) improves glucose tolerance and insulin secretion in an intraperitoneal glucose tolerance test (76). Mice moderately overexpressing cardiac SIRT1 respond better to oxidative stress and exhibit less cardiac hypertrophy, apoptosis or fibrosis, cardiac dysfunction and expression of senescence markers with aging (83). Finally, both SIRT1 activators and overexpression of SIRT1 have been shown to slow in vitro neural cell death as well as in vivo neurodegeneration (84). In summary, activation of SIRT1 appears to have broad favorable metabolic effects.

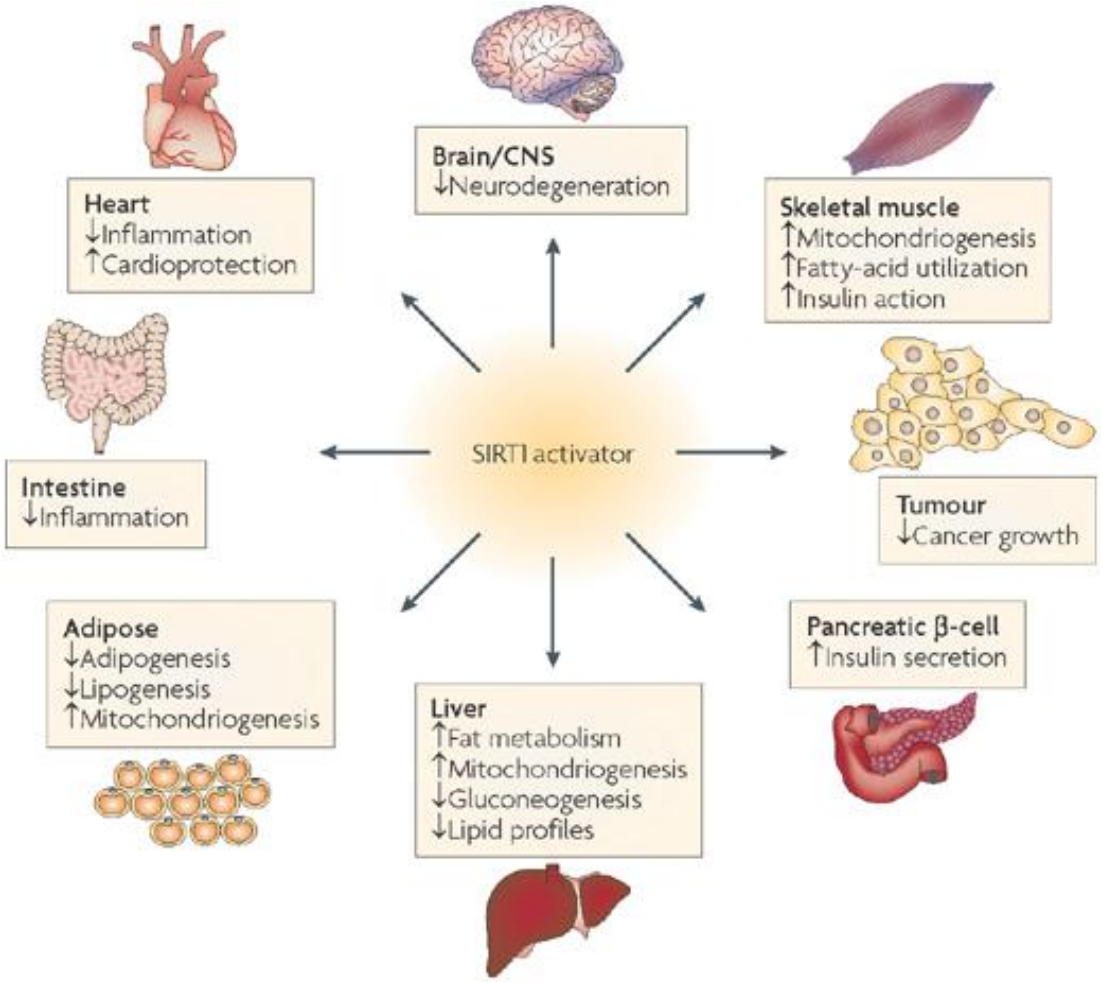

Figure 9. Multiple target organs in which SIRT1 activators can potentially have effects to treat diseases of aging. The effects on inflammation, mitochondriogenesis and metabolism may be seen in more than one tissue. The broad actions of SIRT1 activation in these target tissues are illustrated. (Modified from Philip D. Lambert et al, Nature Reviews Drug Discovery, October 2008. Reprint permission from Macmillan Publishers Ltd).

SIRT1 and the Kidney SIRT1 is expressed in almost all mammalian tissues albeit at different levels. The expression pattern or functional role of SIRT1 in the kidney remains largely unknown.

A large body of evidence supports potent anti-oxidant functions of SIRT1 in diverse tissues and cell types (83, 85-86). This cytoprotective role for SIRT1 has also been reported in renal cells. Pre-treatment with the SIRT1 activator resveratrol reduces acute ischemia/reperfusion injury in rats (87). SIRT1 protects against oxidative stress induced apoptosis in cultured mesangial cells through deacetylation and inactivation of p53 (88). SIRT1 also protects mesangial cells from TGF-β1-mediated apoptosis via deacetylating Smad7, which accelerates its degradation (89). In HK-2 cells SIRT1 is protective through activation of FOXO3α and up-regulation of catalase (90).

Besides being an anti-stress molecule, SIRT1 also acts as a metabolic master switch. Caloric restriction or starvation has been reported to increase SIRT1 expression in multiple tissues of the rodents including the brain, liver and kidney (70) (75). Interestingly intermittent fasting is reported to attenuate the progression of type 1 diabetic nephropathy in rats and is associated with increased renal SIRT1 expression (91), suggesting that SIRT1 may play a positive role in preserving renal functions in diabetic renal disease.

SIRT1 may also participate in blood pressure regulation. Miyazaki and colleagues reported that overexpression of SIRT1 in vascular smooth muscle cells (VSMC) reduced angiotensin II AT1 receptor (AT1R) expression (92).

Furthermore, Mattagajasingh and colleagues showed that inhibition of SIRT1 inhibited vasodilation and decreased NO bioavailability. These studies suggest a role for SIRT1 in regulating vascular tone. SIRT1 is also reported to regulate sodium balance by repressing the transcription of the α-subunit of the epithelial sodium channel ENaC through interacting with disruptor of telomeric silencing-1 (Dot1) in cultured inner medullary collecting duct cells (IMCD) (93). However, its relevance to the in vivo condition of IMCD cells and renal function in general remains to be investigated.

Overall Hypothesis

Hypothesis: SIRT1 plays important roles in promoting resistance of renal medullary cells to oxidative injury. Three specific aims have been developed to test this hypothesis.

Specific aim I: Characterize the histological distribution of SIRT1 expression in the mouse kidney.

Specific aim II: Examine the cytoprotective role of SIRT1 in mouse renal medullary cells against oxidative injury.

Specific Aim III: Examine the mechanism by which SIRT1 exerts cytoprotective functions in renal medullary cells. *(This aim stands only if the answer to aim II is true.)*

CHAPTER II

MATERIAL AND METHODS

Animals Mice were maintained in the animal facility of Vanderbilt University Medical Center, where they were housed at constant temperature with a 12-hour dark/12-hour light circle, and allowed free access to standard rodent chow and water. Wild type C57Bl/6J male mice at 8wks old were obtained from Jackson Laboratory.

The floxed-SIRT1 mouse was generated by Dr. Yansong Gu and coworkers (Harvard University Medical School, Boston, MA) (94), and deposited at the Jackson Laboratory (strain name: B6;129-*SIRT1*^{tm1Ygu}/J). Mice with one allele of SIRT1 gene deletion were obtained by crossing a SIRT1$^{floxed/+}$ mouse with a universal Cre mouse (EIIA-Cre mice on B6 background, kindly provided by Dr. Richard Breyer at Vanderbilt University, Nashville, TN). This mouse was further bred with C57Bl/6J to generate heterozygous SIRT1 knockout mice (SIRT1$^{+/-}$) and their wild type littermates (SIRT1$^{+/+}$). Male mice between 8 to 10wks of age were used in the present study.

To examine the effect of a high-salt diet on renal medullary COX and prostanoid synthase expression, mice were fed with either a high-salt diet (8% NaCl, Research Diet) or a normal-salt diet (0.3% NaCl) for 3 days.

The effect of high salt diet on renal medullary NFκB activity was examined in transgenic mice carrying a luciferase reporter driven by an NFκB response promoter, HIV long-terminal-repeat (LTR) (HLL mice) (19). HLL mice were provided with either normal salt diet or high salt diet for 3 days, after which renal medullary luciferase activity was determined using a commercial luciferase assay kit, according to manufacturer's protocol (Promega Corp, Madison, WI). Luciferase activity was quantified with a luminometer (Monolight 3010, PharMingen, San Diego, CA) and adjusted for the total amount of protein (19).

The cellular location of NFκB activation was examined using transgenic mice that carry an enhanced green fluorescent protein (EGFP) fusion protein under the control of an NFκB response promoter LTR (95). The expression of EGFP was determined by immunofluorescence staining using an anti-EGFP antibody (Invitrogen, Carlsbad, CA) as previously described (95).

Tenascin-C promoter driven inducible Cre knockin mouse (TNC-CreER2-EGFP mouse) was generated in Transgenic Mouse/ES Cells Shared Core at Vanderbilt University. ROSA26-lacZ reporter mice and genotyping methods were previously reported (96).

All animal studies were approved by the Institutional Animal Care and Use Committee of Vanderbilt University

Compounds SIRT1 activators SRT1720 and SRT2183 were provided by Drs. Christoph Westphal and Jill Milne (Sirtris, a GSK company, Cambridge, MA). For

1ml of 50mg/ml stock dosing solution used for in vivo studies, 50mg of SRT1720 was added to 400μl PEG400 and vortexed to form a homogenous suspension. Tween-80 (5μl) was added to 595μl water and vortexed. Then Tween-80/water was added into SRT1720/PEG400 and vortexed until homogeneous. In about 5-10 min the suspension became a translucent-opaque suspension. The final vehicle composition was 40% PEG400, 0.5% Tween-80 and 59.5% water. SRT1720 (100mg/kg body weight) was given to mice by oral gavage once a day according to the company's recommendation. For in vitro studies, SRT compounds were dissolved in DMSO. A final concentration of 0.5 to 10μM of SRT1720 and a final concentration of 1 to 20μM of SRT2183 were used.

COX2 selective inhibitor SC58236 was provided by Drs. Karen Siebert and Peter Isakson (Pfizer/Searle, New York, NY). For in vitro studies, compounds were dissolved in DMSO. A final concentration of 0.5μM or 2.5μM was used.

To test the hypothesis that NFκB is responsible for mediating high salt diet induced COX2 expression in the renal medulla, mice on normal salt diet were pretreated with an NFκB inhibitor, IMD-0354, (Sigma, St. Louis, MO) or vehicle for 2 days, followed by high salt diet for 3 days in the presence of IMD-0354 or vehicle. IMD-0354, dissolved in 0.5% carboxymethylcellulose (CMC, Sigma), was administered by gavage once daily at a dose of 8mg/kg, which effectively blocks NFκB activation. Drug-free vehicle (0.5% CMC solution) was used as a control.

Unilateral ureteral obstruction (UUO) Mice (male, 8 weeks of age) were anesthetized with 50mg/kg body weight ketamine and 100mg/kg body weight xylazine. The left ureter was exposed via a lateral incision and ligated by two sutures at the level of the lower renal pole. Mice were sacrificed at day 3 or 7 post operation. Both contralateral and obstructed kidneys were collected and assessed for gene expression, apoptosis and fibrosis.

Immunoblot Protein concentration was determined using the bicinchoninic acid protein assay (Sigma). 50 micrograms of protein was loaded in each lane of a 10% SDS-PAGE mini-gel and run at 100V. Proteins were transferred to a PVDF membrane at 100V for 1 hour on ice. The membrane was washed 3 times with TBST (50mM Tris, pH7.5, 150mM NaCl, 0.05% Tween-20), incubated in blocking buffer (150mM NaCl, 50mM Tris, 0.05% Tween-20, and 5% Carnation nonfat dry milk, pH7.5) for 1 h at RT, and then incubated with primary antibody in blocking buffer overnight at 4°C. The primary antibodies used were: anti-SIRT1 antibody (Millipore rabbit polyclonal, 1:1,000; Sigma mouse monoclonal, 1:2,000), anti-cleaved caspase-3 antibody (Cell signaling rabbit monoclonal, 1:200), anti-COX2 antibody (Cayman rabbit polyclonal, 1:1,000), anti-COX1 antibody (Cayman rabbit polyclonal, 1:1,000), anti-Col1 antibody (MD Biosciences rabbit polyclonal, 1:10,000), anti-β-actin antibody (Jackson ImmunoResearch Laboratories mouse monoclonal, 1:5,000), anti-α-tubulin antibody (Sigma mouse monoclonal, 1:2,000). After three washes (15min each), the membrane was incubated with horseradish peroxidase–conjugated secondary antibody (Jackson

ImmunoResearch Laboratories, 1:5,000) for 1 h at RT, followed by 3 washes (15min each) with TBST. Antibody labeling was visualized by the addition of chemiluminescence reagent (PerkinElmer Life Sciences) and the membrane was exposed to Kodak XAR-5 film. Due to heterogeneous expression of SIRT1 in the kidney as well as distorted morphology of the obstructed kidney, tissue sampling (dissecting cortex from medulla) may easily introduce artifacts into data. For this reason, the entire kidney was homogenized and whole kidney lysates were used for all the immunoblot studies of Figures 4, 5, 6 and 8.

Immunohistochemistry Deparaffinized 5μm sections were briefly incubated with 3% H_2O_2, and then with primary antibody for 60 min, rinsed with Tris-buffered saline containing 0.1% Tween-20 and incubated with a biotinylated secondary antibody for 30 min. After three PBS washes (5min each), sections were incubated with horseradish peroxidase–conjugated anti-biotin labeling solution (ABC Elite Kit, Vector) for 30 min at 22°C followed by washing and incubation with 3,3-diaminobenzidine solution (DAB). Counterstaining with hematoxylin and eosin was then performed before examination under a light microscope. The primary antibodies used were as follows: anti-SIRT1 antibody (Millipore rabbit polyclonal, 1:500), anti-nitrosylated tyrosine antibody and anti-4-hydroxynonenal antibody (R&D biosystems mouse monoclonal, 1:500).

Immunofluorescent Staining Kidney tissues were fixed in 4% paraformaldehyde and then incubated in 30% sucrose overnight. Cryostat

sections (5 μm) were blocked with 3% normal donkey serum for 20 min, and then incubated with primary antibody for 60 min at RT. After washing in PBS, the sections were incubated with a Cy2 or Cy3 conjugated anti-IgG secondary antibody (Jackson ImmunoResearch Laboratories, 1:200) for 30 min, washed in PBS for 5 times and examined using microscopy with a Zeiss Axioskop and spot-cam digital camera (Diagnostic Instruments) or confocal microscope (Zeiss LSM510). The primary antibodies used for immunofluorescent studies were: anti-SIRT1 antibody (Millipore rabbit polyclonal, 1:500), anti-aquaporin-1 (AQP1) antibody (Santa Cruz mouse monoclonal, 1:100), anti-Tamm Horsfall protein (THP) antibody (MP Biomedical goat polyclonal, 1:1,000), anti-aquaporin-2 (AQP2) antibody (Santa Cruz goat polyclonal, 1:400), anti-COX2 antibody (Cayman rabbit polyclonal, 1:500).

In Situ Hybridization In situ hybridization was performed as described previously (19). Mouse tissues were fixed in 4% paraformaldehyde and then embedded in paraffin. Sections (7 μm) were cut and hybridized at 50–55°C for approximately 18 hours with labeled riboprobes recognizing specific genes. After hybridization, sections were washed at 50°C in 50% formamide, 2´ SSC, and 100μM β-mercaptoethanol for 60 minutes, treated with RNase A (10 mg/ml) at 37°C for 30 minutes, followed by washes in 19 mM Tris, 5 mM EDTA, 500 mM NaCl (37°C), 2´ SSC (50°C), and 0.1´ SSC (50°C). Slides were dehydrated with ethanol containing 300 mM ammonium acetate. Photomicrographs were taken from slides dipped in K5 emulsion (Ilford Ltd., Knutsford, Cheshire, United

Kingdom) diluted 1:1 with 2% glycerol/water and exposed for 7 days at 4°C. After development in Kodak D-19, slides were counterstained with hematoxylin. Photomicrographs were taken with a Zeiss Axioskop microscope using bright-field optics.

Southern Blot Crude ES cell DNA was first digested with restriction enzymes and run in 1% agarose gel. The DNA in the gel was depurinated by rocking it in 0.25M HCl for exactly 10 min, followed by alkaline denaturation in 0.4M NaOH for 3 x 15 min and shaking in 20XSSC for 5 min. The blot was set up from bottom to top: 1) A large dish filled with 20xSSC with glass plate on top of it to rest the gel, 2) Two pieces of wick- blotting paper cut to the width of the gel and length such that the wick was in contact with the bottom of the dish, 3) Agarose gel that was turned upside down, with a nick in the bottom right hand corner for orientation, 4) Hybond N+ nylon membrane cut to the exact size of the gel, with a nick in the corner for orientation, 5) Four pieces of blotting paper cut to size of the gel, 6) Glass plate and additional weight to keep blot in place. The blot was transfered overnight. The next day, the gel and membrane was taken off together, and flipped. The wells were marked using a pencil. The membrane was auto X-linked with Stratalinker, followed by pre-hybridization at 65˚C for at least 1h. The probes were then added and the hybridization was continued at 65˚C overnight. The next day, the membrane was washed 3x for 10min at 65˚C and then exposed at -80˚C for 4-7 days. Primers used for synthesizing 5' probe were: 5'-TAGAGCAGGTGGTCCCAAACAT-3' and 5'-

CCAGGAGCCAGGAAATAGCCTTA-3'. Primers used for synthesizing 3' probe were: 5'-GATGACGACTACACTGGGGAA-3' and 5'-ACTGGGGCACCTTTGCTCTT-3'.

Culture of renal medullary interstitial cells Mouse renal medullary interstitial cells were prepared as described (97-98). Briefly, 8 kidneys were harvested from donor C57Bl6/J mice under sterile conditions, and medullary regions were excised, minced, and suspended in Dulbecco's Modified Eagle's Medium (DMEM, Invitrogen) containing 10% (v/v) fetal bovine serum and penicillin/streptomycin. The pooled suspension containing renal medullary tissues from the donor mice was then injected intracutaneously at 3 or 4 different locations of the ventral abdominal wall of an isogeneric recipient mouse. Four days later, the recipient mouse was sacrificed, and the firm yellow nodules were removed and minced, and cells trypsinized in 0.05% trypsin-EDTA at 37ºC for 15 min, washed and pelleted at 1200rpm. The pellet was resuspended and cultured in DMEM supplemented with 10% fetal bovine serum and penicillin/streptomycin, at 37°C in 95% air /5% CO_2 incubator. The cultured mouse renal medullary interstitial cells contained Oil Red O staining-positive lipid rich droplets, which is a characteristic feature of type 1 medullary interstitial cells (1).

SIRT1 knockdown by Lentivirus carrying selective SIRT1 shRNA HEK293T cells were co-transfected with lentiviral pLKO.1 plasmid carrying SIRT1 selective

shRNA (Sigma MISSION shRNA library, SHCLNG-NM_019812), psPAX2 packaging plasmid and pMD2.G envelop plasmid using FuGENE (Roche). Twelve hours later, the medium containing the transfection reagent was removed and replaced with fresh complete DMEM + 10% FBS + penicillin/streptomycin. Twenty-four hours later, the culture medium containing lentiviral particles was harvested from HEK293T cells and transferred to a polypropylene storage tube. Virus was stored in aliquots at -80^{o}C. Primary cultured mouse renal medullary interstitial cells (RMICs) were then infected with appropriate amount of lentiviral particles containing medium. Twenty-four hours later, virus containing medium was removed and replaced with fresh medium. Infected mouse RMIC were cultured for 3 days and then RT-PCR or immunoblot was performed to examine the efficiency of mRNA or protein knockdown. Controls included empty pLKO.1 plasmid or pLKO.1 plasmid containing scrambled shRNA. In addition, two different SIRT1 selective shRNAs from Sigma were used side by side in all the knockdown experiments to determine whether they resulted in similar phenotypes.

RT-PCR Total RNA was extracted from cultured mouse renal medullary interstitial cells by using TRIZOL reagent (Invitrogen) and reverse transcribed using high capacity cDNA reverse transcription kit (Applied Biosystems). The primers used for PCR were: SIRT1: sense 5'GCAACAGCATCTTGCCTGAT3', antisense 5'GTGCTAC TGGTCTCACTT3'; SIRT2: sense 5'CTTCCTGGGCATGATGAT3', antisense 5'ACCCTGACTGGGCATCTAT3';

SIRT3: sense 5'CAGCAACCTTCAGCAGTA3', antisense 5'CCGTGCATGTAGCTGTTA3'. PCR program used: 30 circles (94^{o} C, 30s; 58^{o} C, 30s; 72^{o} C, 45s).

quantitative RT-PCR Total RNA was extracted from renal tissues or cultured renal medullary interstitial cells using TRIZOL reagent (Invitrogen). Reverse transcription was performed using a high capacity cDNA reverse transcription kit (Applied Biosystems). Quantitative real time PCR was performed using Taqman gene expression assay system (Applied biosystems). The probes used were: Mm01168521_m1 (mouse SIRT1), Mm00478374_m1 (mouse COX2), Mm00477214_m1 (mouse COX1), Mm00801666_g1 (mouse Col1a1), Mm00802372_m1 (mouse Col4a1). Probes for eukaryotic 18S rRNA (4319413E) were used as endogenous control. Gene expression values were calculated based on the comparative threshold cycle (Ct) (method detailed in Applied Biosystems User Bulletin Number 2), normalized to the expression values of 18S rRNA, and displayed as fold induction relative to control.

Crystal violet staining Cell viability was assessed using crystal violet staining (99-101). Culture medium was first removed and culture plates were washed with PBS. The remaining viable attached cells were stained with 0.5% crystal violet in 50% methanol for 15 min at room temperature, and gently rinsed with water and dried. Crystal violet in each well of a 12-well plate was then re-dissolved by 500μl

of 0.1M citrate sodium in 20% methanol, pH 5.4. 30 min later, the absorbance at 570nm was read using a spectrophotometer. Untreated control wells were arbitrarily considered as 100% survival and the crystal violet absorbance in treated wells was compared to control wells to obtain the relative cell survival percentage.

TUNEL (Terminal dUTP nick-end labeling) TUNEL assays of cultured renal medullary interstitial cells were performed according to manufacture's protocols (In situ cell death detection kit, Fluorescein, Cat#11684795910, Roche). Vectorshield mounting medium for fluorescence with DAPI (Vector) was used. Immunofluorescent microscopy was performed using a Zeiss Axioskop and spot-cam digital camera (Diagnostic Instruments). Apoptotic cell % was quantified by calculating the ratio of TUNEL-positive cells to DAPI stained total nuclei number on $\geqslant$15 random high power fields (HPF, 400X as final magnification).

For TUNEL assays on kidney sections, 5μm thick sections of paraffin embedded tissue were deparaffinized and hydrated, quenched in 3% H_2O_2 for 15 min to remove endogenous hydroxyl peroxidase activity, and then subjected to microwave antigen retrieval and proteinase K treatment to expose DNA. Slides were incubated in humidified chamber for 1 h at RT in a reaction solution containing TdT terminal transferase (Fisher), Bio-14-dATP (Gibco) and One-Phor-All buffer (supplied with TdT terminal transferase). The reaction was terminated by washing in PBS, 2 x 3 min followed by 2% BSA in water for 10 min at RT, incubated in horseradish peroxidase conjugated anti-biotin labeling

solution (ABC Elite kit, Vector), and stained with 3,3-diaminobenzidine (DAB). Quantification of apoptotic cells was performed by counting TUNEL-positive cells in $\geqslant$6 random high power fields in the renal medulla (including outer and inner medulla) of one kidney section.

Sirius red staining Collagen accumulation in kidney sections was determined by staining for Sirius Red (102), and quantified by image analysis. Analysis was performed without knowledge of treatment protocol. In brief, paraffin embedded sections were cut into 5μm thick sections and deparaffinized. The slides were incubated in picro-sirius red solution (0.5g Sirius red F3B (C.I. 35782, Sigma) in 500ml saturated aqueous solution of picric acid) for one hour, and then washed in two changes of acidified water (5ml acetic acid in 1L water). After physically removing most of the water from the slides by vigorous shaking or blotting with dam filter paper, the slides were dehydrated in three changes of 100% ethanol, cleared in xylene, and mounted in a resinous medium. A Zeiss Axioskop and spot-cam digital camera (Diagnostic Instruments) was used to capture 15-25 non-overlapping fields per one kidney section at 200X for final magnification through crossed polars. Image analysis was performed using ImageJ with modifications of techniques described previously (103). Data was presented as the mean tubulointerstitial area occupied by collagen fibrils reactive with sirius red compared to total area (%).

Dual Luciferase Reporter Assay An 891bp human COX2 promoter driven *firefly* luciferase reporter construct was generously provided by Dr. Lee-Ho Wang (Department of Hematology, University of Texas Health Science Center at Houston, Houston, TX) (104). The COX2 reporter *firefly* luciferase plasmid and a plasmid containing *renilla* luciferase driven by the TK promoter (Promega) were co-transfected into primary cultured mouse renal medullary interstitial cells using FuGENE (Roche). Dual Luciferase assay kit (Promega) was used to measure both *firefly* and *renilla* luciferase activity in the transfected RMIC with or without treatment. Relative luciferase activity was defined as COX2 reporter *firefly* luciferase activity adjusted by *renilla* luciferase activity. Data is presented as fold induction compared to control group.

Chromatin Immunoprecipitation Assay Chromatin immunoprecipitation Assay was performed according to the manufacture's protocol (Millipore, ChIP Assay kit, Cat# 17-295). Cultured mouse renal medullary interstitial cells were cross-linked using 1% formaldehyde for 10 min at 37ºC. After washing twice using ice cold PBS containing protease inhibitors, cells were scraped into 1.7ml eppendorff tubes and spun down for 4 min at 2,000 rpm at 4ºC. The cell pellet was re-suspended in SDS Lysis Buffer and incubated for 10 min on ice. The lysates were sonicated on ice to shear DNA to lengths between 200 and 1,000 base pairs, and then diluted 10 fold in ChIP Dilution Buffer with protease inhibitors. The immunoprecipitating antibody (Millipore, rabbit anti-SIRT1, working concentration 5μg/ml) was added to the supernatant fraction for overnight-

incubation at 4ºC with rotation (For a negative control, pre-immune IgG was added for immunoprecipitation). Then, Salmon Sperm DNA/Protein A Agarose Slurry (50ul into 2ml supernatant) was added for one hour-incubation at 4ºC with rotation. The agarose was pelleted by gentle centrifugation (700 to 1,000 rpm at 4ºC, ~1min). The supernatant containing unbound, non-specific DNA was removed. The protein A agarose complex was washed for 3-5 min on a rotating platform with the washing buffers supplied with the kit. The precipitated complex was eluted from the antibody by adding freshly prepared elution buffer (1%SDS, 0.1M $NaHCO_3$), vortexed briefly and incubated at room temperature for 15 min. The agarose was then spun down, and the supernatant fraction (eluate) was transfered to another tube and elution was repeated. Eluates were combined and protein-DNA crosslinks were reversed by adding 5M NaCl (20ul into 500µl) and heating at 65ºC for 4 h. The reverse-crosslinked eluates were further treated with Proteinase K, and DNA was recovered by phenol/chloroform extraction and ethanol precipitation. Pellets were washed with 70% ethanol and air dried. Pellets were then resuspended in an appropriate buffer for PCR. The primers used were as follows: [-712, -396] region: sense 5'CAGCAGGGGGAAAATACCTT3', antisense 5'CGGGATCTAAGGTCCT AACT3'; [-4166, -3946] region: sense 5'GGACTGGCTAGAGACATTGA3', antisense 5' AGCAGGGAACACATGGATGA3'. PCR program used: 30 circles (94^{o} C, 30s; 60 ^{o} C, 1min; 72^{o} C, 1min).

X-gal Staining Frozen sections were cut and fixed with cold formalin for 10 minutes at 4ºC. After 3 PBS washes for 5 minutes each, the slides were rinsed in distilled water and washed in β-gal wash buffer (0.1M Phosphate buffer, 2mM $MgCl_2$, 5mM EGTA, 0.01% Sodium Deoxycholate, 0.02% NP40, pH7.3) for 10 minutes at RT. Then, the slides were placed in X-gal staining solution (5mM Potassium Ferrocyanide, 5mM Potassium Ferricyanid, 1mg/ml X-gal in β-gal wash solution) in a humidified chamber for 24 hours at 37ºC. After 2 PBS washes for 5 minutes each, the slides were rinsed with distilled water and mounted with aqueous mounting medium.

Statistical Analysis Data are shown as mean±SEM. Statistical analysis was performed by using GraphPad Prism. Unpaired two-tailed student *t* tests were used to evaluate the differences in means between two independent groups. $P < 0.05$ was considered to be significant. (* In the *t* test, the following assumption should be met: Each of the two populations being compared should follow a normal distribution, which can be evaluated by looking at the distribution of the data or by performing a normality test.)

CHAPTER III

CYTOPROTECTIVE ROLES OF SIRT1 IN RENAL MEDULLA

Introduction

Mammalian SIRT1 belongs to a highly conserved family of nicotinamide adenine dinucleotide (NAD^+)-dependent protein deacetylases and is widely expressed throughout most mammalian tissues (54-55). Because of its dependence on cellular NAD^+ levels, SIRT1 activity responds to redox reactions in cell metabolism (58). Intriguingly, both overexpression of SIRT1 and activation of SIRT1 using the naturally occurring compound resveratrol or newly developed specific activators have been shown to promote cell resistance to different stressors (e.g. oxidative stress or genotoxic stress) in diverse tissues and cells (83, 85-86), This stress defensive function of SIRT1 is thought to contribute to its diverse beneficial effects including protection from diseases (e.g. metabolic syndrome or neurodegenerative diseases) and extension of lifespan in rodents (57, 79, 81, 105).

Although SIRT1 has been extensively studied in many organs including the liver, pancreas, brain, adipose tissue and muscle, a functional role of SIRT1 in the kidney has only been partially established. SIRT1 has been suggested to play a protective role in diabetic renal disease (91) as well as in acute renal

ischemia/reperfusion injury models (106) (87) (107). In cultures, SIRT1 protects mesangial cells or HK-2 cells from oxidative stress or cytokines induced apoptosis (88) (89) (90). These observations are consistent with a cytoprotective role for SIRT1 in the kidney.

Notably, the renal medulla is characterized by pronounced oxidative stress that results from rapidly changing interstitial tonicity as well as high osmotic stress, low blood flow and oxygen tension (18-19, 108). Aging and diseased conditions such as the metabolic syndrome further increase oxidative stress in the kidney and are associated with reduced renal function (21-22). Given that the renal medulla is critical for normal kidney function including regulation of water and sodium balance as well as maintaining normal blood pressure (28, 33, 36, 98, 109), strategies to maintain robust anti-oxidant mechanisms in the renal medulla is of paramount importance.

In this chapter, we characterized the histological distribution of SIRT1 in the kidney and examined the potential anti-oxidant role of SIRT1 in the renal medulla.

Results

SIRT1 is abundantly expressed in the renal medullary interstitial cells. Both immunoblot (Figure 10A) and qRT-PCR (Figure 10B, $P<0.05$) show significantly higher levels of SIRT1 expression in the renal medulla than in the renal cortex. Immunohistochemistry confirmed abundant nuclear SIRT1 immunoreactivity in the renal inner medulla (Figure 10C). Co-staining for SIRT1 (red) and the renal

segmental markers (green) showed abundant SIRT1 positive cells in the inner medullary interstitium (Figure 10D). Some aquaporin-2 (AQP2) positive collecting duct cells also expressed SIRT1 (Figure 10D, right panel). We confirmed SIRT1 expression in the renal medullary interstitial cells as SIRT1 (red) co-localized with a COX2-reporter EGFP that is specifically expressed in these cells (Figure 10E).

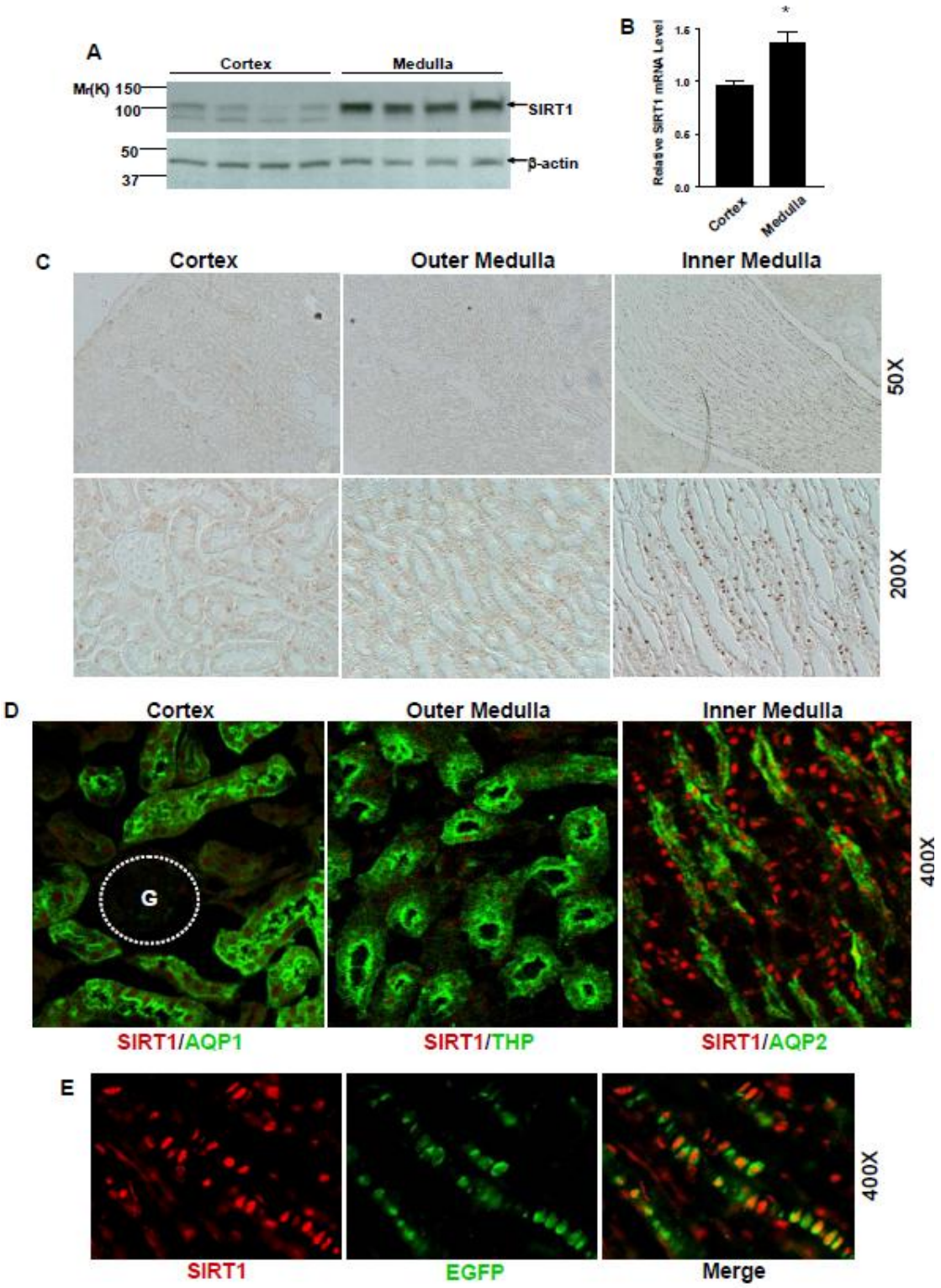
A
Cortex
Medulla
Mr(K) 150
100
50
37
SIRT1
β-actin
B
*
Relative SIRT1 mRNA Level
1.6
1.0
0.6
0.0
Cortex
Medulla
C
Cortex
Outer Medulla
Inner Medulla
50X
200X
D
Cortex
Outer Medulla
Inner Medulla
G
400X
SIRT1/AQP1
SIRT1/THP
SIRT1/AQP2
E
400X
SIRT1
EGFP
Merge

Figure 10. SIRT1 expression in mouse kidney. (A) SIRT1 protein expression in the C57Bl/6J mouse renal medulla (including outer and inner medulla) and the renal cortical region was examined by immunoblot. Each lane represents a lysate from a single mouse. **(B)** SIRT1 mRNA expression in the renal medulla and the cortex was examined by qRT-PCR (n=4, *P<0.05). **(C)** Immunohistochemistry for SIRT1 expression in the mouse kidney. **(D)** Immunofluorescent costaining for SIRT1 (red) and renal segmental markers (green): AQP1 (proximal tubule), THP (thick ascending limb), AQP2 (collecting duct). (G: glomerulus) **(E)** Immunofluorescence stained SIRT1 (red) in the EGFP-positive renal medullary interstitial cells of COX2 promoter driven EGFP reporter transgenic mice.

SIRT1 protects cultured renal medullary interstitial cells against oxidative stress Because SIRT1 is abundantly expressed in the renal medullary interstitium where high levels of oxidative stress are present (see Figure 5, Page 11), we tested the role of SIRT1 in promoting cellular resistance to oxidative stress using primary cultured mouse renal medullary interstitial cells (RMIC).

Down-regulation of SIRT1 was achieved using a lentivirus carrying a SIRT1 selective shRNA. SIRT1 shRNA reduced endogenous SIRT1 protein expression by 85% (Figure 11A, $P<0.0001$). RT-PCR also showed that SIRT1 shRNA decreased SIRT1 mRNA expression, while SIRT2 and SIRT3 mRNA expression remained unaltered (Figure 11B). Exposure of RIMC to oxidative stress (250μM H_2O_2, 12h) significantly reduced cell viability and this effect was accentuated by knockdown of SIRT1 (Figure 11C, 22±4% versus 51±5%, $P<0.0001$). TUNEL-positive apoptosis also increased following H_2O_2 treatment (500μM, 6h), which was further increased by knockdown of SIRT1 (Figure 11D, $P<0.05$). Sensitization to H_2O_2 treatment induced apoptosis by knockdown of SIRT1 was also confirmed by an immunoblot showing increased cleaved caspase-3 expression (Figure 11E, $P<0.001$).

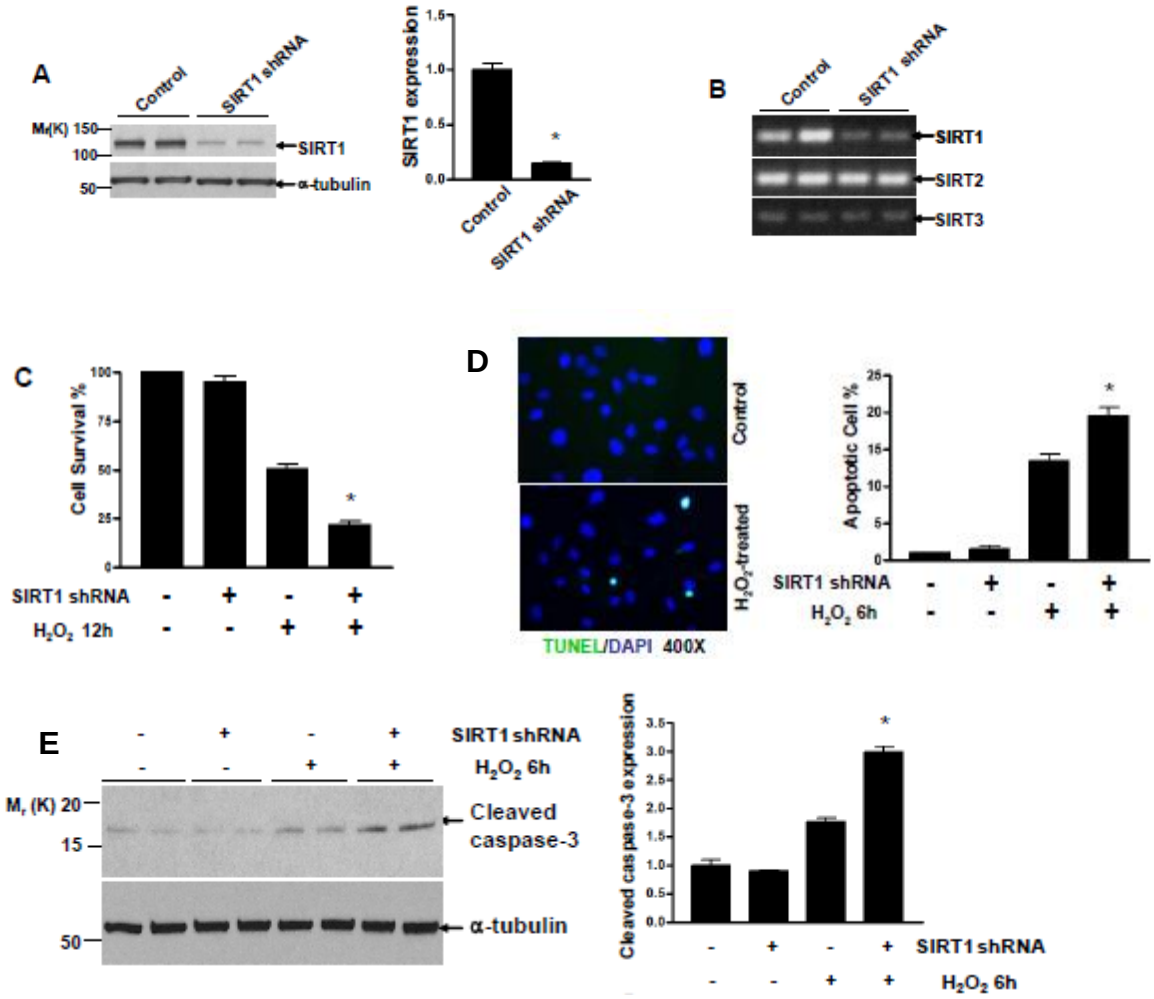

Figure 11. SIRT1 deficiency increases oxidative stress induced apoptosis in cultured renal medullary interstitial cells. (A, B) Primary mouse renal medullary interstitial cells (RMIC) were infected with lentivirus carrying SIRT1 selective shRNA or control virus. SIRT1, SIRT2 and SIRT3 expression were examined by immunoblot (A, densitometry, n=4, *P<0.0001) and RT-PCR (B). **(C)** Control or SIRT1 shRNA treated RMIC were challenged with H_2O_2 (250μM) for 12 hours. Cell viability was examined by crystal violet staining (n=6, *P<0.0001 versus control virus treated cells with H_2O_2). **(D)** Control or SIRT1 shRNA treated RMIC were challenged with H_2O_2 (500μM) for 6 hours. Cell apoptosis was examined by TUNEL assay (n=15, *P<0.05 versus control virus treated cells with H_2O_2). **(E)** Control or SIRT1 shRNA treated RMIC were challenged with H_2O_2 (500μM) for 6 hours. Cellular apoptosis marker, cleaved caspase-3 expression, was examined by immunoblot (n=4, densitometry, *P<0.001 versus control virus treated cells with H_2O_2).

We next examined whether the SIRT1 activator resveratrol protected RMIC from oxidative stress. Resveratrol (5μM) significantly enhanced the ability of RMIC to tolerate oxidative stress (500μM H_2O_2, 12h) (Figure 12A, $54 \pm 8\%$ versus $35 \pm 3\%$, $P<0.001$). Knockdown of SIRT1 using shRNA abolished the protective effect of Resveratrol (Figure 12A). Treatment of RMIC with SRT2183 (5μM), another specific and potent SIRT1 activator, also significantly reduced TUNEL-positive apoptosis following H_2O_2 treatment (Figure 12B, $P<0.001$). This was further confirmed by reduced cleaved caspase-3 level in H_2O_2 treated RMIC also treated with SRT2183 (Figure 12C, $P<0.05$). These observations are consistent with an anti-oxidant role of SIRT1 in renal medullary interstitial cells.

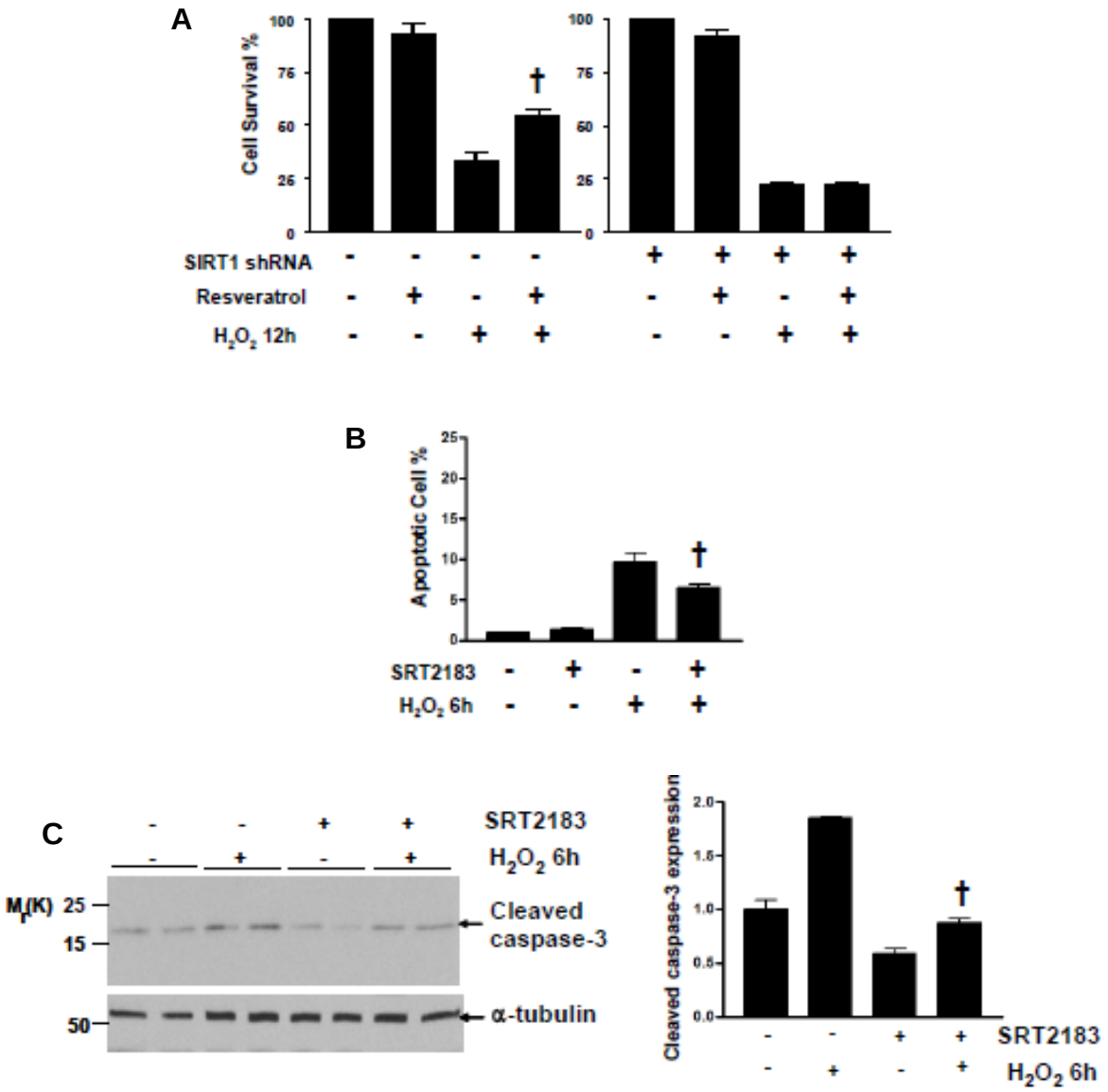

Figure 12. SIRT1 activation protects against oxidative stress induced apoptosis in cultured renal medullary interstitial cells. (A) Control or SIRT1 shRNA treated RMIC were pretreated with or without SIRT1 activator resveratrol (5μM) and challenged with H_2O_2 (250μM) for 12 hours. Cell viability was examined by crystal violet staining (n=6, †P<0.001 versus control virus treated cells with H_2O_2 without resveratrol). **(B)** RMIC were pretreated with or without SIRT1 activator SRT2183 (5μM) and challenged with H_2O_2 (500μM) for 6 hours. Cell apoptosis was examined by TUNEL assay (n=15, †P<0.001 versus cells with H_2O_2 without SRT2183). **(C)** RMIC were pretreated with or without SIRT1 activator SRT2183 (5μM) and challenged with H_2O_2 (500μM) for 6 hours. Cellular apoptosis marker, cleaved caspase-3 expression, was examined by immunoblot (n=4, densitometry, †P<0.05 versus cells with H_2O_2 without SRT2183).

SIRT1 deficiency increases UUO injury induced apoptosis and fibrosis. To investigate the potential protective role of SIRT1 in kidney injury, we used the unilateral ureteral obstruction (UUO) model, which has been associated with increased renal oxidative stress (110-111). Although homozygous SIRT1 knockout mice exhibit severe developmental defects (94), heterozygous SIRT1 knockout mice develop normally, and their kidneys are histologically normal (Figure 13). qRT-PCR (Figure 14A, $P<0.01$) and immunoblot (Figure 14B, $P<0.05$) confirmed significantly decreased SIRT1 mRNA and protein expression in the kidney of heterozygous SIRT1 knockout mice (SIRT1+/-). A significant increase of SIRT1 protein expression was observed in the obstructed kidney at day 3 of both SIRT1+/+ mice (Figure 14C, $P<0.0001$) and SIRT1+/- mice (Figure 14C, $P<0.0001$). In addition, SIRT1 induction was significantly less in the kidney of SIRT1+/- mice than in SIRT1+/+ mouse kidney (Figure 14C, $P<0.001$).

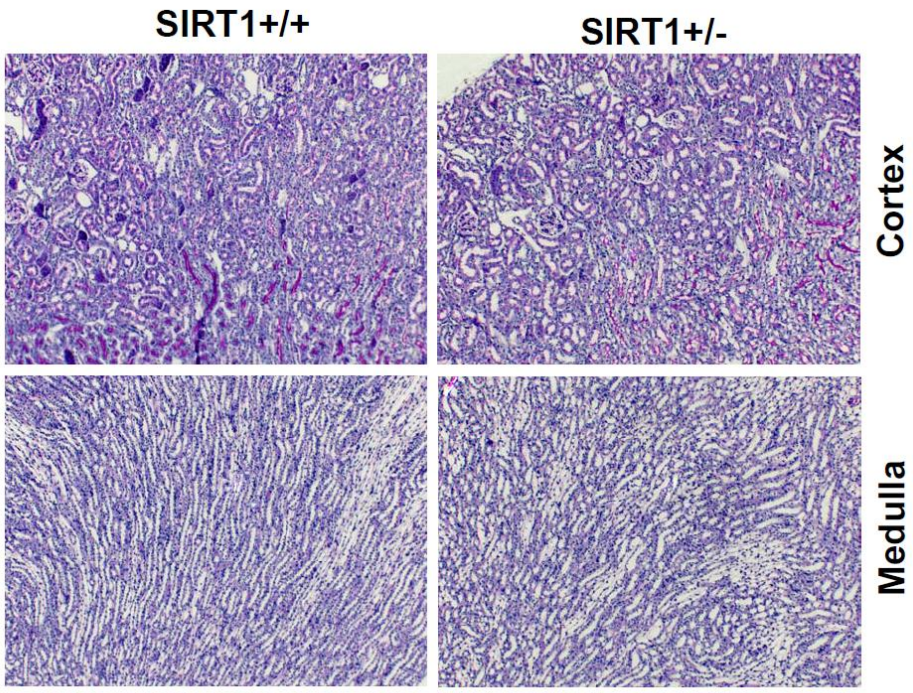

Figure 13. The kidney of heterozygous SIRT1 knockout mice develops normally. Representative pictures of PAS staining showing the histology of the renal cortex and renal medulla from wild type mice (SIRT1+/+) and heterozygous SIRT1 knockout mice (SIRT1+/-) (200X).

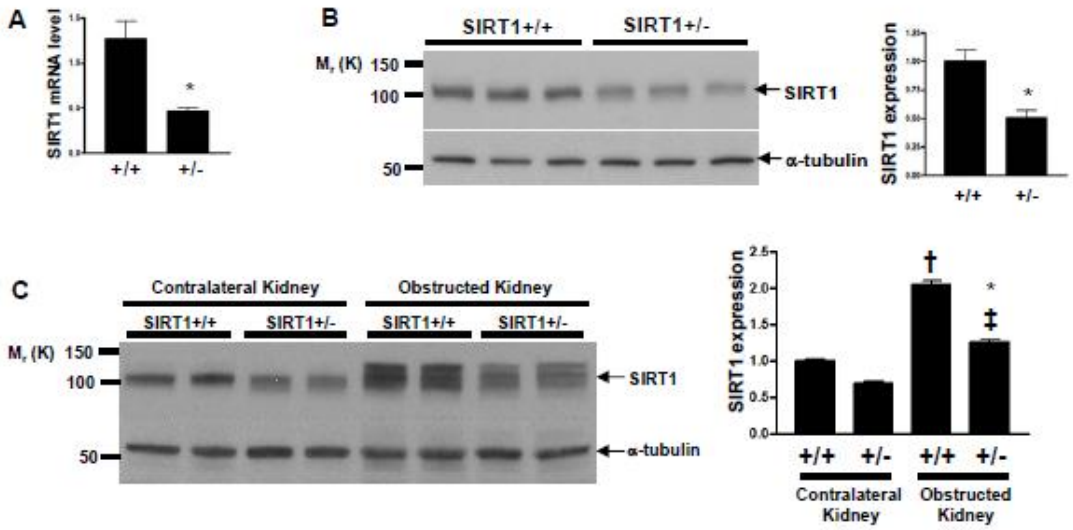

Figure 14. Reduced SIRT1 expression in the kidney of heterozygous SIRT1 knockout mice. (A) Relative SIRT1 mRNA expression level in the entire kidney of wild type mice (SIRT1+/+) and heterozygous SIRT1 knockout mice (SIRT1+/-) was examined by qRT-PCR (n=4, *P<0.01). **(B)** SIRT1 protein expression level in the entire kidney of SIRT1+/+ mice and SIRT1+/- mice was examined by immunoblot (n=6, densitometry, *P<0.05). **(C)** SIRT1 expression in the entire kidney of SIRT1+/+ mice and SIRT1+/- mice following 3 days unilateral ureteral obstruction (UUO) was examined by immunoblot (n=4, densitometry, †P<0.0001 versus contralateral kidney of SIRT1+/+ mice, ‡P<0.0001 versus contralateral kidney of SIRT1+/- mice, *P<0.001 versus obstructed kidney of SIRT1+/+ mice).

Renal cell apoptosis was predominantly seen in the renal medulla of mice following UUO (3d) as assessed by TUNEL. TUNEL-positive apoptosis was significantly greater in the renal medulla of SIRT1+/- mice than that of SIRT+/+ mice (Figure 15A, $P<0.05$). Increased apoptosis in the obstructed kidney of SIRT1+/- mice was further confirmed by higher levels of cleaved caspase-3 expression when compared to SIRT1+/+ mice (Figure 15B, $P<0.01$). Following 7 days UUO, sirius red staining, a marker of collagen, was greater in the obstructed kidney of SIRT1+/- mice versus SIRT1+/+ mice (Figure 15C, $P<0.05$). This result was confirmed by higher levels of type I collagen expression in the obstructed kidney of SIRT1+/- mice (Figure 15D, $P<0.05$). Thus SIRT1 deficiency increases renal apoptosis and fibrosis following UUO injury.

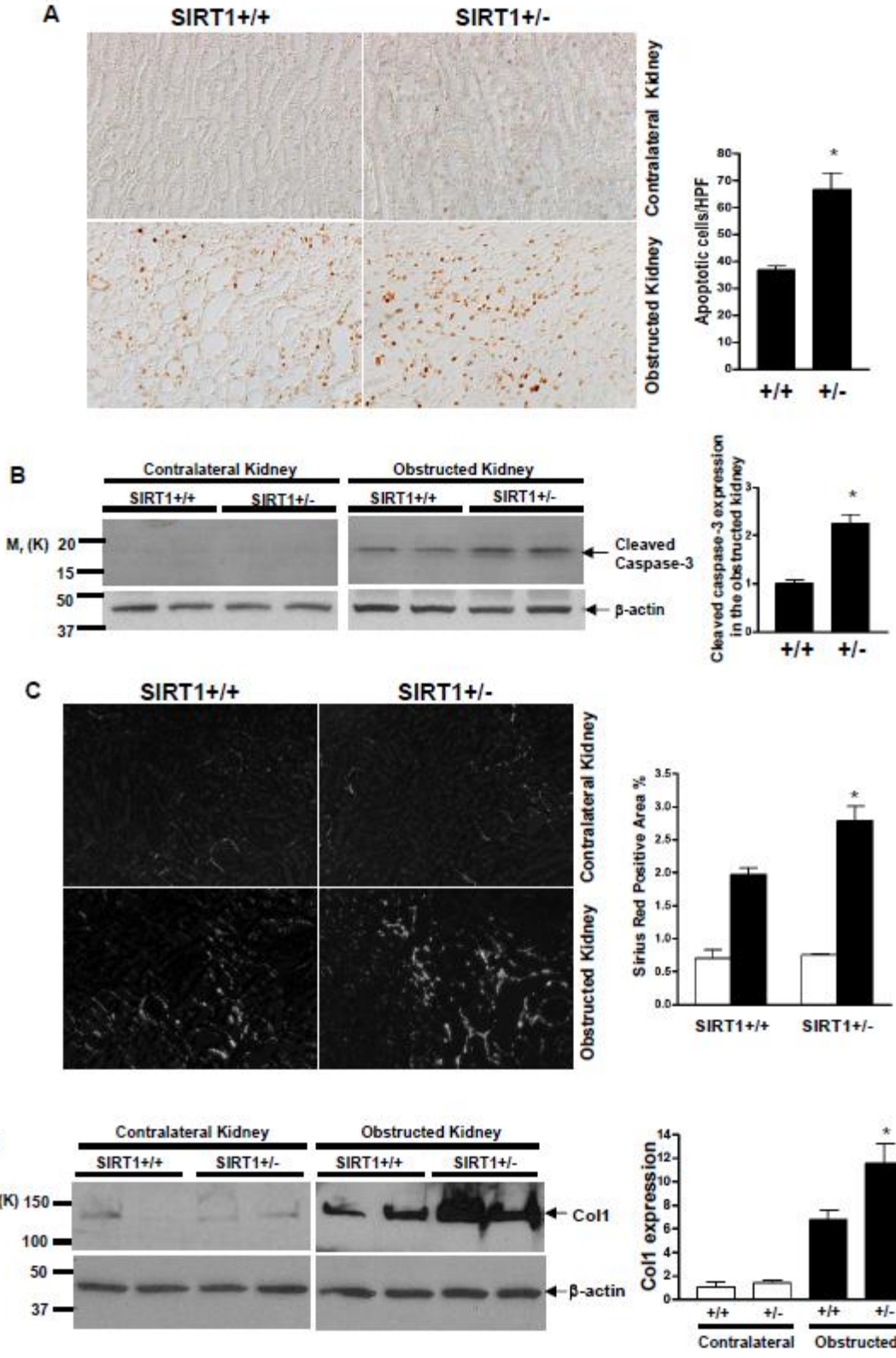
A
SIRT1+/+
SIRT1+/-
Contralateral Kidney
Obstructed Kidney
Apoptotic cells/HPF
+/+
+/-
B
Contralateral Kidney
Obstructed Kidney
SIRT1+/+
SIRT1+/-
M, (K) 20
15
50
37
Cleaved Caspase-3
β-actin
Cleaved caspase-3 expression in the obstructed kidney
C
SIRT1+/+
SIRT1+/-
Contralateral Kidney
Obstructed Kidney
Sirius Red Positive Area %
D
Contralateral Kidney
Obstructed Kidney
M, (K) 150
100
50
37
Col1
β-actin
Col1 expression
Contralateral
Obstructed

Figure 15. SIRT1 deficiency is associated with increased apoptosis and fibrosis in ureteral obstructed kidney. (A) Representative pictures (200X) and quantification of TUNEL-positive apoptosis in the renal medulla of SIRT1+/+ mice and SIRT1+/- mice following 3 days UUO (*P<0.05). **(B)** Immunoblot for the apoptosis marker cleaved caspase-3 expression in the entire kidney of SIRT1+/+ mice and SIRT1+/- mice following 3 days UUO (n=4, densitometry, *P<0.01 versus SIRT1+/+ mice). **(C)** Representative pictures (200X) and quantification of sirius red staining on kidney sections of SIRT1+/+ mice and SIRT1+/- mice following 7 days UUO (*P<0.05 versus obstructed kidney of SIRT1+/+ mice). **(D)** Levels of type I collagen (Col1) protein expression in the entire kidney of SIRT1+/+ and SIRT1+/- mice following 7 days UUO were assessed by immunoblot (n=5, densitometry, *P<0.05 versus obstructed kidney of SIRT1+/+ mice). (open bar: contralateral kidney; filled bar: obstructed kidney).

SIRT1 activation reduces UUO injury induced apoptosis and fibrosis. In contrast to SIRT1 deficiency, treatment of wild type mice with the SIRT1 activator SRT1720 (100mg/kg/d) significantly reduced TUNEL-positive apoptosis in the medulla of the obstructed kidney following UUO (3d) (Figure 16A, $P<0.05$). Reduced apoptosis was further confirmed by reduced cleaved caspase-3 expression in the obstructed kidney of SRT1720-treated mice versus vehicle-treated mice (Figure 16B, $P<0.0001$). Furthermore, SRT1720 treatment significantly reduced sirius red staining (Figure 16C, $P<0.05$) and type I collagen (Col1) expression in the obstructed kidney following UUO (7d) (Figure 16D, $P<0.05$). Thus increasing SIRT1 activity decreases renal apoptosis and fibrosis following UUO injury, suggesting a protective role of SIRT1 in the obstructed kidney.

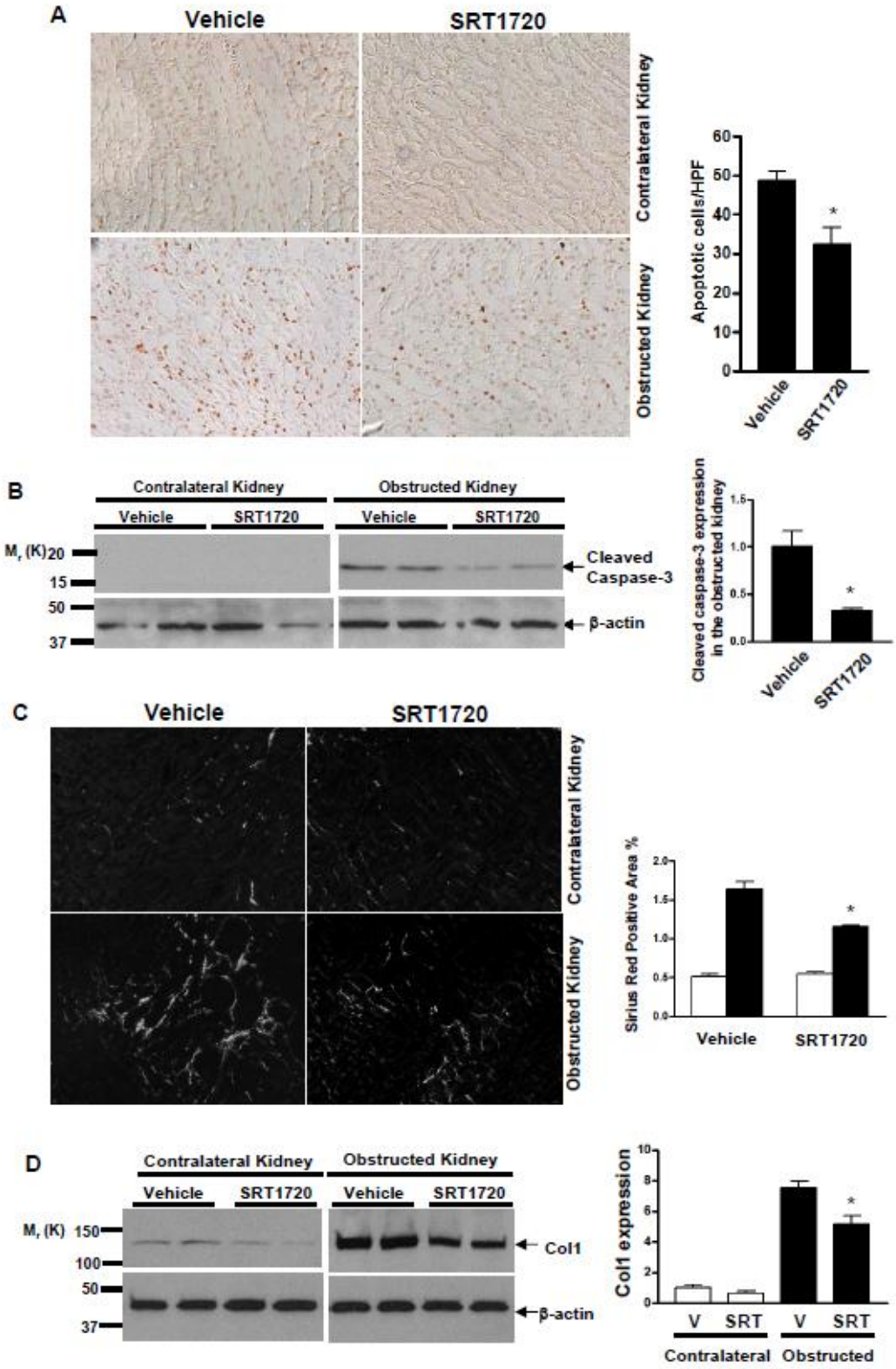
A
Vehicle
SRT1720
Contralateral Kidney
Obstructed Kidney
Apoptotic cells/HPF
60
50
40
30
20
10
0
*
Vehicle
SRT1720
B
Contralateral Kidney
Obstructed Kidney
Vehicle
SRT1720
Vehicle
SRT1720
M, (K) 20
15
50
37
Cleaved Caspase-3
β-actin
Cleaved caspase-3 expression in the obstructed kidney
1.5
1.0
0.5
0.0
*
Vehicle
SRT1720
C
Vehicle
SRT1720
Contralateral Kidney
Obstructed Kidney
Sirius Red Positive Area %
2.0
1.5
1.0
0.5
0.0
*
Vehicle
SRT1720
D
Contralateral Kidney
Obstructed Kidney
Vehicle
SRT1720
Vehicle
SRT1720
M, (K) 150
100
50
37
Col1
β-actin
Col1 expression
10
8
6
4
2
0
*
V
SRT
V
SRT
Contralateral
Obstructed

Figure 16. SIRT1 activation is associated with reduced apoptosis and fibrosis in ureteral obstructed kidney. (A) Representative pictures (200X) and quantification of TUNEL-positive apoptosis in the renal medulla of vehicle-treated or SIRT1 activator SRT1720 (100mg/kg/d)-treated wild type mice following 3 days UUO (*P<0.05). **(B)** Immunoblot for cleaved caspase-3 expression in the entire kidney of vehicle-treated or SRT1720-treated wild type mice following 3 days UUO (n=4, densitometry, *P<0.0001 versus obstructed kidney of vehicle-treated mice). **(C)** Representative pictures (200X) and quantification of sirius red staining on kidney sections of vehicle-treated or SRT1720-treated mice following 7 days UUO (*P<0.05 versus obstructed kidney of vehicle-treated mice). **(D)** Levels of type I collagen (Col1) protein expression in the entire kidney of vehicle-treated or SRT1720-treated wild type mice following 7 days UUO were assessed by immunoblot (n=5, densitometry, *P<0.05 versus obstructed kidney of vehicle-treated mice). (open bar: contralateral kidney; filled bar: obstructed kidney).

Discussion

The present studies demonstrate that the stress responsive protein SIRT1 is preferentially expressed in the renal inner medulla including medullary interstitial cells. SIRT1 deficiency accentuates renal medullary cell apoptosis and renal fibrosis and conversely SIRT1 activation promotes the resistance of renal medullary cells to oxidative stress both in vitro and in vivo. These results therefore suggest that targeting SIRT1 with pharmacological activators might improve renal function in conditions that induce oxidative stress in renal medulla including ureteral obstruction. It remains to be determined if SIRT1 activation also protects renal cell viability in other types of kidney diseases including diabetic nephropathy and/or hypertensive nephropathy.

Anti-oxidant function of SIRT1 has previously been reported in other organs such as the heart, neurons and pancreatic β cells (83, 85-86). In the kidney, we found that SIRT1 is abundantly expressed in the interstitial cells of renal inner medulla, where it also plays a critical role against excessive oxidative stress. This result is consistent with the observation that there are high levels of oxidative markers under physiological conditions in the renal inner medullary interstitium (Figure 5 in Chapter I). Multiple unique features of renal medullary interstitium are known to contribute to excessive oxidative stress including low blood flow and oxygen tension, high osmotic stress due to high concentrations of sodium chloride and urea (18, 112). Besides oxidative stress, high concentrations of ammonia and pH changes in the renal medullary interstitium may also

compromise cell viability (113). Whether the cytoprotective effect of SIRT1 activity in the renal medullary interstitial cells is limited to oxidative stress remains to be investigated. The present study also shows SIRT1 expression in some renal inner medullary collecting duct cells in vivo. Whether SIRT1 exerts anti-oxidant function in these cells was not determined. Nonetheless, a physiological role for SIRT1 in regulating the epithelial Na^+ channel α-subunit (α-ENaC) expression has been reported in cultured renal inner medullary collecting duct cells (93). However, its relevance to the in vivo condition is to be investigated. Furthermore, increased oxidative stress and phenotypic changes have been reported in aging kidneys (21, 114-115). Given the reported anti-stress and anti-aging nature of SIRT1 function (57, 83, 116-117), targeting SIRT1 by SIRT1 activators may have therapeutic potentials to protect the kidney from developing age related renal diseases.

SIRT1 responds to UUO injury as SIRT1 protein expression is induced in the kidney following ureteral obstruction (Figure 14C). Higher shifted bands recognized by anti-SIRT1 antibody are present in the obstructed kidney, which is consistent with the possibility of protein modification of SIRT1 (118-119). Distribution of SIRT1 in the obstructed kidneys remains similar to normal kidneys, with preferential expression in renal inner medulla (Figure 17). Abundant SIRT1 expression is still present in the interstitial cells of the inner medulla. In addition, elevated SIRT1 immunoreactivity appears in both renal cortical and medullary cells. Whether this reflects potential stress-responsive functions of SIRT1 in other renal cell types besides renal medullary interstitial cells remains uncertain.

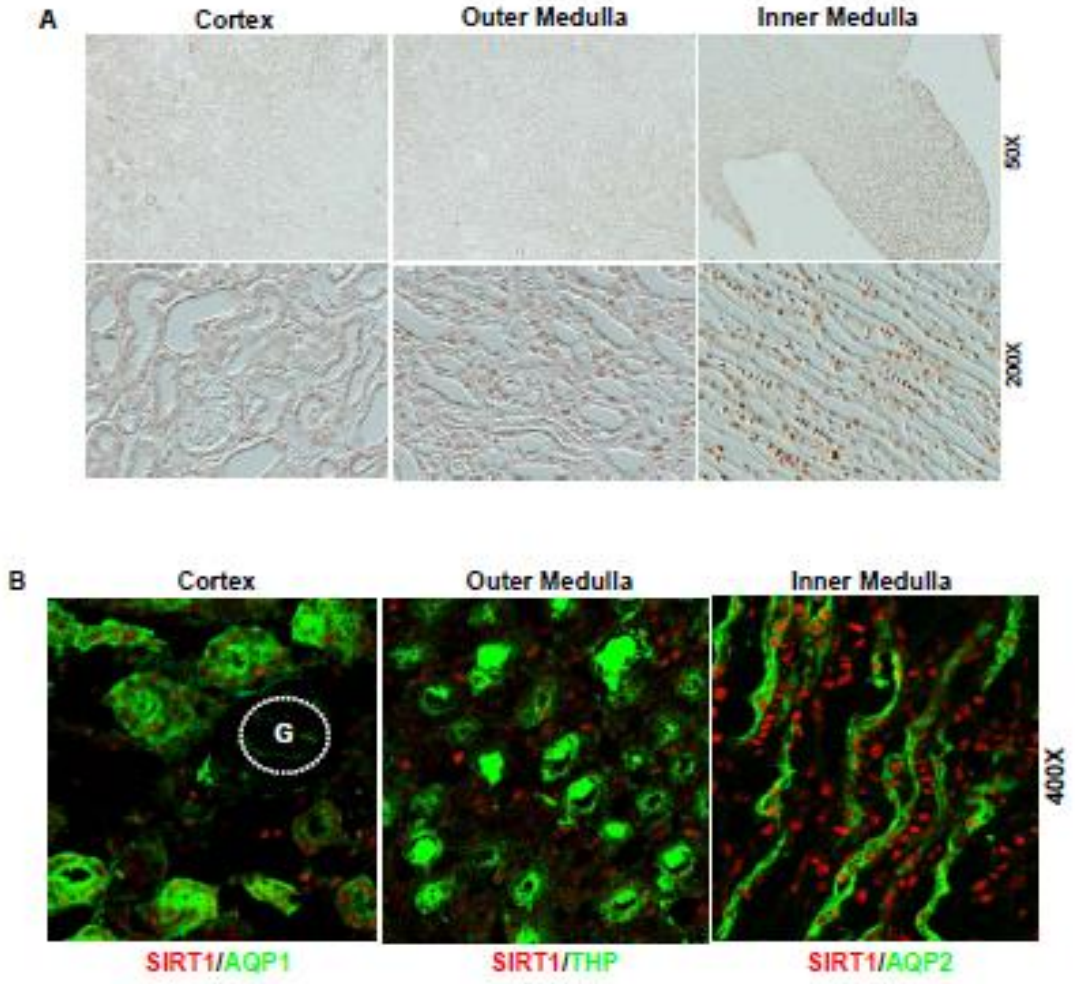

Figure 17. SIRT1 expression in the ureteral obstructed kidney. (A) Immunohistochemistry for SIRT1 expression in the obstructed kidney following 3 days UUO. **(B)** Immunofluorescent costaining for SIRT1 (red) and renal segmental markers (green) in the obstructed kidney: AQP1 (proximal tubule marker), THP (thick ascending limb marker), AQP2 (collecting duct marker). (G: glomerulus).

The present findings are consistent with a beneficial role for SIRT1 in protecting the kidney from fibrosis, supporting previous studies showing an anti-fibrotic effect of resveratrol (120-122). Although the detailed mechanisms of renal fibrosis following ureteral obstruction are still incompletely understood, fibrosis appears to be a maladaptive response to injury. If apoptosis and loss of resident renal medullary cells are considered as primary injury following UUO, reduced apoptosis and loss of resident renal medullary cells by SIRT1 activity may consequently result in a reduced fibrotic response. In addition, the present observations that activation of SIRT1 promotes renal medullary interstitial cell viability and that SIRT1 activity reduces renal fibrosis following UUO injury further implies that renal medullary interstitial cells actively protected by SIRT1 are probably not the cells contributing to fibrosis. Other cell populations such as type 3 medullary interstitial cells (perivascular pericytes) or infiltrating circulating cells may transform into fibroblasts.

In summary, the renal medullary environment is characterized by high oxidative stress. As the renal medulla is critical for the renal regulation of water and sodium balance as well as maintenance of normal blood pressure, maintaining robust anti-oxidant mechanisms in the renal medulla is of great importance. My work supports an important role of SIRT1 activity, which is tightly modulated by oxidative metabolism, in protecting renal medullary interstitial cells in the setting of oxidative stress. Recently specific and potent small molecule SIRT1 activators show therapeutic efficacy in alleviating symptoms in metabolic syndrome and neurodegenerative diseases. Targeting SIRT1 with SIRT1 activators may also be

a potential therapeutic strategy for minimizing or preventing renal damage or fibrosis resulting from increased oxidative stress. Such conditions include metabolic syndrome and aging.

CHAPTER IV

THE ANTI-OXIDANT ACTIVITY OF SIRT1 IS PARTIALLY MEDIATED THROUGH INCREASING COX2 EXPRESSION

Introduction

In Chapter III, my work demonstrated that SIRT1 immunoreactive proteins are preferentially expressed in the mouse inner renal medulla, especially renal medullary interstitial cells. Both in vitro studies using primary cultured mouse renal medullary interstitial cells and in vivo studies using unilateral ureteral obstruction (UUO) model demonstrated an essential anti-oxidant activity of SIRT1 in the renal medullary interstitial cells. SIRT1 is known to regulate cellular response to oxidative stress via modulating the expression and/or activity of the cell cycle control protein FOXO, the DNA damage repair protein Ku70 and proteins involved in apoptosis, p53 and E2F1 in a tissue or cell type specific manner (123). However, the molecular mechanism by which SIRT1 exerts cytoprotective functions in renal medullary cells is to be investigated.

Renal medulla is a major site of prostaglandin synthesis. Prostaglandin signaling is known to protect multiple organs and tissues such as the liver, kidney, retina and neurons against injury of diverse causes (124-128). An important role of COX2 in protecting the renal medullary interstitial cells from apoptosis in hypertonic stress challenged cultured cells and in water-deprived animals has

been reported (19, 29-30, 129) (130) (24). Interestingly, several transcription factors that are important regulators of COX2 gene expression have also been demonstrated to be deacetylase substrates of SIRT1. These transcription factors include NFκB and p53 (19) (74-75, 131-132) (19, 133).

To further explore the underlying mechanisms by which SIRT1 exerts potent anti-oxidant function in renal medulla, we set out to examine the potential interaction of SIRT1 and COX2, the two important survival factors that are co-localized in the renal medullary interstitial cells.

Results

SIRT1 regulates renal medullary interstitial cell COX2 expression in vitro. SIRT1 co-localizes with COX2 in renal medullary interstitial cells and COX2 activity is an important survival factor in renal medullary interstitial cells (25, 30, 129). To further explore the mechanism by which SIRT1 activation protects RMIC from injury, we examined whether SIRT1 activity promotes expression of COX2 in RMIC. RMIC COX2 protein and mRNA expression was significantly increased by H_2O_2 (500μM, 6h) (Figure 18A and 18B). H_2O_2-induced COX2 protein expression was nearly completely abolished by SIRT1 shRNA (Figure 18A). SIRT1 shRNA also dramatically reduced H_2O_2-induced COX2 mRNA expression (Figure 18B, $P<0.0001$).

Moreover, treatment of RMIC with the SIRT1 activator SRT2183 increased COX2 expression in a dose dependent manner (Figure 18C). In contrast, neither H_2O_2 nor down-regulation of SIRT1 altered COX1 expression (Figure 18A), and SIRT1 activator did not induce COX1 expression (data not shown), supporting a specific effect of SIRT1 on COX2 expression. Furthermore, induction of COX2 by hypertonic stress was not affected by down-regulation of SIRT1 (Figure 18D), suggesting that SIRT1 is specifically involved in the COX2 response to oxidative stress.

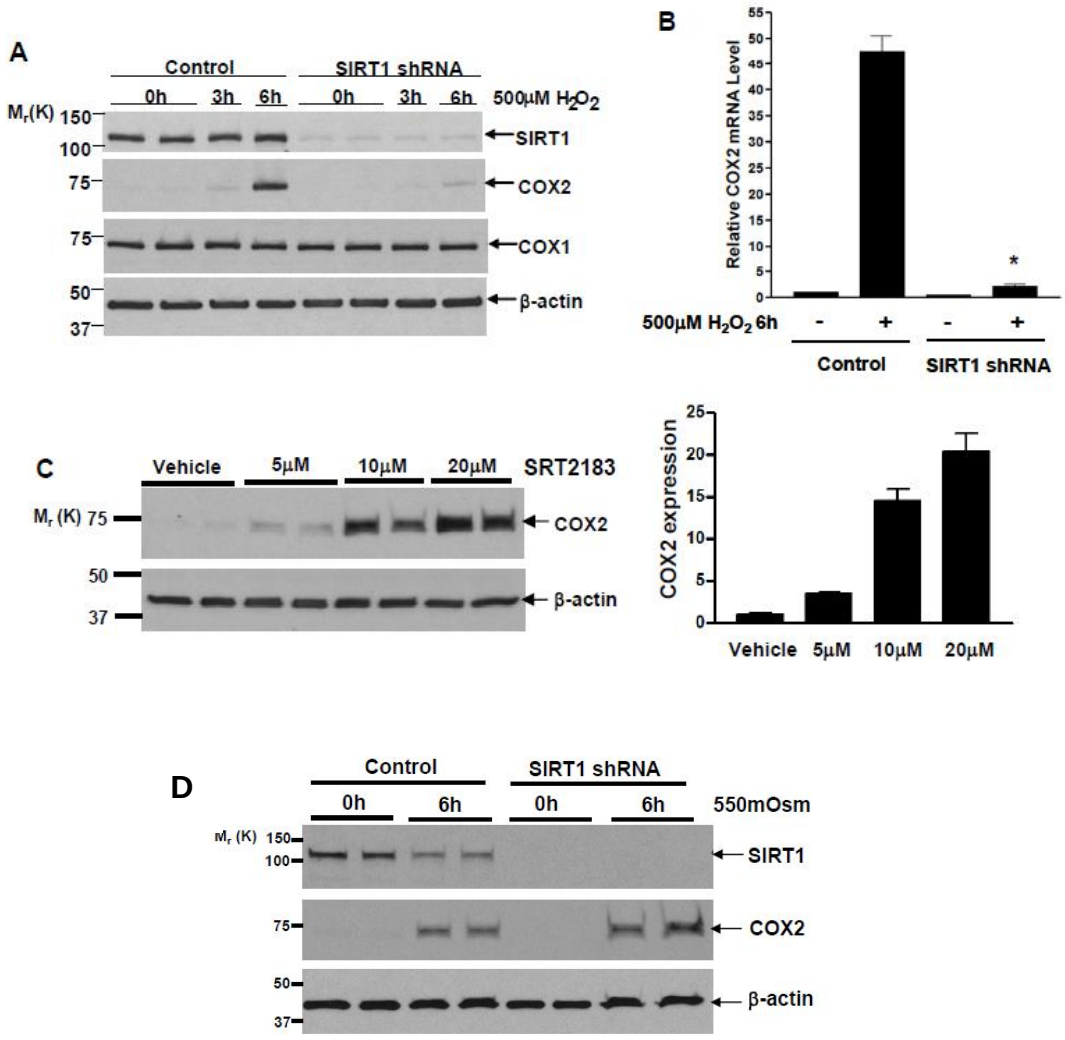

Figure 18. SIRT1 regulates COX2 expression in cultured renal medullary interstitial cells. (A) Wild type or SIRT1 knockdown cultured RMIC were challenged with H_2O_2 (500μM) for 0, 3 or 6 hours. SIRT1, COX2 and COX1 expression were examined by immunoblot. **(B)** Wild type or SIRT1 knockdown RMIC were challenged with H_2O_2 (500μM) for 0 or 6 hours. COX2 mRNA expression was assessed by qRT-PCR (n=4, *P<0.0001 versus wild type cells with H_2O_2). **(C)** RMIC were treated with SIRT1 activator SRT2183 (0, 5, 10, 20μM) for 8 hours, and COX2 expression was examined by immunoblot (n=4). **(D)** Wild type or SIRT1 knockdown cultured RMIC were challenged with hypertonic stress (550mosm) for 0 or 6 hours. SIRT1 and COX2 expression were examined by immunoblot.

SIRT1 activity appears to regulate cultured RMIC COX2 expression at the transcriptional level, since SIRT1 shRNA significantly blunted H_2O_2 (250μM, 12h)-induced COX2 luciferase reporter activation (Figure 19A, $P<0.0001$). To determine whether SIRT1 physically associates with the COX2 promoter, a chromatin immunoprecipitation (ChIP) assay was performed on H_2O_2-treated RMIC. The presence of sequence from the mouse COX2 promoter region (5' sequence -712 to -396) in the DNAs immunoprecipitated with SIRT1 antibody was confirmed by PCR (Figure 19B). SIRT1 associated COX2 promoter sequence was detected in both non-treated cells and H_2O_2-treated cells, suggesting that SIRT1 may be associated in a transcriptional complex on the COX2 promoter region. In contrast, PCR using primers recognizing a random DNA sequence about 4,000 bp upstream of COX2 gene transcription start site, showed no bands, supporting the specificity of the association of SIRT1 with COX2 promoter region. As a negative control, immunoprecipitation with normal rabbit IgG also showed no bands.

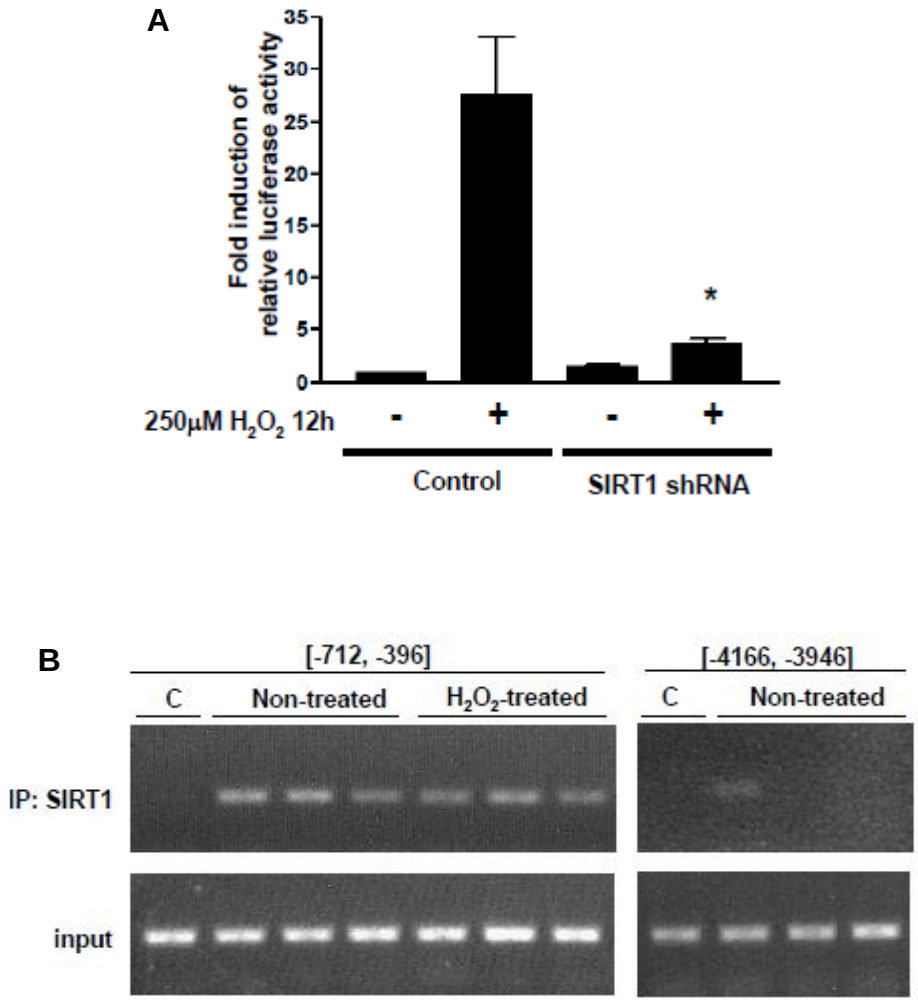

Figure 19. SIRT1 regulates COX2 gene expression at its transcriptional level. (A) COX2 luciferase reporter activity was measured in wild type or SIRT1 knockdown RMIC with H_2O_2 (250μM) for 0 or 12 hours by using dual luciferase assay kit. (n=12, *P<0.0001 versus wild type cells with H_2O_2). **(B)** ChIP assay was performed on non-treated or H_2O_2 (500μM, 3 hours)-treated RMIC using anti-SIRT1 antibody and PCR primers recognizing mouse COX2 5' sequences upstream of the transcription start site [-712, -396] or [-4166,-3946]. (C: immunoprecipitation with normal rabbit IgG). Data are representative of three independent experiments.

SIRT1 regulates renal medullary interstitial cell COX2 expression in vivo

Since SIRT1 activity regulates COX2 expression in vitro, we further investigated the role of SIRT1 in regulating renal COX2 expression in vivo. Abundant COX2 induction (red) was observed primarily in the renal medulla of the obstructed kidney, but not in the contralateral kidney (Figure 20A). Co-staining confirmed COX2 expression (red) in renal medullary interstitial cells between AQP2 (green) stained collecting ducts (Figure 20A, right panel). Deletion of one allele of SIRT1 gene significantly reduced COX2 induction in the obstructed kidney following UUO (3d) (Figure 20B, $P<0.05$). Furthermore, treatment of wild type mice with the SIRT1 activator SRT1720 (100mg/kg/d) markedly induced COX2 expression (red) predominantly in the renal medullary interstitial cells between AQP2 (green) stained collecting ducts (Figure 20C). This result was further confirmed by increased renal COX2 expression in SRT1720-treated mice versus vehicle-treated mice as assessed by immunoblot (Figure 20D, $P<0.05$). Taken together, these in vivo observations are consistent with the in vitro results, and support an important role for SIRT1 to increase COX2 expression in renal medullary interstitial cells.

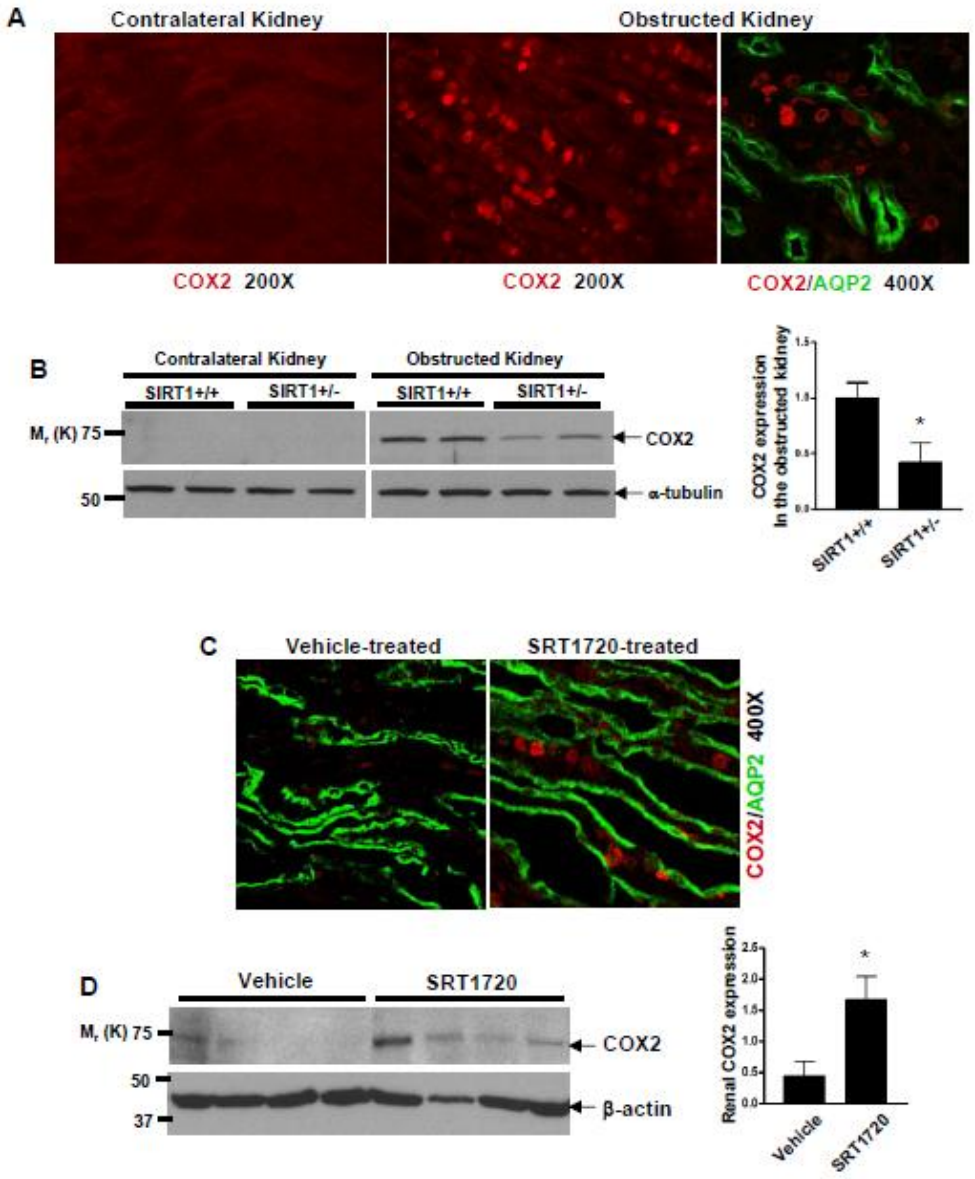

Figure 20. SIRT1 regulates COX2 expression in renal medullary interstitial cells in vivo. (A) Representative immunofluorescent pictures show COX2 induction (red) in the renal medulla of the obstructed kidney of wild type mice following 3 days UUO. Co-staining further shows induced COX2 (red) in renal medullary interstitial cells between AQP2 (green)-positive collecting ducts (right panel). **(B)** Immunoblot for COX2 expression in the entire kidney of SIRT1+/+ mice and SIRT1+/- mice following 3 days UUO (n=5, densitometry, *P<0.05 versus obstructed kidney of SIRT1+/+ mice). **(C)** Wild type mice were treated with vehicle or SIRT1 activator SRT1720 (100mg/kg/d) for 5 days. Immunofluorescent co-staining shows that SRT1720 induces COX2 expression (red) in renal medullary interstitial cells between AQP2 (green)-positive collecting ducts. **(D)** COX2 expression in the entire kidney of vehicle or SRT1720-treated mice was examined by immunoblot (n=4, densitometry, *P<0.05 versus vehicle-treated mice).

COX2 derived PGE2 protects cultured renal medullary interstitial cells from oxidative stress The ability of RMIC to tolerate H_2O_2 is dependent on COX2 activity, since COX2 inhibition with SC58236 (2.5μM) reduced cell viability from 60±9% to 30±6% (Figure 21A, P<0.0001). Reduced cell resistance to oxidative stress by COX2 inhibition was further confirmed as increased H_2O_2-induced TUNEL-positive apoptosis was observed in RMIC treated with SC58236 (2.5μM) (Figure 21C, P<0.001). Conversely, pre-incubation of RMIC with the COX2 derived arachidonic metabolite prostaglandin E2 (PGE2) (100nM or 1μM) dose dependently restored viability of SIRT1-deficient RMIC exposed to H_2O_2 (Figure 21B, 69±6%, 82±9% versus 43±5%, P<0.05). TUNEL assay (Figure 21D, P<0.05) and immunoblot for cleaved caspase-3 expression (Figure 21E, P<0.05) further showed reduced H_2O_2-induced apoptosis in SIRT1-deficient RMIC treated with PGE2 (100nM). Taken together, these observations support SIRT1-dependent COX2 induction as an important anti-oxidant mechanism in the renal medullary interstitial cells.

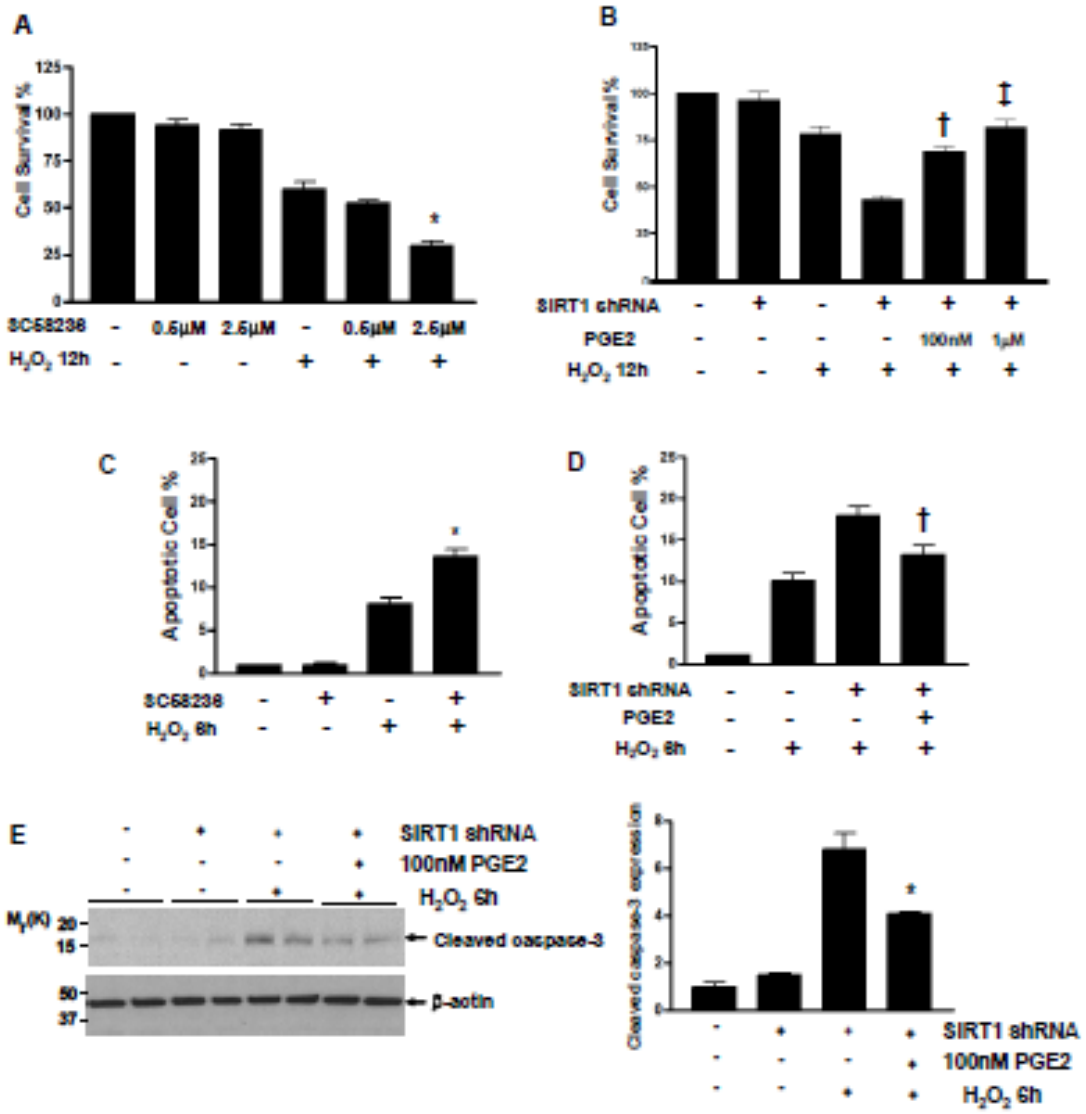

Figure 21. COX2 activity and its derived PGE2 protect cultured renal medullary interstitial cells from oxidative stress. (A, B) Wild type or SIRT1 knockdown cultured RMIC were pretreated with COX2 selective inhibitor SC58236 (0.5μM, 2.5μM) or PGE2 (100nM, 1μM) and challenged with H_2O_2 (250μM) for 12 hours. Cell viability was examined by crystal violet staining (n=6, *P<0.0001 versus cells with H_2O_2 alone, †P<0.0001 versus SIRT1 knockdown cells with H_2O_2 without PGE2, ‡P<0.05 versus SIRT1 knockdown cells with H_2O_2 and 100nM PGE2). **(C, D)** Wild type or SIRT1 knockdown RMIC were pretreated with SC58236 (2.5μM) or PGE2 (100nM) and challenged with H_2O_2 (500μM) for 6 hours. Cell apoptosis was examined by TUNEL assay (n=15, *P<0.001 versus cells with H_2O_2 alone, †P<0.05 versus SIRT1 knockdown cells with H_2O_2 without PGE2. **(E)** Wild type or SIRT1 knockdown RMIC were pretreated with 100nM PGE2 and challenged by H_2O_2 (500μM) for 6 hours. Cellular apoptosis marker, cleaved caspase-3 expression, was examined by immunoblot (n=4, densitometry, *P<0.05 versus SIRT1 knockdown cells with H_2O_2 without PGE2).

Discussion

COX2 is required for renal medullary interstitial cell survival against hypertonic stress. Interestingly, a stress defensive protein SIRT1 is also found preferentially expressed in the renal inner medulla including medullary interstitial cells. In this chapter, I was able to find data to support that these two essential survival factors COX2 and SIRT1 are uniquely linked in the renal medullary interstitial cells, and they together exert anti-oxidant functions. By showing that SIRT1 regulates COX2 induction in the setting of oxidative stress and that PGE2 rescues oxidative stress-induced apoptosis in SIRT1-deficient cells, the present study places COX2 induction and PGE2 production downstream of SIRT1 in the renal medullary interstitial cells in the setting of oxidative stress.

COX2 has been shown to be a pre-requisite for renal medullary interstitial cell survival from hypertonic stress (19, 25, 29, 129). Previous study by Hao and colleagues suggests that hypertonicity activates COX2-derived prostacyclin (PGI2) production, which promotes cell viability through PPARδ (29). The present study, however, identified a cytoprotective effect of PGE2 on renal medullary interstitial cells against oxidative stress. Protective effects of COX2 derived PGE2 have been reported in multiple organs and tissues such as the liver, kidney, retina and neurons against injury of diverse causes (124-128). The underlying molecular mechanisms involve an activation of PGE2 coupled cAMP-PKA or PI3K-Akt signaling pathways (128, 134-136). These kinases may therefore be responsible for the anti-apoptotic effect of COX2 derived PGE2

observed in my study in the setting of oxidative stress. Interestingly, RT-PCR analysis showed the presence of two PGE2 receptors EP1 and EP4 in the cultured renal medullary interstitial cells (Figure 22). Interestingly, the expression of EP4 mRNA dramatically increased following H_2O_2 treatment, implicating a potential role for EP4 receptor in response to oxidative stress.

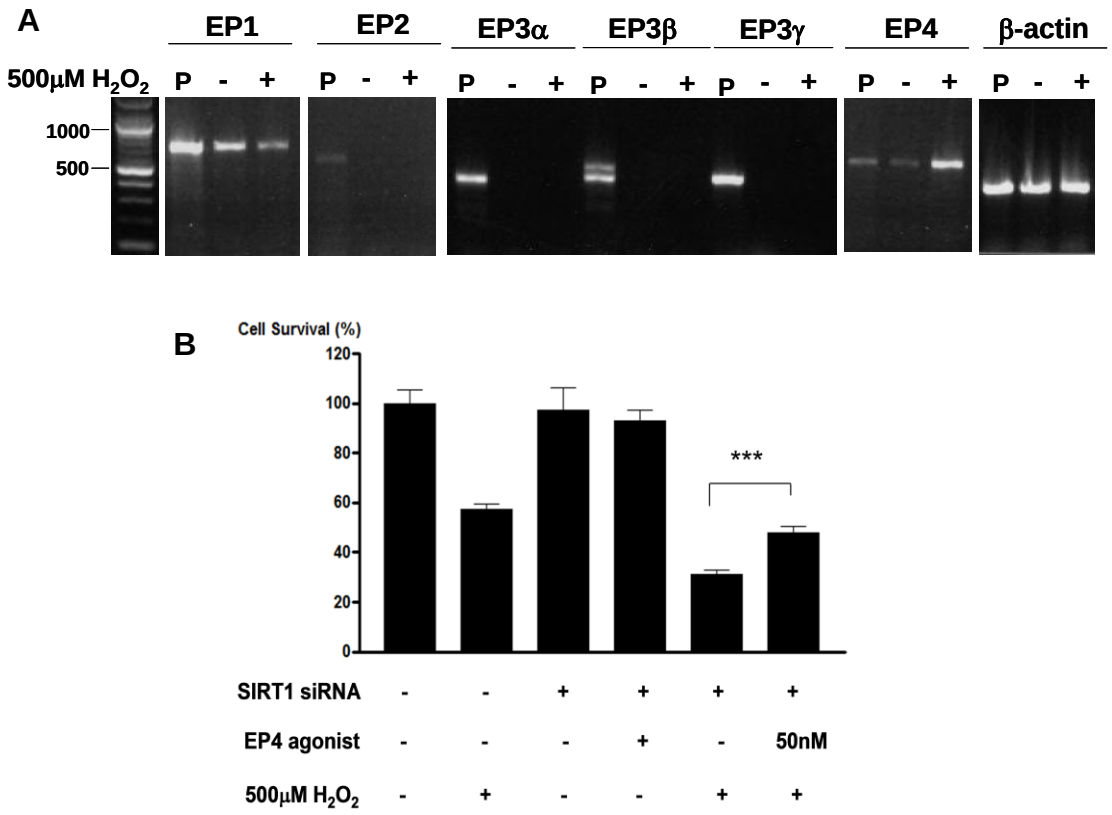

Figure 22. EP4 agonist protects cultured renal medullary interstitial cells from oxidative stress. (A) The expression of PGE2 receptors EP1-4 in the non-treated or 500μM H_2O_2 (6h)-treated cultured mouse renal medullary interstitial cells was examined by RT-PCR using specific primers. (P: positive control using RNA extracted from mouse renal medullary tissues). **(B)** Wild type or SIRT1 knockdown cultured RMIC were pretreated with EP4 agonist (50nM) and challenged with H_2O_2 (500μM) for 12 hours. Cell viability was examined by crystal violet staining (n=6, ***P<0.0001).

Given the fact that neither UUO injury nor the SIRT1 activator induces COX2 expression in renal medullary collecting duct cells in vivo, the SIRT1-dependent COX2 induction and PGE2 production may be a specific effect on renal medullary interstitial cells. Since prostaglandins can act through both autocrine and paracrine mechanisms, it is possible that SIRT1 in renal medullary interstitial cells may protect adjacent renal tubules and vessels through locally diffused PGE2. Different mechanisms are reported in cultured mesangial cells, where a cytoprotective role of SIRT1 against oxidative stress or TGF-β1 induced apoptosis is mediated via deacetylating p53 or Smad7 respectively (88) (89). However, whether SIRT1 interacts with these proteins in renal cells in vivo remains undetermined.

The present finding is supportive of a regulatory role of SIRT1 on COX2 expression at the transcriptional level. Since SIRT1 is a protein deacetylase, one possibility is that SIRT1 deacetylates and activates DNA-binding proteins in a transcriptional complex on COX2 gene promoter, thus leading to activation of the COX2 gene transcription. As SIRT1 knockdown suppressed the activation of the COX2 promoter-driven luciferase reporter in an exogenous plasmid (Figure 19A), SIRT1-regulated COX2 induction may be mediated through modification of transcription factors or co-factors. Several transcription factors and co-factors have been demonstrated to be deacetylase substrates of SIRT1 in a variety of tissues and cell types in a tissue and cell specific manner. These transcription factors or co-factors include NFκB, p53, FOXO, and PGC-1α (74-75, 131-132).

Notably NFκB and p53 have been implicated in the regulation of COX2 gene expression (19, 133) (137) (138). Unfortunately my preliminary studies were unable to detect direct effect of SIRT1 on NFκB or p53 in renal medullary interstitial cells.

To summarize, SIRT1 and COX2 are essential survival factors that are co-localized in the renal medullary interstitial cells. One of the mechanism by which SIRT1 exerts its cytoprotective role in the renal medulla is through increasing COX2 expression in the renal medullary interstitial cells. COX2 derived PGE2 may activate EP4 receptor, triggering downstream anti-apoptotic signaling pathways in the interstitial cells. Locally diffused PGE2 may also protect the adjacent renal tubular and vascular cells. However, the present study was unable to identify the molecular mechanism by which SIRT1 regulates COX2 expression. Further experiments are required to determine which molecule or molecules mediate the interaction between SIRT1 and the COX2 promoter in the renal medullary interstitial cells.

CHAPTER V

RENAL MEDULLARY INTERSTITAL COX2 IN THE REGULATION OF RENAL SODIUM EXCRETION AND BLOOD PRESSURE

Introduction

Besides playing a critical cytoprotective role, renal medullary COX2 participates in the regulation of sodium balance and blood pressure (45) (43) (44). COX inhibiting NSAID was associated with the development of edema, systemic hypertension or impaired blood pressure control in patients with preexisting salt sensitive hypertension (24). Furthermore, animal studies show that high salt diet increases renal medullary COX2 expression (41) (42), and that selective renal medullary COX2 inhibition via an intra-medullary infusion catheter significantly increases blood pressure in uninephrectomized rats on a high salt diet (43). This suggests an important role of renal medullary COX2 in renal response to sodium loading. However, the cellular location of COX2 induction in the renal medulla following high salt diet has not been clearly defined.

Nor is the signaling mechanism by which a high salt diet induces renal medullary COX2 expression fully established. The 5' flanking region of the COX2 gene possesses consensus sequences for several transcriptional factors, including CRE, NFκB and NF-IL6 (25). Regulation of COX2 gene expression by these transcription factors has been shown to be cell type and stressor specific.

Interestingly, an increase of tonicity has been reported in the renal medulla of mice on a high salt diet (139-140) (141), and in vitro studies have demonstrated that hypertonicity activated NFκB signaling is essential for COX2 induction in renal medullary interstitial cells (19), supporting a role for NFκB signaling in high salt diet induced COX2 expression in renal medulla. NFκB is a group of nuclear transcriptional factor that are normally sequestered in the cytoplasm of unstimulated cells as inactive homo- or heterodimers by a group of inhibitory proteins — IκBs. Phosphorylation of IκB by IKK leads to disassociation of IκB from NFκB and degradation of IκB, allowing translocation of NFκB into the nucleus and binding to DNA. Bortezomib, a NFκB inhibiting drug for treating multiple myeloma by acting as a proteasome inhibitor that inhibits the degradation of IκB and activation of NFκB, has been reported to cause edema in patients, consistent with a potential role of NFκB in regulating body sodium and fluid balance.

In this chapter, we examined renal medullary NFκB activity following a sodium loading as well as its role in renal medullary COX2 induction via two approaches: (1) use of transgenic NFκB reporter mice to determine the activation of NFκB as well as its cellular location; (2) use of an NFκB inhibitor IMD-0354 to examine whether NFκB is required for high salt diet induced medullary COX2 expression. Furthermore, whether global inhibition of COX2 activity by using selective COX2 inhibitor might cause sodium retention and hypertension in a high salt diet mouse model was also examined.

Results

High salt diet induces COX2 expression in renal medullary interstitial cells

Renal medullary COX2 expression was substantially increased after 2 days of high salt diet, and remained elevated throughout the study (Figure 23a and 23b). On the contrary, COX1 immunoreactive protein level was constitutively high, and not altered by high salt diet.

To examine the cellular location of COX2 expression in the renal medulla following high salt diet, in situ hybridization was performed. COX2 mRNA expression was primarily localized in the renal medulla (Figure 23c), specifically in renal medullary interstitium between renal tubules. COX1 mRNA was constitutively expressed in the renal medulla, but was detected primarily in the collecting ducts.

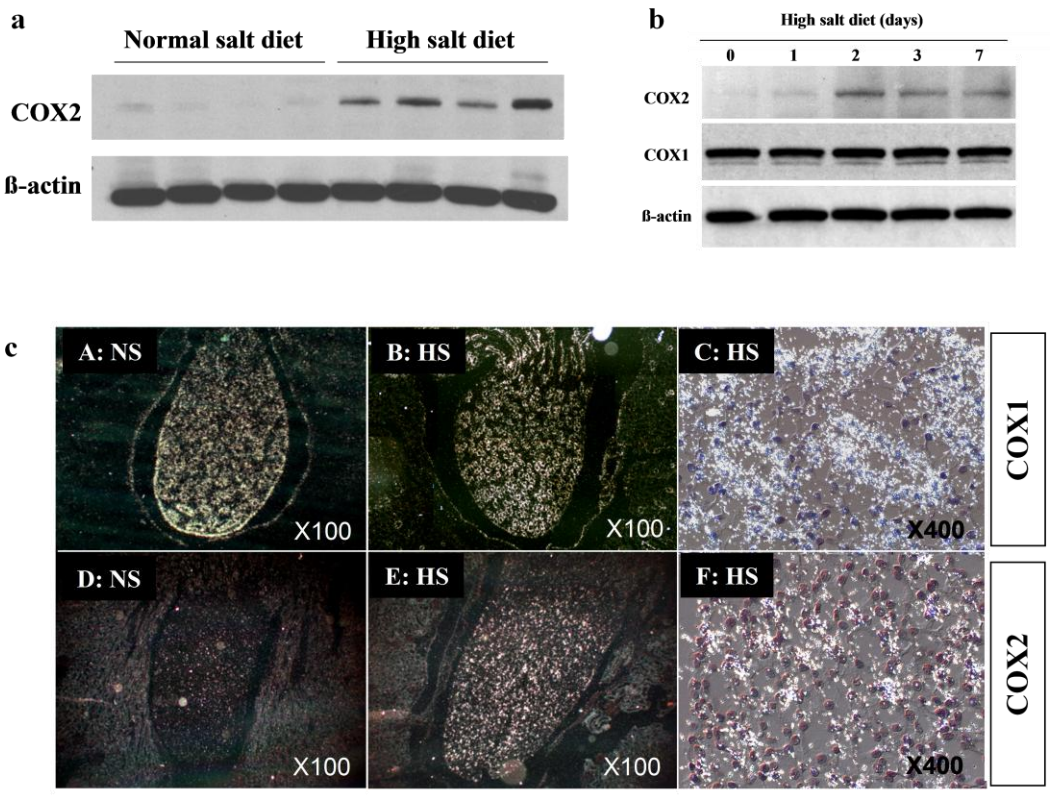

Figure 23. High salt diet increases renal medullary COX2 expression. (a) Immunoblotting was performed to examine the COX2 expression in the renal medullary tissues of C57Bl6/J mice fed with high salt diet (8% NaCl) or normal salt diet (0.4% NaCl) for 3 days. Expression of β-actin was also examined as a loading control. Each lane represents an individual mouse sample. **(b)** C57Bl/6J mice were fed with high salt diet for 0, 1, 2, 3 or 7 days. Renal medullary COX2 and COX1 protein expression was determined by immunoblotting. **(c)** In situ hybridization of COX1 (A, B, C) and COX2 (D, E, F) in the renal medulla of C57Bl6/J mice fed with normal salt diet (A, D) or high salt diet (B, C, E and F) for 5 days. (NS, normal salt diet; HS, high salt diet).

Cryostat sections from the kidneys of mice fed with high salt diet were examined by co-immunofluorescence staining using antibodies against COX2 and distinct cell markers for different structures in renal medulla: AQP2 for collecting duct, AQP1 for thin descending limb of Henle's loop, ClC-K channel for thin ascending limb of Henle's loop, CD31 for vasa recta, and Tam-Horsfall protein (THP) for thick ascending limb in outer medulla. Results revealed perinuclear localization of COX2 in the inner medullary cells that were arranged in rows, which are typical renal medullary interstitial cells (Figure 24). COX2 immunofluorescence did not co-localize with any of the cell markers used, suggesting that COX2 is localized exclusively in renal medullary interstitial cells. Additionally, COX2 induction was not observed in the renal outer medulla, as no COX2 immunofluorescence co-localized with THP at the same renal region.

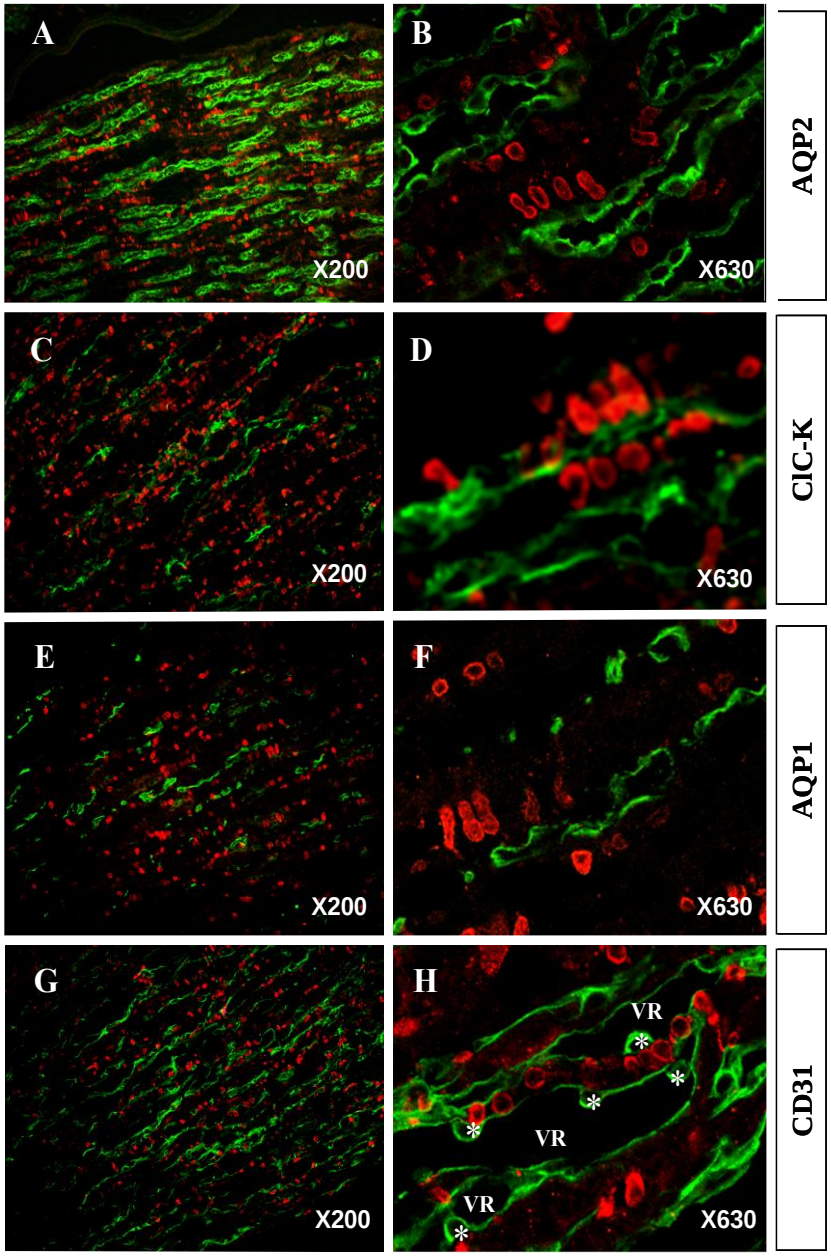

Figure 24. High salt diet induces COX2 expression in the renal medullary interstitial cells. C57Bl6/J mice were fed with high salt diet for 3 days. The cellular location of COX2 expression in the renal medulla was examined by co-immunofluorescence staining using the antibody against COX2 in red and different antibodies respectively against distinct structure markers in green: AQP2 for collecting duct (A and B); AQP1 for thin descending limb (E and F); ClC-K for thin ascending limb(C and D) and CD31 for vasa recta (G and H). (VR, vasa recta; * endothelial cell body)

High salt diet induces NFκB activation in renal medullary interstitial cells

To further investigate the molecular mechanisms that induces COX2 expression in renal medullary interstitial cells following a sodium loading, we examined if NFκB signaling was activated in the kidney of high salt diet fed mice. Transgenic mice carrying an NFκB response promoter driven a luciferase reporter were fed with normal salt diet or high salt diet for 3 days, and then sacrificed. High salt diet significantly increased luciferase reporter activity in the renal medulla by 7 fold compared to normal salt diet (Figure 25a, 3626±1045 vs 513±248 unit/mg protein, n=10, $P<0.05$), indicating that NFκB is activated in renal medulla following high salt diet.

To determine the cellular location of NFκB activation, cryostat sections of the kidneys from transgenic mice carrying an EGFP reporter driven by an NFκB response promoter either on normal salt diet or high salt diet were examined by immunofluorescence staining using anti-EGFP antibody. Strong EGFP immunofluorescence was only detected in mice fed with high salt diet, but not in mice on normal salt diet (Figure 25b). In addition, the EGFP expression was mainly localized in the renal medullary cells that were arranged in rows, which are typical renal medullary interstitial cells.

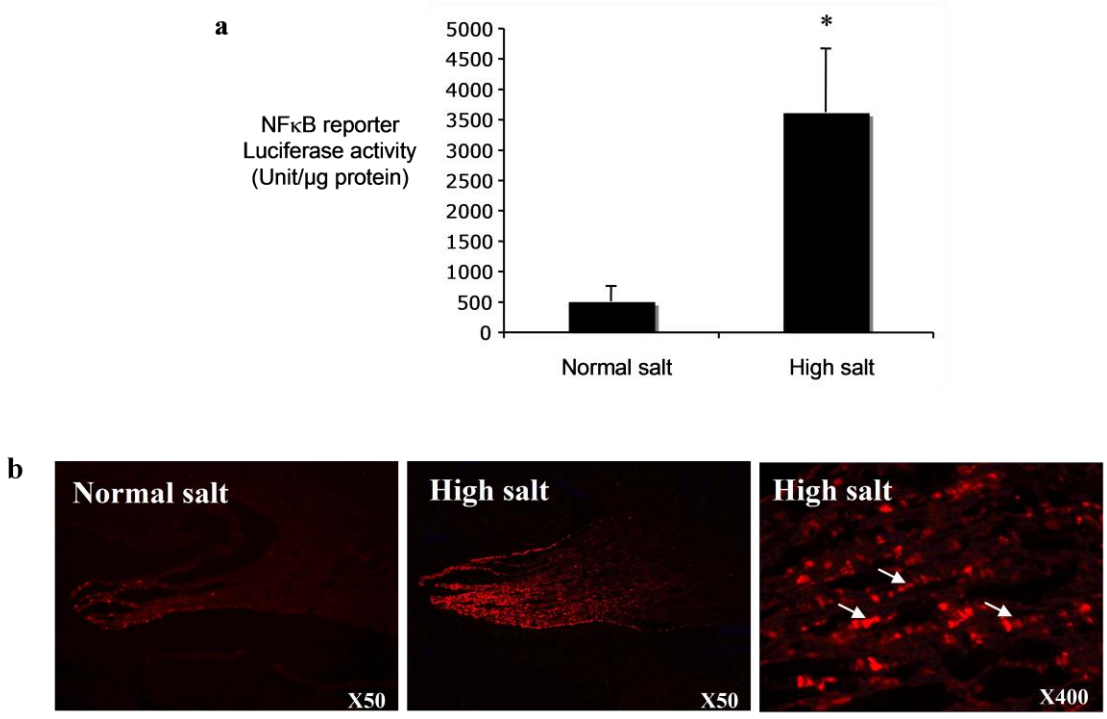

Figure 25. High salt diet activates NFκB in renal medullary interstitial cells. NFκB response promoter driven luciferase (a) or EGFP (b) reporter transgenic mice were fed with normal salt diet or high salt diet for 3 days. **(a)** Luciferase activity in the renal medulla was determined using the Promega luciferase assay kit to assess endogenous NFκB activity. Protein content was also measured by BCA protein assay for normalization (* $P<0.05$, n=15, student's t test). **(b)** The cellular location of NFκB activation was examined by immunofluorescence staining using the antibody against NFκB reporter EGFP. Arrows indicate the EGFP expressing cells that are arranged in rows, which are typical renal medullary interstitial cells.

NFκB activation is required for high salt diet induced renal medullary COX2 expression To find out whether NFκB mediates renal medullary COX2 induction following high salt diet in vivo, mice were treated with NFκB selective inhibitor IMD-0354 to block NFκB activation. Treatment with the NFκB inhibitor IMD-0354 significantly attenuated COX2 induction following high salt diet (Figure 26a), suggesting that NFκB activation is essential for renal medullary COX2 induction. Consistently, the NFκB inhibitor also significantly reduced high salt induction of urinary PGE_2 production following high salt diet (Figure 26b, 809±267 vs 1798±578 pg/24h, n=3, $P<0.05$).

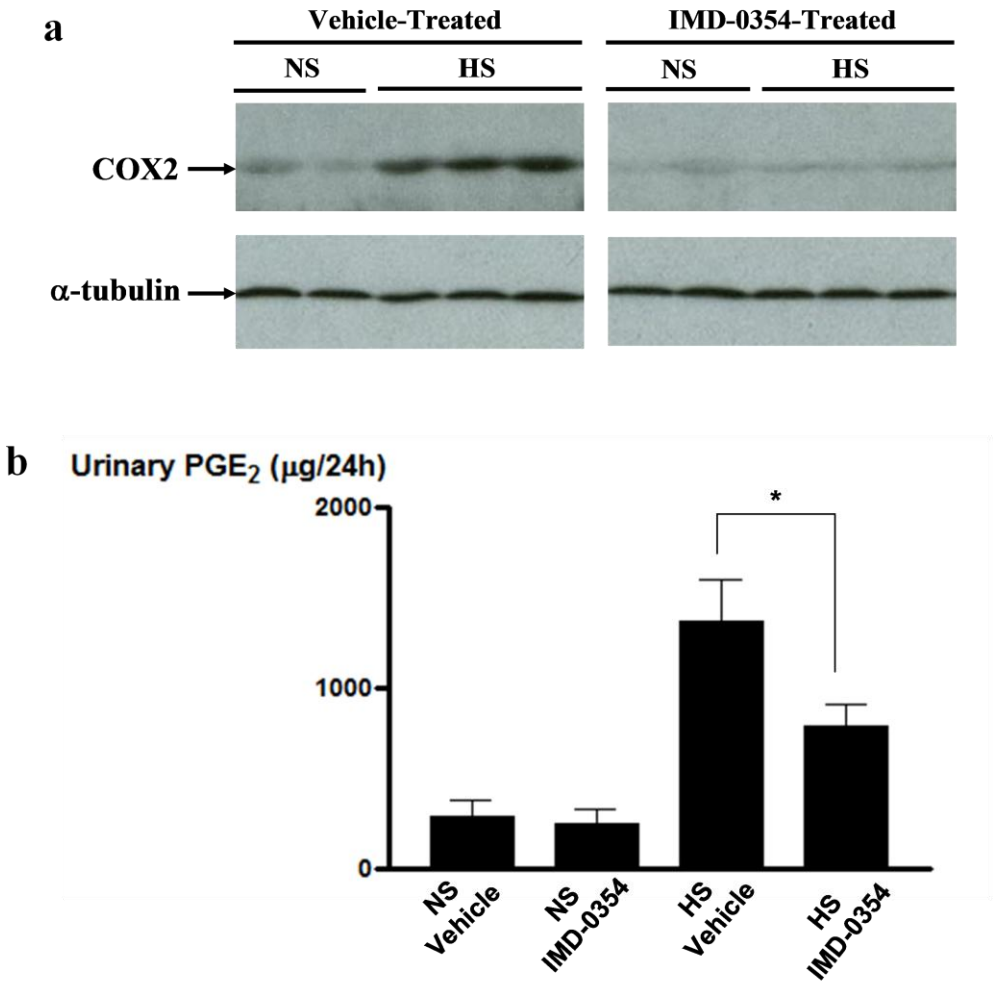

Figure 26. NFκB activation is required for renal medullary COX2 induction following high salt diet. (a) C57Bl/6J mice were pretreated with NFκB inhibitor IMD-0354 (8mg/kg bw daily) or vehicle for 2 days, then fed with high salt diet (8% NaCl) or kept on normal salt diet (0.4% NaCl) in addition to IMB-0354 or vehicle treatment for another 3 days. COX2 expression in the renal medullary tissues was determined by immunoblotting. Each lane represents an individual mouse sample. **(b)** C57Bl/6J mice were put in the metabolic cages and treated in the same way as in (a). 24 hour urine of each mouse was collected at the last day of the experiment. Urinary PGE_2 production was measured by using Cayman ELISA kit. (* $P<0.05$, n=3, ANOVA) (NS, normal salt diet; HS, high salt diet)

Global COX2 inhibition failed to cause sodium retention or hypertension in high salt diet fed mice Intra-medullary infusion of COX2 inhibitors causes sodium sensitive hypertension in uninephrectomized rats (43), suggesting a role for renal medullary COX2 in regulating sodium excretion and blood pressure. To further confirm this, we examined the effect of global COX2 inhibition on renal sodium excretion and blood pressure in a more physiologically relevant high salt diet fed mouse model. Male C57Bl/6J mice at the age of 2 months were implanted with a catheter in their artery to remotely real time monitor blood pressure. Mice were first kept on normal salt diet (0.4% NaCl) for one week and then switched to high salt diet (8% NaCl) with or without selective COX2 inhibitor SC58236 treatment (1:5,000 dilution in drinking water according to pharmaceutical company's recommendation). Daily 24 hour mean arterial blood pressure (MAP) of each mice was recorded. High salt diet was unable to increase MAP (Figure 27a), which is consistent with existing evidence suggesting that the blood pressure of C57 mouse strain is sodium insensitive. In addition, the COX2 inhibitor didn't produce significant effect on the MAP (Figure 27a).

In contrast to C57 background, the blood pressure of 129 mouse strain is reported to be sodium sensitive. Male 129/SvJ mice at the age of 2 months were treated with high salt diet with or without COX2 inhibitor. Systemic blood pressure (SBP) of each mouse was measured by tail cuff. As expected, these mice developed hypertension following high salt diet (Figure 27b). However, COX2 inhibitor SC58236 didn't produce any significant effect on the increase of

blood pressure following sodium loading, nor on the recovery of blood pressure after the mice were placed back on their normal diet (Figure 27b).

Additionally, several attempts failed to show any effect of global COX2 inhibition on urinary sodium excretion in neither C57Bl/6J or 129/SvJ mice on a high salt diet using metabolic cage studies (data not shown).

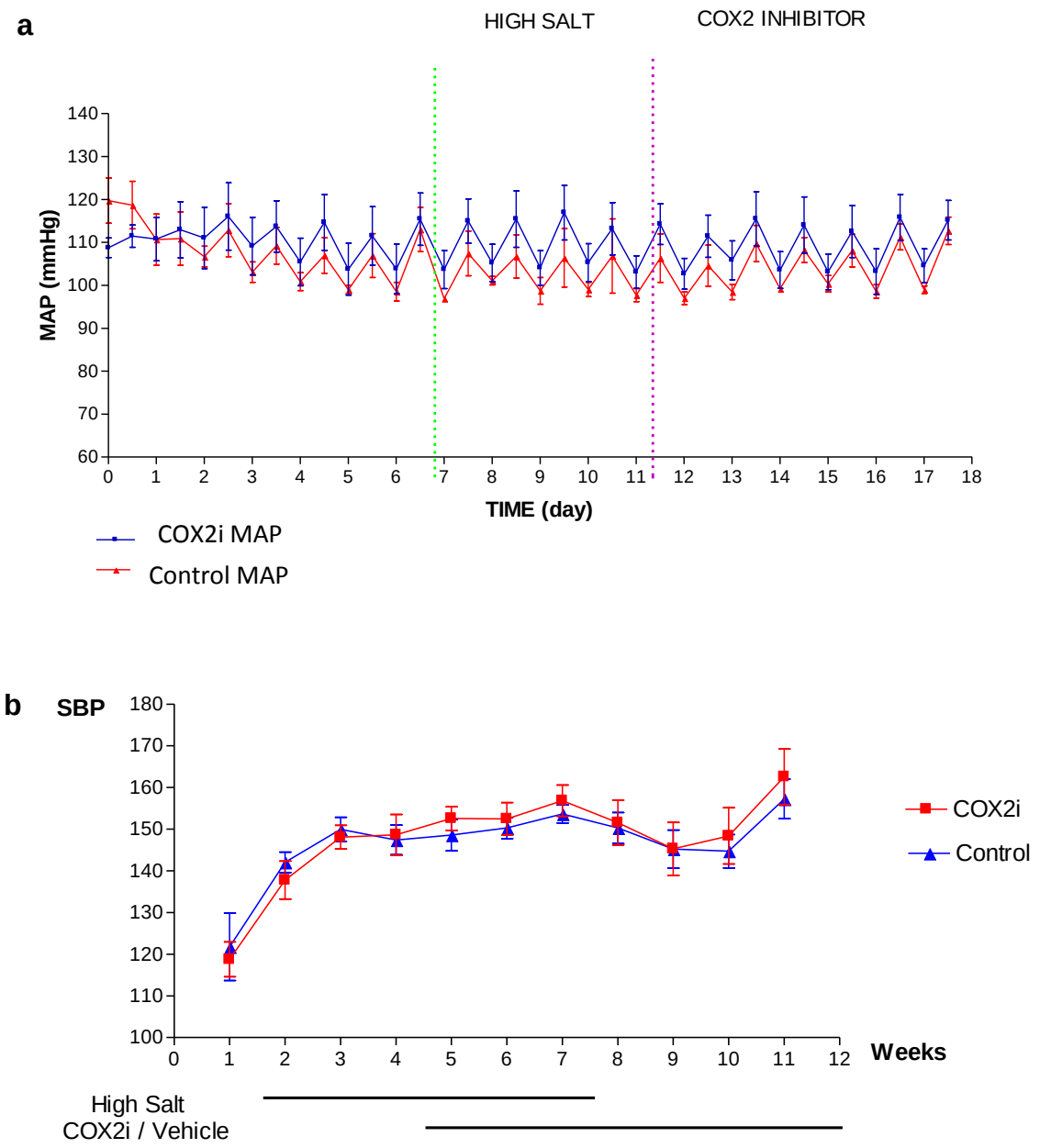

Figure 27. Global COX2 inhibition has no effect on blood pressure of high salt diet fed mice. (a) Telemetry recording of mean arterial pressure (MAP) of high salt diet fed C57Bl/6J male mice with or without selective COX2 inhibitor (SC58236 in drinking water) (n=8). **(b)** Tail cuff recording of systemic blood pressure (SBP) of high salt diet fed 129/SvJ mice with or without selective COX2 inhibitor (SC58236 in drinking water).

Discussion

Renal medullary COX2 induction has been suggested to play a role in renal response to a sodium loading (43) (44). To further examine the physiological roles of high salt diet-induced renal medullary COX2 expression, the present study examined the cellular location of COX2 induction and found that the renal medullary interstitial cells are the major site of COX2 induction following high salt diet. In addition, NFκB activation is demonstrated to play a critical role in mediating high salt diet induced COX2 expression in renal medulla. However, global inhibition of COX2 activity did not show any effect on neither renal sodium excretion nor blood pressure of mice on a high salt diet.

The cellular localization of the two isoforms of COX within the kidney has been documented (24). COX1 is predominantly expressed in the collecting ducts, while COX2, the inducible form of COX, is predominantly expressed in the renal medulla and the cortical thick ascending limb/macula densa. COX2 expression in the cortical thick ascending limb/macula densa can be induced by low salt diet or in certain conditions with volume contraction. On the other hand, renal medullary COX2 is induced under stressed conditions like water deprivation and obstructive nephropathy, or following high salt diet. The present study co-stained COX2 with the markers of distinct structures in renal medulla, and demonstrated high salt diet induced COX2 expression exclusively in renal medullary interstitial cells. Renal medullary interstitial cells are essential components of the kidney that participate in regulating sodium balance and maintaining blood pressure (142).

Chemical ablation of these cells with bromoethylamine (BEA) leads to systemic hypertension (36). By locating high salt diet induced COX2 in these cells, my work suggests that the underlying mechanisms of an important physiological role of renal medullary interstitial cells in regulating blood pressure may involve a sodium loading responsive COX2 interstitial cell expression. Although COX2 was first cloned in endothelial cells, COX2 immunoreactive protein was not detected in vasa recta of renal medulla.

COX2 expression can be regulated at multiple levels, including transcriptional and post-transcriptional regulation (143). The present study demonstrated a critical role of a known transcriptional regulator of COX2 gene, NFκB, in mediating high salt diet induced COX2 expression in renal medullary interstitial cells. High salt diet is reported to increase renal medullary NaCl concentration (139-141). Previous studies show that hypertonic induction of COX2 expression in renal medullary interstitial cells depends on NFκB activation (19). Taken together, all the above observations suggest that high salt diet, probably through increasing NaCl concentration in renal medulla, activates NFκB transcriptional activity, leading to COX2 induction in renal medullary interstitial cells.

As a sensor of redox and energy state in the cells, SIRT1 integrates cellular metabolism with stress or nutritional changes. In Chapter III and IV, SIRT1 has been located in the renal medullary interstitial cells and some of the inner medullary collecting duct cells. As high salt diet increases tonicity and generates free radical species in the renal medulla, which are known to impact cellular oxidative metabolism, SIRT1 activity in the renal medulla is very likely to respond

to a sodium loading as well. Although NFκB is reported as SIRT1 deacetylase substrate in other cellular contexts, preliminary studies failed to identify an interaction of SIRT1 with NFκB in cultured renal medullary interstitial cells in the setting of oxidative stress, However, whether SIRT1 and NFκB interact in the renal medullary interstitial cells in vivo following a sodium loading remains to be determined. Recently SIRT1 is reported to regulate the epithelial sodium channel expression in cultured inner medullary collecting ducts, which may suggest a role for SIRT1 in regulating renal sodium balance in vivo.

Following NFκB activation and COX2 induction in the renal medullary interstitial cells, COX2 derived prostaglandins may diffuse and act on adjacent renal tubular epithelial cells and vasa recta. Through activating diverse prostaglandin receptors and triggering a series of downstream cellular signaling pathways, COX2 derived prostaglandins from renal medullary interstitial cells may increase renal medullary blood flow and promote renal sodium excretion (45) (142), thus normal blood pressure can be maintained following sodium loading. Surprisingly, global inhibition of COX2 activity by COX2 selective inhibitor SC58236 did not cause sodium retention or increased blood pressure in two different mouse strains (C57Bl/6J and 129/SvJ) on high salt diet. One possibility is that inhibition of COX2 activity in vasculature, kidney macula densa may counteract the effect of COX2 inhibition in renal medullary interstitial cells. In particular, the kidney macula densa COX2 may have a pro-hypertensive effect through its role in promoting renin release (109). A better strategy is to generate a mouse with COX2 gene conditionally disrupted in renal medullary interstitial

cells. To achieve this, we generated a renal medullary interstitial cell specific inducible Cre mouse, Tenascin-C promoter driven inducible Cre knockin mouse (see Chapter VI). By crossing the floxed COX2 mice which have been available to us, with this renal medullary interstitial cell specific Cre mice, the effect of renal medullary interstitial cell COX2 ablation on renal ability to excrete excess sodium and maintain blood pressure following dietary sodium loading can be further examined.

In summary, my work has demonstrated that high salt diet induced COX2 expression in renal medulla is exclusively localized to the interstitial cells and nuclear factor NFκB plays an important role in inducing COX2 expression in these cells. Since renal medullary COX2 is suggested to regulate renal sodium balance and blood pressure, the present study also implies a role of renal medullary NFκB signaling in the regulation of renal sodium balance and blood pressure. Inhibition of renal medullary NFκB may hence contribute to altered sodium balance in patients taking NFκB inhibitors, such as Bortezomib.

CHAPTER VI

A RENAL MEDULLARY INTERSTITIAL CELL SPECIFIC INDUCIBLE CRE MOUSE, TENASCIN-C-CreER2-EGFP KNOCKIN MOUSE

Introduction

As previously mentioned, in addition to structurally supporting the renal tubules and vessels, RMICs are thought to have important physiological functions. RMICs are characterized by abundant cytoplasmic lipid droplets that contain triglycerides, cholesterol esters and free long-chain fatty acids including arachidonic acid. The number, size as well as lipid component of those lipid droplets varies dramatically upon different physiological or metabolic state of the animal (7) (8), implying potential roles of RMICs in physiology and metabolism. RMICs are also the potential target of multiple hormones such as angiotensin II and endothelin, actions of which have been suggested to regulate renal medullary hemodynamics (144) (145). Chemical ablation of RMICs with bromoethylamine (BEA) leads to systemic hypertension (36), further supporting an indispensible role of these cells in the maintenance of blood pressure.

In previous chapters, important physiological roles of SIRT1 and COX2 in RMICs have been investigated. SIRT1 mediated COX2 expression and PGE2 production from RMICs may act in autocrine and/or paracrine pathways to protect renal medullary cells from stress or injury. Renal medullary COX2 is also

suggested to play roles in regulating renal medullary blood flow, renal sodium excretion and blood pressure (24).

Given the important roles of RMICs in kidney function, in order to study genes of interest particularly in those cells, we set out to generate a renal medullary interstitial cell specific Cre mouse. A modified Cre/LoxP-based technology where recombinase activity of an inducible Cre-estrogen fusion protein (CreER2) is dependent on tamoxifen was used (146) (147). Cre expression was driven by the promoter of a renal medullary interstitial cell specific gene, tenascin-C. Tenascin-C gene is one of the four members of the tenascin family (tenascin-C, -X, -R, -W) that encode glycoproteins found in the extracellular matrix of many tissues, where they play important roles not only in supporting the tissues structurally but also regulating the functions of the different cells populating the extracellular matrix, especially when active tissue modeling during embryogenesis or re-modeling after injury occurs (148) (149) (150). Although tenascin-C is abundantly expressed in the mesenchyme surrounding developing epithelia in virtually every organ during development, its expression in normal adult tissues is relatively low and highly restricted in stromal cells.

By crossing this Cre mouse with the mouse carrying floxed gene, we sought to conditionally knock out the gene of interest (e.g. SIRT1 or COX2) from renal medullary interstitial cells. The effect of selective gene disruption in RMICs on renal physiology or pathophysiology can be further studied.

Results

Tenascin-C is specifically expressed in the interstitial cells of renal inner medulla. Evidence supporting tenascin-C gene promoter as a candidate for driving Cre expression specifically in renal medullary interstitial cells are as follows: Tenascin-C expression is reported in adult mouse renal medullary stroma (151) (152) (153); Our microarray data have shown that tenascin-C mRNA is selectively expressed in mouse renal medullary interstitial cells versus renal medullary collecting duct cells (Table 1); Finally high levels of tenascin-C expression in the renal medullary interstitium are demonstrated by in situ hybridization (Figure 28).

Table 1. Microarray reveals several genes that are selectively expressed in renal medullary interstitial cells (RMICs).

Gene Name	Ratio
Mus musculus DAN	0.033
Mus musculus HIC-5 mRNA	0.042
Mus musculus GDP-dissociation in	0.049
Reticulocalbin	0.056
Tenascin-C	0.06
Retinol binding protein 1, cecul	0.087
Mus musculus lysyl oxidase-2	0.099
G-protein coupled receptor 26	0.101

Ratio represents the mRNA level of a gene in inner medullary collecting ducts (IMCDs) as compared to that in renal medullary interstitial cells (RMICs).

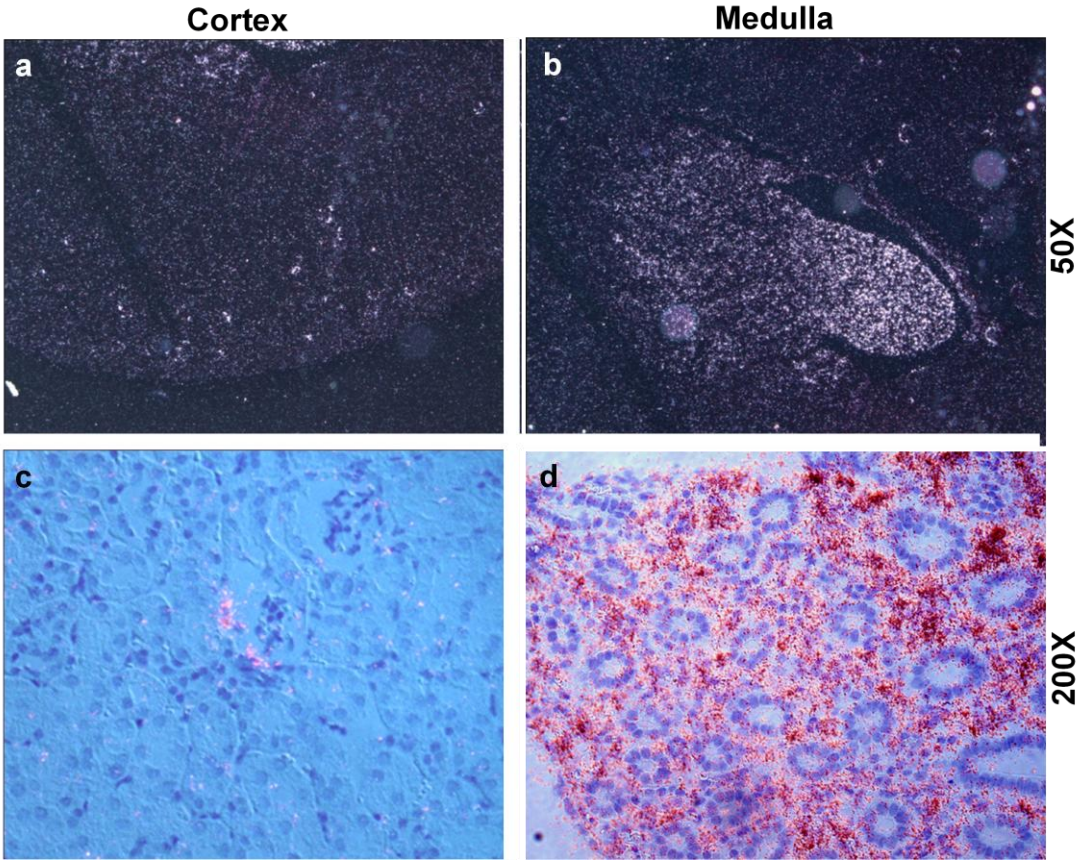

Figure 28. High levels of tenascin-C mRNA expression in the mouse renal medullary interstitium. (a, b) Dark field in situ hybridization pictures show high levels of tenascin-C mRNA in the mouse renal medulla with low levels in the renal cortex. **(c, d)** Bright field in situ hybridization pictures further show tenascin-C mRNA is highly expressed in the renal medullary interstitium.

Generation of tenascin-C-CreER2-EGFP knockin mice. Considering that the mouse tenascin-C gene has a 31kb intron1 (Figure 29a) that may contain important transcriptional regulatory elements, and heterozygous tenascin-C knockout mice have normal phenotypes (154) (155), we decided to knock in Cre directly downstream of tenascin-C gene translation start site to ensure Cre expression in the same pattern as endogenous tenascin-C gene.

Mouse genomic tenascin-C gene was obtained from a BAC library screen. The targeting construct included a 4kb 5' arm comprised of 5' region upstream of tenascin-C gene translation start codon in exon 2, an inducible CreER2, an IRES (internal ribosome entrance site)-EGFP (enhanced green fluorescence protein), a PGK-Neo selection cassette flanked by FRT, and a 2kb 3' homogenous arm (Figure 29a). The targeting construct was linearized by Ahd I and injected into E14 129SvJ ES cells with established protocols. Following homologous recombination, the CreER2-IRES-EGFP-Neo allele was expected to be inserted right after the translation start site ATG (Figure 29a). ES cell clones were screened by southern blot analysis, and four clones were identified as correctly targeted (Figure 29b). Germline transmission was obtained from two of the correctly targeted clones (3D4 and 5C3). The genotype of the mice was determined by PCR of genomic DNA. Mice heterozygous for the tenascin-C-CreER2 allele were viable, of normal size, and did not exhibit any overt developmental or functional abnormalities. The IRES-EGFP cDNA included in the targeting construct was expected to give rise to co-expression of a detectable

marker protein (EGFP) with the CreER2 and hence allows for detecting the expression of Cre in mice carrying the transgene.

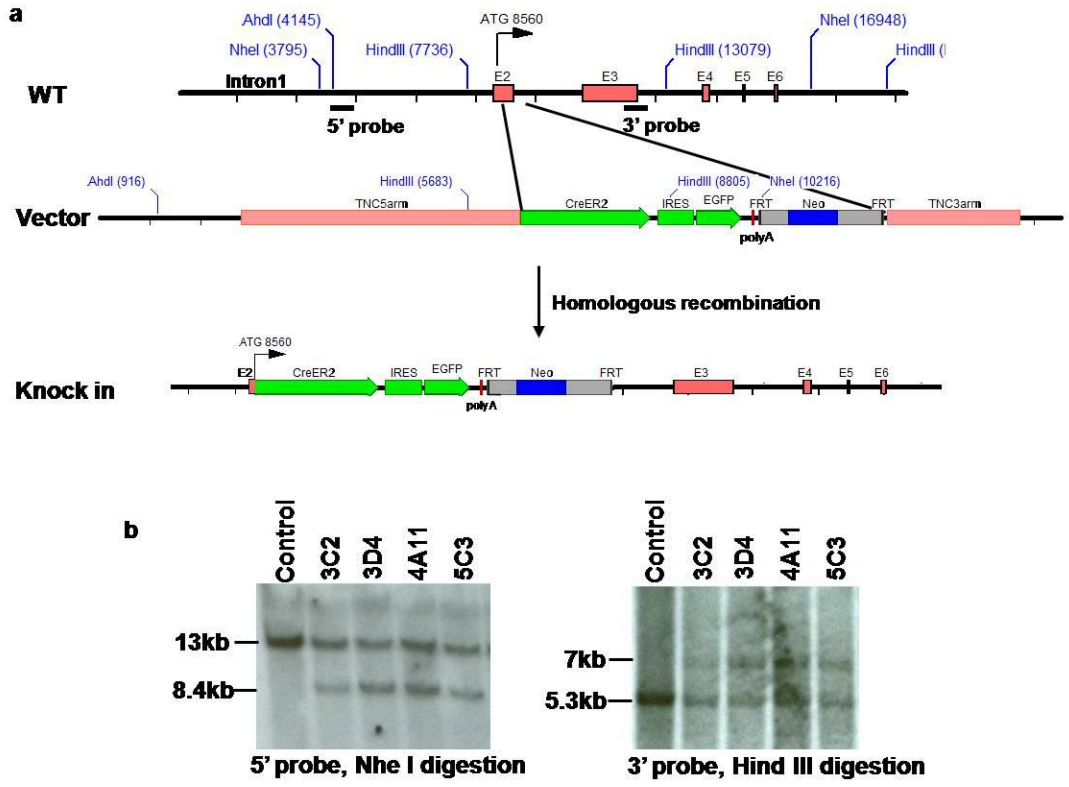

Figure 29. Generating Tenascin-C-CreER2-EGFP Knockin Mice. (a) Targeting strategy. The targeting construct has a 4kb 5' arm that locates immediately upstream of the tenascin-C gene ATG, an inducible CreER2, IRES-EGFP reporter, a PGK neo selection cassette flanked by FRT and a 2kb 3' arm that locates after exon2. **(b)** Southern blots show four targeted ES cell clones that give expected hybridization patterns. 5' probe and 3' probe are indicated in (a).

EGFP is exclusively expressed in renal medullary interstitial cells of Tenascin-C-CreER2-EGFP mice. To test if the ectopic genes are expressed with the same pattern as endogenous tenascin-C gene, EGFP expression was examined in mice heterozygous for the tenascin-C-CreER2 allele. Abundant EGFP expression was observed in the inner renal medulla but not in the cortex or outer medulla (Figure 30a). Higher power field picture (400X) showed EGFP-positive cells arranged in rows. Co-labeling studies showed that the EGFP did not co-localize with renal collecting duct marker AQP2 or descending thin limb of loop of henle marker AQP1 but co-localized with renal medullary interstitial specific COX2 (Figure 30b), consistent with selective expression of EGFP in renal medullary interstitial cells. EGFP was not observed in other organs or tissues examined including the heart, spleen, liver, skin and brain (data not shown).

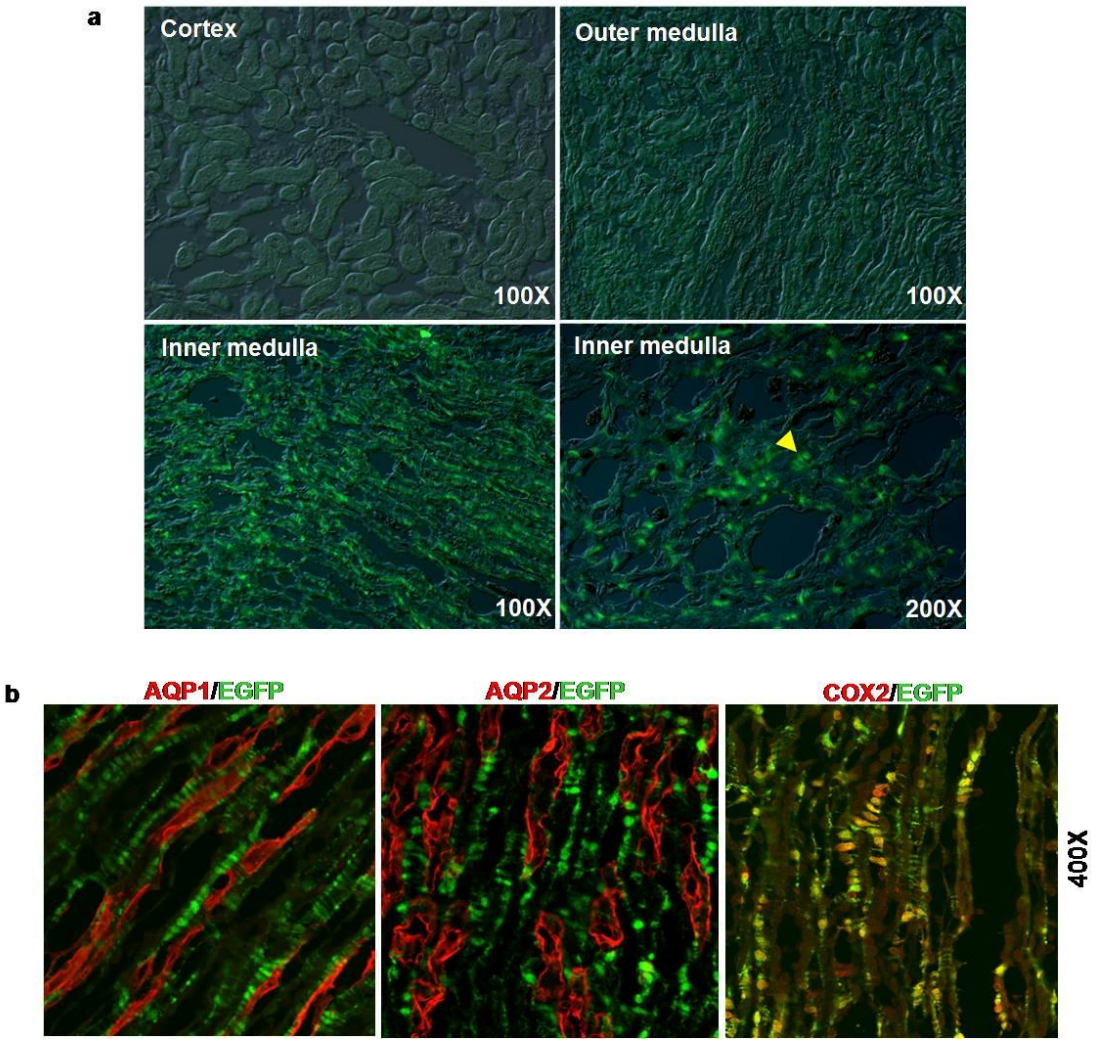

Figure 30. Exclusive EGFP expression in the renal medullary interstitial cells of tenascin-C-CreER2-EGFP mice. (a) EGFP expression was examined in the kidney of adult tenascin-C-CreER2-EGFP$^{+/-}$ mice. Yellow arrow indicates EGFP positive cells arranged like rug of ladder resembling renal medullary interstitial cells. **(b)** Co-staining with renal structural markers (red). AQP1, thin limb of loop of henle; AQP2, collecting duct; COX2: renal medullary interstitial cell specific.

Cre recombinase is exclusively activated in renal medullary interstitial cells of Tenascin-C-CreER2-EGFP mice. ROSA26-lacZ reporter mice were used to monitor Cre activity by virtue of β-galactosidase (β-gal) expression that is dependent on Cre recombinase mediated release of a stop codon before β-gal cDNA. Tamoxifen (1.5mg/25g bw/day) was administered to tenascin-C-CreER$^{+/-}$ /ROSA26-lacZ$^{+/-}$ mice at the age of 8wks continuously for two weeks. Three days after the last injection, β-gal activity was examined in major organs was by X-gal staining. The recombination reporter β-gal activity appeared to be highly restricted to the inner medulla of the kidney but not in the renal cortex or outer medulla (Figure 31a). β-gal positive cells were arranged in a rows when observed under higher power field (200X). This was further confirmed by co-labeling with renal collecting duct marker AQP2 (Figure 31b). No significant β-gal activity was observed in the heart, spleen, liver, skin and cerebrum of the brain (Figure 32). However, there was detectable β-gal activity in some cells between different layers of cerebellum (Figure 32), consistent with previous studies showing tenascin-C expression in the forebrain and cerebellum of adult mice (156). No β-gal activity was detected in the renal medulla or any other organs or tissues of tenascin-C-CreER2$^{+/-}$/ROSA26-lacZ$^{+/-}$ mice without tamoxifen treatment, suggesting no leak of the inducible Cre recombinase activity (data not shown).

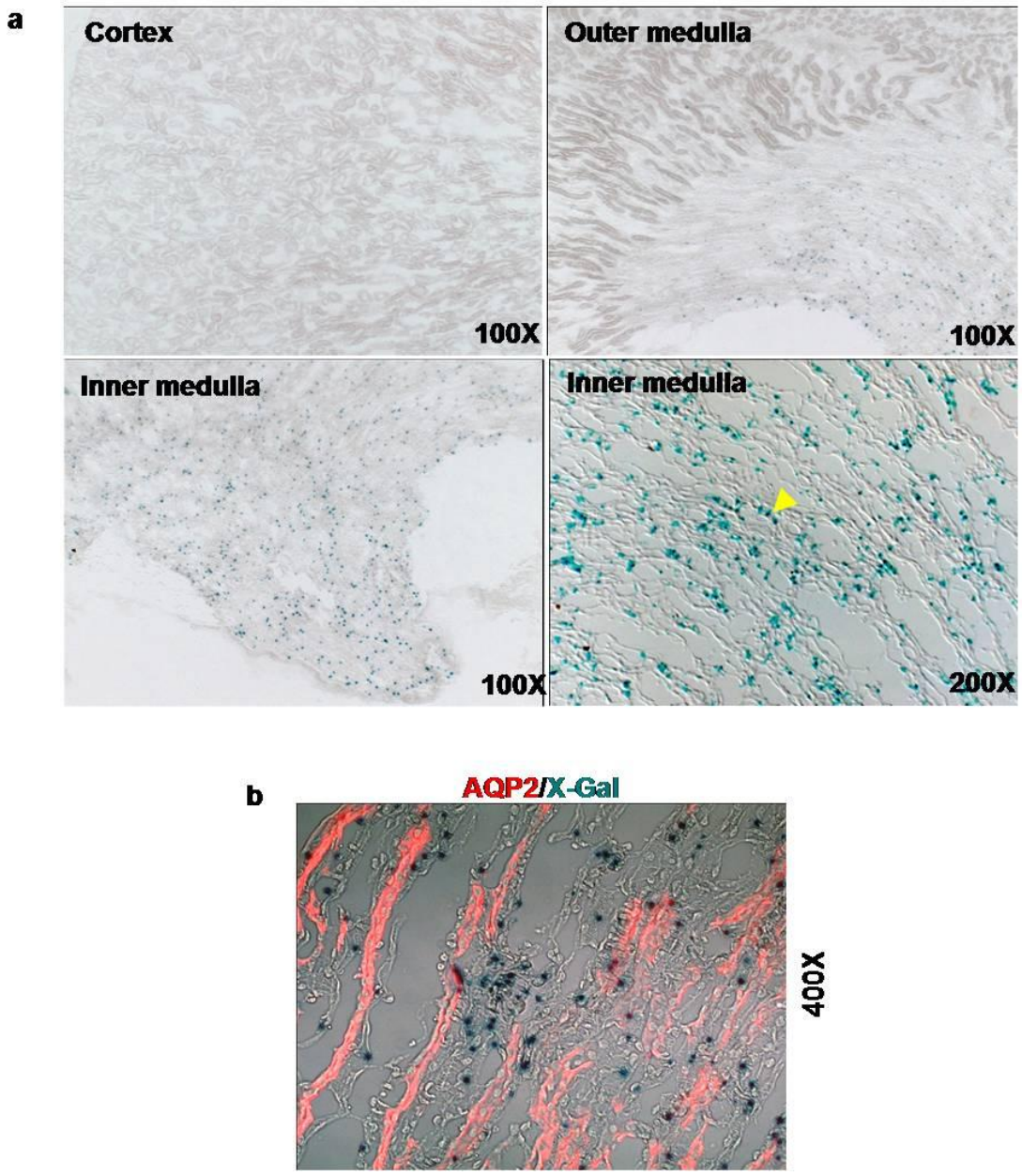

Figure 31. Cre recombinase is exclusively activated in the renal medullary interstitial cells of tenascin-C-CreER2$^{+/-}$/ROSA26-lacZ$^{+/-}$ mice with tamoxifen injection. (a) X-gal staining shows β-gal activity in the kidney of tenascin-C-CreER2$^{+/-}$/ROSA26-lacZ$^{+/-}$ mice with tamoxifen injection. **(b)** X-gal stained renal medullary section co-stained with renal collecting duct marker AQP2 (red).

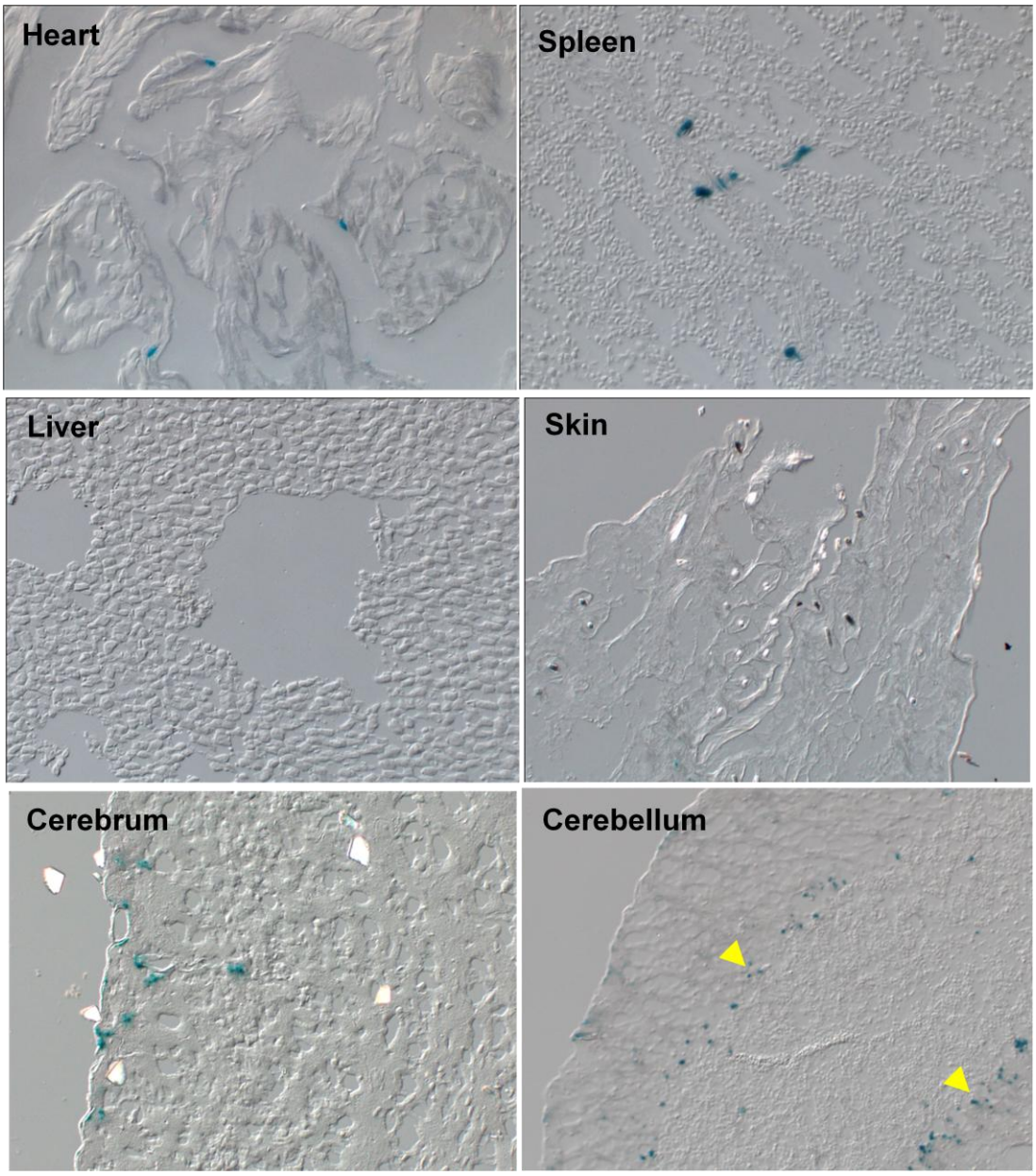

Figure 32. Cre recombinase activity in major organs of tenascin-C-CreER2$^{+/-}$/ROSA26-lacZ$^{+/-}$ mice with tamoxifen injection. Pictures of X-gal staining (200X) shows no significant β-gal activity in the heart, spleen, liver, skin and cerebrum but in certain cells lining between different layers of cerebellum (indicated by yellow arrows) of tenascin-C-CreER2$^{+/-}$/ROSA26-lacZ$^{+/-}$ mice with tamoxifen injection.

Discussion

In summary, we have generated a tenascin-C-CreER2-IRES-EGFP knock-in mouse, and demonstrated that this mouse exhibits inner medullary interstitial cell specific reporter EGFP expression and inducible Cre recombinase activity in the kidney. The tenascin-C-CreER2-EGFP knock-in mouse is therefore able to induce DNA recombination specifically in the medullary interstitial cells together with driving expression of an EGFP reporter. Through inactivating genes of interest (e.g. SIRT1 or COX2) or driving ectopic gene expression specifically in these cells, our understanding of the functional roles of renal medullary interstitial cells in renal physiology and pathophysiology should be greatly facilitated.

In Chapter V, global inhibition of COX2 activity failed to cause sodium retention or promote hypertension in high salt diet fed mice. This is contradictory to a large body of pre-existing evidence which provided the basis of our original hypothesis. One possibility is that besides renal medullary interstitial cells, treating mice with COX2 inhibitor orally also inhibited COX2 activity in other COX2-expressing tissues including cortical macula densa and vasculature. These other effects could counteract the effect of COX2 inhibition in renal medullary interstitial cells. In particular, cortical macula densa COX2 may exert a pro-hypertensive effect through its role in promoting renin release (109). A conditional gene targeting strategy provides means of specifically studying the role of renal medullary interstitial COX2 in medullary sodium excretion and blood pressure. Crossing

floxed COX2 mice with the tenascin-C-CreER2 mice should specifically delete the COX2 gene in renal medullary interstitial cells.

Interestingly, we also observed abundant EGFP expression in the stroma of the developing kidney of tenascin-C-CreER2$^{+/-}$ mice (data not shown). This observation is consistent with previous studies showing tenascin-C expression in the stroma of the developing kidney (156). The tenascin-C-CreER2 mouse with an EGFP reporter may therefore also provide a tool for studying stromal cells during kidney development.

Finally elevated tenascin-C expression has been suggested to play important roles in pathological conditions such as inflammation, infection and cancer in multiple organs including the kidney (157) (149, 153). The tenascin-C-CreER2 mouse may also be useful for tracing the localization of tenascin-C expression in these pathological conditions.

CHAPTER VII

CONCLUSIONS AND FUTURE DIRECTIONS

Conclusions

My thesis project has focused on a specific population of renal cells, the renal medullary interstitial cells, which are predominantly located in the interstitium of the renal inner medulla. Renal inner medulla is a very harsh environment with widely fluctuating and high osmolarity (over 1,000mosm), low blood flow (less than 5% of total renal blood flow) and low oxygen tension (less than 10mm Hg), which all contribute to excessive oxidative stress. It has been a longstanding issue to understand how the renal medullary cells manage to survive and function under such stressful conditions.

My work first examined the distribution of an anti-stress and anti-aging molecule SIRT1 in the kidney, and we were able to show that SIRT1 is preferentially expressed in the renal inner medulla including the renal medullary interstitial cells. The heterogeneous expression pattern strongly implied that SIRT1 may be uniquely needed for cells living in such a hostile environment in the renal inner medulla. Through a series of in vitro as well as in vivo experiments, I gathered data supporting a potent anti-oxidant role of SIRT1 in the renal medullary cells. SIRT1 deficiency accentuates renal medullary cell apoptosis and renal fibrosis and conversely SIRT1 activation promotes the resistance of renal medullary cells

to oxidative stress both in vitro and in vivo. Further studies demonstrated that one of the principal mechanisms by which SIRT1 mediates its protective effects in renal medullary interstitial cells is through increasing COX2 expression and PGE2 production. COX2 derived PGE2 production may in turn act through autocrine and/or paracrine pathways to protect renal medullary cells from stress or injury. Previous studies by our lab as well as by other groups have demonstrated that COX2 is an essential factor for renal medullary interstitial cell survival under hypertonic stress. By showing that SIRT1 and COX2 co-localize in the renal medullary interstitial cells and that SIRT1 regulates COX2 expression in the setting of oxidative stress, my work has linked these two important survival factors uniquely in the renal medullary interstitial cells. Taken together, these findings in Chapter III and IV are of interest and importance, as the identification of SIRT1 as a molecule that confers cytoprotection in the renal inner medulla, and the delineation that such protection is in part mediated through COX2 and production of PGE2, have contributed to our understanding of the protective mechanisms in these "born-tough" renal medullary cells.

In addition to structurally supporting adjacent renal tubules and vessels, renal medullary interstitial cells also serve important physiological functions. A long ongoing project in our lab has been studying the potential roles of renal medullary COX2 in promoting renal sodium excretion and maintaining blood pressure in the renal response to a sodium loading. In Chapter V, my work has precisely located high salt diet induced COX2 expression exclusively in the renal medullary interstitial cells. COX2 derived PGE2 from these cells may promote

excretion of excess sodium through acting on the adjacent renal vasa recta to modulate renal blood flow and/or the adjacent renal tubular epithelial cells to modulate sodium absorption, as a result of which, normal blood pressure following sodium loading is maintained. The molecular mechanism by which high salt diet induces COX2 expression in medullary interstitial cells was further examined and a critical role for NFκB was revealed. High salt diet activates NFκB in renal medullary interstitial cells and inhibition of NFκB significantly attenuates high salt diet induced COX2 expression. As high salt diet increases tonicity in the renal medulla and hypertonicity induced COX2 is mediated by NFκB activation in cultured renal medullary interstitial cells, my work support a model whereby renal medullar interstitial cells respond to a sodium loading through sensing increased tonicity, which activates NFκB. NFκB subsequently mediates COX2 induction in the medullary interstitial cells, followed by production of locally diffusible PGE2 that coordinates the functions of vasa recta and renal tubules to promote renal sodium excretion and maintain body sodium balance and blood pressure.

Lastly, in chapter VI, I together with my laboratory coworkers generated a tenascin-C-CreER2-IRES-EGFP knockin mouse. Following careful characterization, we have demonstrated that this mouse has inner medullary interstitial cell specific reporter EGFP expression and inducible Cre recombinase activity. By using this tool, conditional disruption of genes of interest (e.g. SIRT1 or COX2) in renal medullary interstitial cells is now possible. Our understanding

of the physiological roles of renal medullary interstitial cells as well as the underlying molecular mechanisms in these cells may be greatly facilitated.

Future Directions

The molecular mechanism by which SIRT1 regulates COX2 transcription In Chapter IV, my data suggest that the cytoprotective function of SIRT1 is partially attributable to its regulation of COX2 expression in the renal medullary interstitial cells in the setting of oxidative stress. However, the molecular mechanism by which SIRT1 regulates COX2 expression remains to be determined in future studies.

The expression of COX2 gene can be regulated at multiple levels including transcription, mRNA stability, translation and protein stability. The present findings are further supportive of a regulatory role of SIRT1 on COX2 gene transcription, as SIRT1 knockdown reduced both H_2O_2-induced COX2 mRNA expression and COX2 protein induction (Figure 18B), and COX2 promoter-driven luciferase reporter activation following H_2O_2 was also attenuated by SIRT1 knockdown (Figure 19A). Considering SIRT1 is a protein deacetylase but not a direct DNA interacting protein, SIRT1 activity might deacetylate other nuclear proteins (e.g. histones, transcription factors, co-factors) which bind to COX2 gene promoter and modulate the transcription of COX2 gene. Additionally, SIRT1 knockdown suppressed the activation of the COX2 promoter-driven luciferase reporter in an exogenous plasmid with no histones bound (Figure 19A), suggesting that the mediator responsible for SIRT1-regulated COX2 induction

may be transcription factors or co-factors. ChIP assay showed physical association of SIRT1 with COX2 promoter DNA under both normal condition and stressed condition (Figure 33A). Quantitative real time PCR may be performed to determine if association of SIRT1 with this DNA region increases or decreases following oxidative stress. Nonetheless, it is possible that different machineries are involved in SIRT1 regulation of COX2 gene transcription under normal versus stressed conditions. For instance, SIRT1 may interact with a repressor under normal condition, while with an activator under stressed condition. Previous studies (19, 25) together with the present study suggest that COX2 induction is a pre-requisite for renal medullary interstitial cell survival from stresses. Notably, excessive COX2 expression is also known to induce cell apoptosis. Therefore a firm and precise control of COX2 expression is essential for cell vitality. By residing on COX2 promoter and interacting with different nuclear factors that bind to COX2 promoter under different conditions, SIRT1 may play an important role in achieving the finest control of COX2 expression in the renal medullary interstitial cells.

In search of the responsible "nuclear factor" or "nuclear factors" that mediate the function of SIRT1 in regulating COX2 gene transcription, several transcriptional regulators of COX2 gene that are also reported SIRT1 deacetylase substrates are considered potential candidates. These transcription factors include NFκB and p53. Preliminary data, however, were not supportive of a role of SIRT1 in modifying either NFκB or p53 in the cultured RMICs. Co-immunoprecipitation was unable to detect direct association of SIRT1 with either

p65 or p53. Acetylation level of p65 was not affected by knockdown of SIRT1 by SIRT1 selective shRNA or activation of SIRT1 by SIRT1 activators. In addition, H_2O_2 treatment didn't induce the activation of the luciferase reporter driven by a NFκB response promoter, HIV long-terminal repeat (LTR) (158), indicating that NFκB signaling may not be responding to H_2O_2 treatment in the context tested. Interestingly, the levels of both total p53 and acetylated-p53 significantly increased following H_2O_2 treatment, consistent with a role for p53 in mediating cellular response to stress. However, knocking down SIRT1 expression or activating SIRT1 had no significant effect on H_2O_2-induced either total p53 level or acetylated-p53 level. Taken together, all the above observations do not support a direct modification of either p65 or p53 by SIRT1 activity in the cultured RMICs in the setting of oxidative stress.

In order to further explore candidates that mediate the interaction between SIRT1 and COX2 promoter region, I searched for putative transcription factor binding elements on the COX2 promoter region using VISTA tools (http://genome.lbl.gov/vista/index.shtml). Interestingly, in an evolutionarily conserved ~100bp genomic DNA region (among human, dog, rat and mouse) located at around 800bp upstream of COX2 gene transcription start site, there are two adjacent putative FOXO binding elements (Figure 33B). The mammalian FOXO family comprises three major members of transcription factors, FOXO1, FOXO3 and FOXO4, which can associate with a variety of unrelated transcriptional factors and regulate activation or repression of diverse target genes that play crucial roles in diverse cellular processes including proliferation,

apoptosis, stress resistance and metabolic regulation (159). Importantly, FOXO3 expression was observed in both mouse renal medulla in vivo and in cultured mouse renal medullary interstitial cells in vitro by RT-PCR (Figure 33C). The expression of FOXO3 in the renal medulla was also confirmed by in situ hybridization (data not shown). Of note, FOXO3 is also a deacetylase substrate of SIRT1 and SIRT1 has various effects on FOXO3-mediated gene expression, from activation to repression (132) (160). Based on the above observations, I hypothesize that FOXO3 may be "the transcription factor" that binds to COX2 promoter region and mediates the function of SIRT1 in regulating COX2 expression. Importantly, ChIP assay has shown that both SIRT1 and FOXO3 were detected in association with COX2 promoter region (Figure 33A). To confirm whether SIRT1 and FOXO3 are present in the same transcriptional complex on the COX2 promoter, reciprocal reChIP may be performed by immunoprecipitating the protein/DNA complex first with anti-SIRT1 antibody and then immunoprecipitating for the second time with anti-FOXO3 antibody, and vice versa. H_2O_2 treatment induced FOXO3 disassociation with this COX2 promoter region (Figure 33A), suggestive of a suppressive role for FOXO3 in regulating COX2 gene transcription. Further experiments should determine the effect of SIRT1 knockdown or SIRT1 activation on total and acetylated-FOXO3 levels. By using FOXO3-overexpressing plasmids or FOXO3 selective shRNA, I will also examine the effect of FOXO3 overexpression or FOXO3 knockdown on COX2 expression.

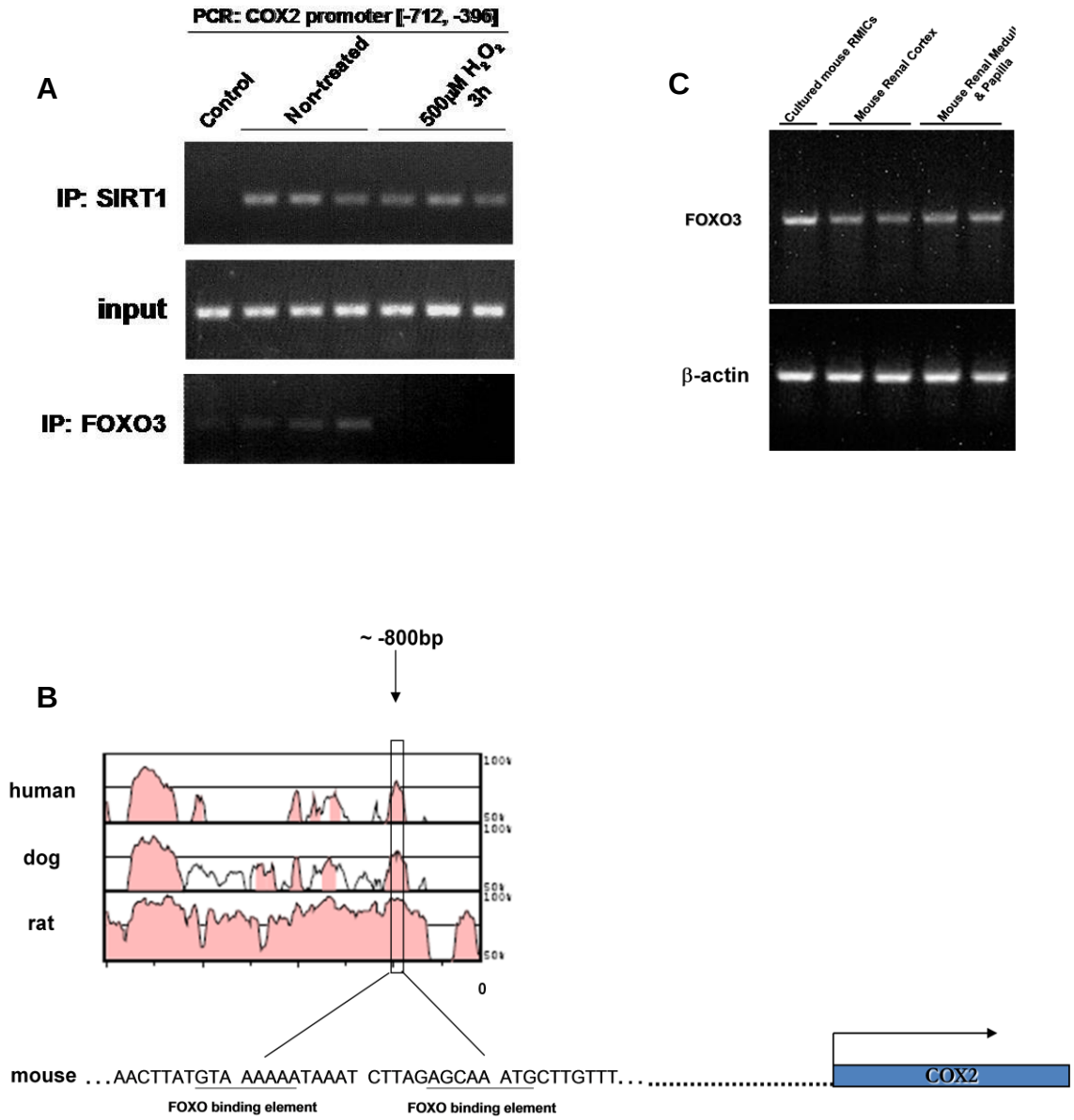

Figure 33. FOXO3 and SIRT1 associate with the same region of the COX2 promoter. (A) ChIP assay showed physical association of SIRT1 and FOXO3 with COX2 promoter region [-712, -396] in non-treated or H_2O_2-treated cultured renal medullary interstitial cells. **(B)** In an evolutionarily conserved genomic DNA region located at ~800bp upstream of COX2 gene transcription start site, there are two adjacent putative FOXO binding elements. **(C)** RT-PCR analysis showed FOXO3 mRNA expression was present in the renal cortical tissue, renal medullary tissue, and cultured renal medullary interstitial cells of mice.

Renal medullary interstitial cell specific gene ablation using Tenascin-C-CreER2 mice In Chapter VI, we generated a Tenascin-C-CreER2 knockin mouse that has inducible Cre recombinase selectively expressed in the renal medullary interstitial cells. This novel tool will be actively used in the further studies on the roles of COX2 and/or SIRT1 in the renal medullary interstitial cells.

As I have discussed briefly in the discussion section of Chapter V, unexpectedly, global inhibition of COX2 by treating mice with pharmacological inhibitors didn't cause sodium retention or increased blood pressure (Figure 27) following sodium loading. One possible explanation is that inhibition of COX2 activity in the vasculature and/or renal cortical thick ascending limb (macula densa) may counteract the effect of inhibiting COX2 activity in the renal medullary interstitial cells. In particular, COX2 activity in macula densa is pro-hypertensive through promoting renin release (109), as opposed to a suggested anti-hypertensive role of COX2 in the renal medullary interstitial cells. In order to specifically study the role of COX2 in the renal medullary interstitial cells, conditional renal medullary interstitial cell specific COX2 knockout mice will be generated by crossing renal medullary interstitial cell specific Cre mice (Tenascin-C-CreER2 mice) with floxed-COX2 mice. Renal sodium excretion and blood pressure following sodium loading will be further examined in these conditional COX2 knockout mice. Previous studies have suggested an important role of renal medullary interstitial COX2 in promoting renal sodium excretion and maintaining blood pressure following sodium loading, I thus expect that the renal medullary interstitial cell

COX2 knockout mice will have impaired renal ability to excrete excess sodium and will develop hypertension following high salt diet.

This Tenascin-C-CreER2 mouse will also be crossed with a floxed-SIRT1 mouse to generate conditional renal medullary interstitial cell specific SIRT1 knockout mice for further studies on the role of renal medullary interstitial cell SIRT1. As compared to SIRT1 heterozygous mice with globally one SIRT1 allele ablation, renal medullary interstitial cell specific SIRT1 knockout mice have both SIRT1 alleles deleted in the renal medullary interstitial cells. Therefore these SIRT1-null renal medullary interstitial cells are expected to be more vulnerable to stress or injury and develop severer phenotypes, when compared with SIRT1-deficient cells. Secondly, although the in vivo observations in Chapter III have clearly supported a protective role of SIRT1 against UUO induced apoptosis, the present study didn't distinguish the role of renal medullary interstitial cell SIRT1 from potential roles of SIRT1 in other tissues (e.g. renal medullary collecting duct cells, inflammatory cells). Previous studies show an anti-oxidant function of SIRT1 in the cultured renal tubular cells (90), suggesting that renal medullary collecting duct cell SIRT1 may also be protective against UUO injury. SIRT1 activity in inflammatory cells, on the other hand, can be complicated. SIRT1 is reported to inhibit inflammatory responses (90), however, the yin-yang roles that inflammation plays during UUO injury have not been fully understood yet and are still under debating. Taken together, conditional renal medullary interstitial cell specific SIRT1 knockout mice should offer significant advantage for future studies versus SIRT1 heterozygous mice. SIRT1-null renal medullary interstitial

cells should exhibit a more pronounced phenotype and concerns regarding SIRT1 activity in other tissues will be mitigated.

Potential role of SIRT1 in renal response to sodium loading As discussed in Chapter III and Chapter IV, SIRT1 is abundantly expressed in the renal medullary interstitial cells. SIRT1 mediated COX2 induction protects renal medullary interstitial cells following oxidative stress or renal injury from obstructive nephropathy. Renal medullary interstitial cells were also shown to be the major site of renal medullary COX2 expression in a high salt diet mouse model in Chapter V. Although my preliminary data using a COX2 selective inhibitor to globally inhibit COX2 activity did not affect renal sodium excretion or blood pressure in mice on a high salt diet, many other studies have suggested an important role of renal medullary COX2 in regulating renal blood flow, renal sodium excretion and blood pressure. In addition, high salt diet increases tonicity and generates free radical species in the renal medulla. This impairs cellular oxidative metabolism. Based on the above observations, considering that SIRT1 is a regulator of COX2 expression in renal medullary interstitial cells and that SIRT1 is sensitive to cellular redox state, it is of interest to explore if SIRT1 plays a role in high salt diet induced COX2 expression in renal medullary interstitial cells and whether SIRT1 participates in the renal regulation of sodium excretion and blood pressure following sodium loading.

Preliminary data using a naturally producing SIRT1 activator resveratrol have suggested a potential role of SIRT1 activation in promoting urinary sodium

excretion in high salt diet fed mice (Figure 34). Further experiments should examine the effect of SIRT1 activation by more specific small molecule SIRT1 activator SRT compounds or SIRT1 deficiency by using heterozygous SIRT1 knockout mice on renal sodium excretion as well as blood pressure following sodium loading. With regard to the underlying mechanism by which SIRT1 activation might promote renal sodium excretion, SIRT1 regulation of renal medullary interstitial COX2 induction following high salt diet could be examined.

Besides a potential role of renal medullary interstitial SIRT1, the possibility that collecting duct SIRT1 may participate in regulating renal sodium balance by affecting epithelial sodium reabsorption must also be considered, since SIRT1 expression is observed in some renal medullary collecting duct cells in vivo. Furthermore, SIRT1 has been reported to regulate the expression of the α-subunit of the epithelial sodium channel ENaC in cultured inner medullary collecting duct cells.

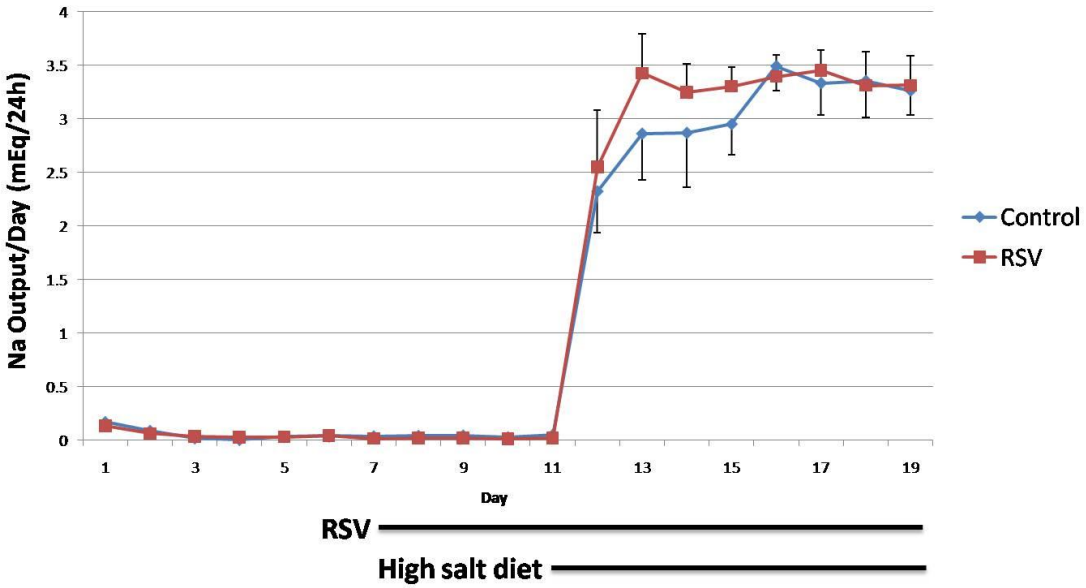

Figure 34. Resveratrol promotes urinary sodium excretion in mice fed with high salt diet. 12 C57Bl/6J male mice were fed with low salt diet and kept in metabolic cages. Each mouse was fed with a certain amount of food everyday to control the daily sodium intake. Daily urine was collected for electrolyte measurement for urinary sodium output throughout the study. After 7 days in the metabolic cages for balance, Sirtuin-1 activator Resveratrol was administered to 6 mice by gavage (shown in purple line), and vehicle to the other 6 mice (shown in blue line). 4 days later, all the mice were switched to high salt diet for another 7 days. Resveratrol treated mice excreted excess sodium more promptly than vehicle treated mice following high salt diet.

Potential Role of SIRT1 in Renal Aging or Metabolic Renal Disease My work has demonstrated an important anti-oxidant function of SIRT1 activity in the renal medulla and suggests that targeting SIRT1 with pharmaceutical activators could provide a strategy to maintain renal function in conditions that induce oxidative stress in the renal medulla such as ureteral obstruction. Aging and diseased conditions such as the metabolic syndrome, increase oxidative stress in the kidney and are associated with impaired renal function (22). Given the important roles of SIRT1 in the biology of aging and metabolism, it will be important to determine if SIRT1 activation also prevents renal aging or protects renal cells in metabolic renal disease such as diabetic nephropathy or hypertensive nephropathy.

To study the role of SIRT1 in renal aging, we first asked if renal SIRT1 expression is reduced with aging. Preliminary data show that although renal SIRT1 expression was not significantly different in C57Bl/6J mice during adulthood (3, 5, 10, 18 months), decreased renal SIRT1 expression in mice was observed at 26 months of age (data not shown). This observation is concordant with previous studies showing that age related renal changes in mice are minimal until an age of at least 22 months (114) (115). Interestingly, reduced renal SIRT1 expression was also observed in mice on a high fat diet (data not shown). However, whether the reduction of SIRT1 expression contributes to renal damage and reduced renal function with aging or in metabolic syndrome remains to be investigated.

REFERENCES

1. Brenner BM. The Kidney, 8th ed. Philadelphia: W. B. Saunders Company; 2008.
2. Lacombe C, Da Silva JL, Bruneval P, Fournier JG, Wendling F, Casadevall N, et al. Peritubular cells are the site of erythropoietin synthesis in the murine hypoxic kidney. J Clin Invest. 1988;81(2):620-3. PMCID: 329613.
3. Bohman SO. The ultrastructure of the rat renal medulla as observed after improved fixation methods. J Ultrastruct Res. 1974;47(3):329-60.
4. Le Hir M, Kaissling B. Distribution of 5'-nucleotidase in the renal interstitium of the rat. Cell Tissue Res. 1989;258(1):177-82.
5. Schiller A, Taugner R. Junctions between interstitial cells of the renal medulla: a freeze-fracture study. Cell Tissue Res. 1979;203(2):231-40.
6. Majack RA, Larsen WJ. The bicellular and reflexive membrane junctions of renomedullary interstitial cells: functional implications of reflexive gap junctions. Am J Anat. 1980;157(2):181-9.
7. Nissen HM. On lipid droplets in renal interstitial cells. II. A histological study on the number of droplets in salt depletion and acute salt repletion. Z Zellforsch Mikrosk Anat. 1968;85(4):483-91.
8. Nissen HM. On lipid droplets in renal interstitial cells. 3. A histological study on the number of droplets during hydration and dehydration. Z Zellforsch Mikrosk Anat. 1968;92(1):52-61.
9. Schmidt-Nielsen B, O'Dell R. Structure and concentrating mechanism in the mammalian kidney. Am J Physiol. 1961;200:1119-24.
10. Tisher CC, Schrier RW, McNeil JS. Nature of urine concentrating mechanism in the macaque monkey. Am J Physiol. 1972;223(5):1128-37.
11. Christoph K, Beck FX, Neuhofer W. Osmoadaptation of Mammalian cells - an orchestrated network of protective genes. Curr Genomics. 2007;8(4):209-18.
12. Brezis M, Rosen S. Hypoxia of the renal medulla--its implications for disease. N Engl J Med. 1995;332(10):647-55.
13. Baumgartl H, Leichtweiss HP, Lubbers DW, Weiss C, Huland H. The oxygen supply of the dog kidney: measurements of intrarenal pO 2. Microvasc Res. 1972;4(3):247-57.
14. Bae YS, Kang SW, Seo MS, Baines IC, Tekle E, Chock PB, et al. Epidermal growth factor (EGF)-induced generation of hydrogen peroxide. Role in EGF receptor-mediated tyrosine phosphorylation. J Biol Chem. 1997;272(1):217-21.
15. Tohyama Y, Takano T, Yamamura H. B cell responses to oxidative stress. Curr Pharm Des. 2004;10(8):835-9.
16. Yu BP. Cellular defenses against damage from reactive oxygen species. Physiol Rev. 1994;74(1):139-62.
17. Zou AP, Li N, Cowley AW, Jr. Production and actions of superoxide in the renal medulla. Hypertension. 2001;37(2 Part 2):547-53.
18. Pallone TL. Is oxidative stress differentially regulated in the renal cortex and medulla? Nat Clin Pract Nephrol. 2006;2(3):118-9.
19. Hao CM, Yull F, Blackwell T, Komhoff M, Davis LS, Breyer MD. Dehydration activates an NF-kappaB-driven, COX2-dependent survival mechanism in renal medullary interstitial cells. J Clin Invest. 2000;106(8):973-82.

20. Mattagajasingh I, Kim CS, Naqvi A, Yamamori T, Hoffman TA, Jung SB, et al. SIRT1 promotes endothelium-dependent vascular relaxation by activating endothelial nitric oxide synthase. Proc Natl Acad Sci U S A. 2007;104(37):14855-60. PMCID: 1976244.
21. Zhou XJ, Rakheja D, Yu X, Saxena R, Vaziri ND, Silva FG. The aging kidney. Kidney Int. 2008;74(6):710-20.
22. Roberts CK, Sindhu KK. Oxidative stress and metabolic syndrome. Life Sci. 2009;84(21-22):705-12.
23. Neuhofer W, Beck FX. Cell survival in the hostile environment of the renal medulla. Annu Rev Physiol. 2005;67:531-55.
24. Hao CM, Breyer MD. Physiological regulation of prostaglandins in the kidney. Annu Rev Physiol. 2008;70:357-77.
25. Hao CM, Komhoff M, Guan Y, Redha R, Breyer MD. Selective targeting of cyclooxygenase-2 reveals its role in renal medullary interstitial cell survival. Am J Physiol. 1999;277(3 Pt 2):F352-9.
26. Murray MD, Brater DC. Renal toxicity of the nonsteroidal anti-inflammatory drugs. Annu Rev Pharmacol Toxicol. 1993;33:435-65.
27. Schlondorff D. Renal complications of nonsteroidal anti-inflammatory drugs. Kidney Int. 1993;44(3):643-53.
28. Bach PH, Nguyen TK. Renal papillary necrosis--40 years on. Toxicol Pathol. 1998;26(1):73-91.
29. Hao CM, Redha R, Morrow J, Breyer MD. Peroxisome proliferator-activated receptor delta activation promotes cell survival following hypertonic stress. J Biol Chem. 2002;277(24):21341-5.
30. Moeckel GW, Zhang L, Fogo AB, Hao CM, Pozzi A, Breyer MD. COX2 activity promotes organic osmolyte accumulation and adaptation of renal medullary interstitial cells to hypertonic stress. J Biol Chem. 2003;278(21):19352-7.
31. Breyer MD, Breyer RM. G protein-coupled prostanoid receptors and the kidney. Annu Rev Physiol. 2001;63:579-605.
32. Breyer MD, Hao C, Qi Z. Cyclooxygenase-2 selective inhibitors and the kidney. Curr Opin Crit Care. 2001;7(6):393-400.
33. Cowley AW, Jr. Renal medullary oxidative stress, pressure-natriuresis, and hypertension. Hypertension. 2008;52(5):777-86.
34. Cowley AW, Jr. Franz Volhard Lecture. Evolution of the medullipin concept of blood pressure control: a tribute to Eric Muirhead. J Hypertens Suppl. 1994;12(10):S25-34.
35. Muirhead EE. Renal vasodepressor mechanisms: the medullipin system. J Hypertens Suppl. 1993;11(5):S53-8.
36. Haugan K, Shalmi M, Petersen JS, Marcussen N, Spannow J, Christensen S. Effects of renal papillary-medullary lesion on the antihypertensive effect of furosemide and development of salt-sensitive hypertension in Dahl-S rats. J Pharmacol Exp Ther. 1997;280(3):1415-22.
37. Cowley AW, Jr., Roman RJ. The role of the kidney in hypertension. JAMA. 1996;275(20):1581-9.
38. Anderson RJ, Berl T, McDonald KM, Schrier RW. Prostaglandins: effects on blood pressure, renal blood flow, sodium and water excretion. Kidney Int. 1976;10(3):205-15.
39. Whelton A, White WB, Bello AE, Puma JA, Fort JG. Effects of celecoxib and rofecoxib on blood pressure and edema in patients > or =65 years of age with systemic hypertension and osteoarthritis. Am J Cardiol. 2002;90(9):959-63.

40. White WB, Kent J, Taylor A, Verburg KM, Lefkowith JB, Whelton A. Effects of celecoxib on ambulatory blood pressure in hypertensive patients on ACE inhibitors. Hypertension. 2002;39(4):929-34.
41. Yang T, Singh I, Pham H, Sun D, Smart A, Schnermann JB, et al. Regulation of cyclooxygenase expression in the kidney by dietary salt intake. Am J Physiol. 1998;274(3 Pt 2):F481-9.
42. Chen J, Zhao M, He W, Milne GL, Howard JR, Morrow J, et al. Increased dietary NaCl induces renal medullary PGE2 production and natriuresis via the EP2 receptor. Am J Physiol Renal Physiol. 2008;295(3):F818-25. PMCID: 2653111.
43. Zewde T, Mattson DL. Inhibition of cyclooxygenase-2 in the rat renal medulla leads to sodium-sensitive hypertension. Hypertension. 2004;44(4):424-8.
44. Ye W, Zhang H, Hillas E, Kohan DE, Miller RL, Nelson RD, et al. Expression and function of COX isoforms in renal medulla: evidence for regulation of salt sensitivity and blood pressure. Am J Physiol Renal Physiol. 2006;290(2):F542-9.
45. Qi Z, Hao CM, Langenbach RI, Breyer RM, Redha R, Morrow JD, et al. Opposite effects of cyclooxygenase-1 and -2 activity on the pressor response to angiotensin II. J Clin Invest. 2002;110(1):61-9. PMCID: 151026.
46. Kennedy CR, Zhang Y, Brandon S, Guan Y, Coffee K, Funk CD, et al. Salt-sensitive hypertension and reduced fertility in mice lacking the prostaglandin EP2 receptor. Nat Med. 1999;5(2):217-20.
47. Francois H, Athirakul K, Howell D, Dash R, Mao L, Kim HS, et al. Prostacyclin protects against elevated blood pressure and cardiac fibrosis. Cell Metab. 2005;2(3):201-7.
48. Hebert RL, Jacobson HR, Fredin D, Breyer MD. Evidence that separate PGE2 receptors modulate water and sodium transport in rabbit cortical collecting duct. Am J Physiol. 1993;265(5 Pt 2):F643-50.
49. Guan Y, Zhang Y, Breyer RM, Fowler B, Davis L, Hebert RL, et al. Prostaglandin E2 inhibits renal collecting duct Na+ absorption by activating the EP1 receptor. J Clin Invest. 1998;102(1):194-201. PMCID: 509081.
50. Taylor NE, Glocka P, Liang M, Cowley AW, Jr. NADPH oxidase in the renal medulla causes oxidative stress and contributes to salt-sensitive hypertension in Dahl S rats. Hypertension. 2006;47(4):692-8.
51. Meng S, Roberts LJ, 2nd, Cason GW, Curry TS, Manning RD, Jr. Superoxide dismutase and oxidative stress in Dahl salt-sensitive and -resistant rats. Am J Physiol Regul Integr Comp Physiol. 2002;283(3):R732-8.
52. Ho YS, Xiong Y, Ma W, Spector A, Ho DS. Mice lacking catalase develop normally but show differential sensitivity to oxidant tissue injury. J Biol Chem. 2004;279(31):32804-12.
53. Makino A, Skelton MM, Zou AP, Cowley AW, Jr. Increased renal medullary H2O2 leads to hypertension. Hypertension. 2003;42(1):25-30.
54. Afshar G, Murnane JP. Characterization of a human gene with sequence homology to Saccharomyces cerevisiae SIR2. Gene. 1999;234(1):161-8.
55. Shi T, Wang F, Stieren E, Tong Q. SIRT3, a mitochondrial sirtuin deacetylase, regulates mitochondrial function and thermogenesis in brown adipocytes. J Biol Chem. 2005;280(14):13560-7.
56. Landry J, Sutton A, Tafrov ST, Heller RC, Stebbins J, Pillus L, et al. The silencing protein SIR2 and its homologs are NAD-dependent protein deacetylases. Proc Natl Acad Sci U S A. 2000;97(11):5807-11. PMCID: 18515.
57. Lavu S, Boss O, Elliott PJ, Lambert PD. Sirtuins--novel therapeutic targets to treat age-associated diseases. Nat Rev Drug Discov. 2008;7(10):841-53.

58. Guarente L, Picard F. Calorie restriction--the SIR2 connection. Cell. 2005;120(4):473-82.
59. Imai S. The NAD World: a new systemic regulatory network for metabolism and aging--Sirt1, systemic NAD biosynthesis, and their importance. Cell Biochem Biophys. 2009;53(2):65-74. PMCID: 2734380.
60. Michan S, Sinclair D. Sirtuins in mammals: insights into their biological function. Biochem J. 2007;404(1):1-13. PMCID: 2753453.
61. Haigis MC, Mostoslavsky R, Haigis KM, Fahie K, Christodoulou DC, Murphy AJ, et al. SIRT4 inhibits glutamate dehydrogenase and opposes the effects of calorie restriction in pancreatic beta cells. Cell. 2006;126(5):941-54.
62. Liszt G, Ford E, Kurtev M, Guarente L. Mouse Sir2 homolog SIRT6 is a nuclear ADP-ribosyltransferase. J Biol Chem. 2005;280(22):21313-20.
63. Michishita E, Park JY, Burneskis JM, Barrett JC, Horikawa I. Evolutionarily conserved and nonconserved cellular localizations and functions of human SIRT proteins. Mol Biol Cell. 2005;16(10):4623-35. PMCID: 1237069.
64. Stern JS, Gades MD, Wheeldon CM, Borchers AT. Calorie restriction in obesity: prevention of kidney disease in rodents. J Nutr. 2001;131(3):913S-7S.
65. Joseph J, Cole G, Head E, Ingram D. Nutrition, brain aging, and neurodegeneration. J Neurosci. 2009;29(41):12795-801.
66. Barger JL, Walford RL, Weindruch R. The retardation of aging by caloric restriction: its significance in the transgenic era. Exp Gerontol. 2003;38(11-12):1343-51.
67. Lin SJ, Defossez PA, Guarente L. Requirement of NAD and SIR2 for life-span extension by calorie restriction in Saccharomyces cerevisiae. Science. 2000;289(5487):2126-8.
68. Howitz KT, Bitterman KJ, Cohen HY, Lamming DW, Lavu S, Wood JG, et al. Small molecule activators of sirtuins extend Saccharomyces cerevisiae lifespan. Nature. 2003;425(6954):191-6.
69. Picard F, Kurtev M, Chung N, Topark-Ngarm A, Senawong T, Machado De Oliveira R, et al. Sirt1 promotes fat mobilization in white adipocytes by repressing PPAR-gamma. Nature. 2004;429(6993):771-6.
70. Cohen HY, Miller C, Bitterman KJ, Wall NR, Hekking B, Kessler B, et al. Calorie restriction promotes mammalian cell survival by inducing the SIRT1 deacetylase. Science. 2004;305(5682):390-2.
71. Bordone L, Cohen D, Robinson A, Motta MC, van Veen E, Czopik A, et al. SIRT1 transgenic mice show phenotypes resembling calorie restriction. Aging Cell. 2007;6(6):759-67.
72. Boily G, Seifert EL, Bevilacqua L, He XH, Sabourin G, Estey C, et al. SirT1 regulates energy metabolism and response to caloric restriction in mice. PLoS One. 2008;3(3):e1759. PMCID: 2258149.
73. Vaziri H, Dessain SK, Ng Eaton E, Imai SI, Frye RA, Pandita TK, et al. hSIR2(SIRT1) functions as an NAD-dependent p53 deacetylase. Cell. 2001;107(2):149-59.
74. Yeung F, Hoberg JE, Ramsey CS, Keller MD, Jones DR, Frye RA, et al. Modulation of NF-kappaB-dependent transcription and cell survival by the SIRT1 deacetylase. EMBO J. 2004;23(12):2369-80. PMCID: 423286.
75. Rodgers JT, Lerin C, Haas W, Gygi SP, Spiegelman BM, Puigserver P. Nutrient control of glucose homeostasis through a complex of PGC-1alpha and SIRT1. Nature. 2005;434(7029):113-8.
76. Moynihan KA, Grimm AA, Plueger MM, Bernal-Mizrachi E, Ford E, Cras-Meneur C, et al. Increased dosage of mammalian Sir2 in pancreatic beta cells enhances glucose-stimulated insulin secretion in mice. Cell Metab. 2005;2(2):105-17.

77. Bordone L, Motta MC, Picard F, Robinson A, Jhala US, Apfeld J, et al. Sirt1 regulates insulin secretion by repressing UCP2 in pancreatic beta cells. PLoS Biol. 2006;4(2):e31. PMCID: 1318478.
78. Sun C, Zhang F, Ge X, Yan T, Chen X, Shi X, et al. SIRT1 improves insulin sensitivity under insulin-resistant conditions by repressing PTP1B. Cell Metab. 2007;6(4):307-19.
79. Baur JA, Pearson KJ, Price NL, Jamieson HA, Lerin C, Kalra A, et al. Resveratrol improves health and survival of mice on a high-calorie diet. Nature. 2006;444(7117):337-42.
80. Lagouge M, Argmann C, Gerhart-Hines Z, Meziane H, Lerin C, Daussin F, et al. Resveratrol improves mitochondrial function and protects against metabolic disease by activating SIRT1 and PGC-1alpha. Cell. 2006;127(6):1109-22.
81. Milne JC, Lambert PD, Schenk S, Carney DP, Smith JJ, Gagne DJ, et al. Small molecule activators of SIRT1 as therapeutics for the treatment of type 2 diabetes. Nature. 2007;450(7170):712-6.
82. Pfluger PT, Herranz D, Velasco-Miguel S, Serrano M, Tschop MH. Sirt1 protects against high-fat diet-induced metabolic damage. Proc Natl Acad Sci U S A. 2008;105(28):9793-8.
83. Alcendor RR, Gao S, Zhai P, Zablocki D, Holle E, Yu X, et al. Sirt1 regulates aging and resistance to oxidative stress in the heart. Circ Res. 2007;100(10):1512-21.
84. Parker JA, Arango M, Abderrahmane S, Lambert E, Tourette C, Catoire H, et al. Resveratrol rescues mutant polyglutamine cytotoxicity in nematode and mammalian neurons. Nat Genet. 2005;37(4):349-50.
85. Lee JH, Song MY, Song EK, Kim EK, Moon WS, Han MK, et al. Overexpression of SIRT1 protects pancreatic beta-cells against cytokine toxicity by suppressing the nuclear factor-kappaB signaling pathway. Diabetes. 2009;58(2):344-51.
86. Della-Morte D, Dave KR, Defazio RA, Bao YC, Raval AP, Perez-Pinzon MA. Resveratrol pretreatment protects rat brain from cerebral ischemic damage via a sirtuin 1 -- uncoupling protein 2 pathway. Neuroscience. 2009;159(3):993-1002.
87. Bertelli AA, Migliori M, Panichi V, Origlia N, Filippi C, Das DK, et al. Resveratrol, a component of wine and grapes, in the prevention of kidney disease. Ann N Y Acad Sci. 2002;957:230-8.
88. Kume S, Haneda M, Kanasaki K, Sugimoto T, Araki S, Isono M, et al. Silent information regulator 2 (SIRT1) attenuates oxidative stress-induced mesangial cell apoptosis via p53 deacetylation. Free Radic Biol Med. 2006;40(12):2175-82.
89. Kume S, Haneda M, Kanasaki K, Sugimoto T, Araki S, Isshiki K, et al. SIRT1 inhibits transforming growth factor beta-induced apoptosis in glomerular mesangial cells via Smad7 deacetylation. J Biol Chem. 2007;282(1):151-8.
90. Hasegawa K, Wakino S, Yoshioka K, Tatematsu S, Hara Y, Minakuchi H, et al. Sirt1 protects against oxidative stress-induced renal tubular cell apoptosis by the bidirectional regulation of catalase expression. Biochem Biophys Res Commun. 2008;372(1):51-6.
91. Tikoo K, Tripathi DN, Kabra DG, Sharma V, Gaikwad AB. Intermittent fasting prevents the progression of type I diabetic nephropathy in rats and changes the expression of Sir2 and p53. FEBS Lett. 2007;581(5):1071-8.
92. Miyazaki R, Ichiki T, Hashimoto T, Inanaga K, Imayama I, Sadoshima J, et al. SIRT1, a longevity gene, downregulates angiotensin II type 1 receptor expression in vascular smooth muscle cells. Arterioscler Thromb Vasc Biol. 2008;28(7):1263-9.
93. Zhang D, Li S, Cruz P, Kone BC. Sirtuin 1 functionally and physically interacts with disruptor of telomeric silencing-1 to regulate alpha-ENaC transcription in collecting duct. J Biol Chem. 2009;284(31):20917-26. PMCID: 2742857.

94. Cheng HL, Mostoslavsky R, Saito S, Manis JP, Gu Y, Patel P, et al. Developmental defects and p53 hyperacetylation in Sir2 homolog (SIRT1)-deficient mice. Proc Natl Acad Sci U S A. 2003;100(19):10794-9.
95. Connelly L, Robinson-Benion C, Chont M, Saint-Jean L, Li H, Polosukhin VV, et al. A transgenic model reveals important roles for the NF-kappa B alternative pathway (p100/p52) in mammary development and links to tumorigenesis. J Biol Chem. 2007;282(13):10028-35.
96. Chen J, Boyle S, Zhao M, Su W, Takahashi K, Davis L, et al. Differential expression of the intermediate filament protein nestin during renal development and its localization in adult podocytes. J Am Soc Nephrol. 2006;17(5):1283-91.
97. Dunn MJ, Staley RS, Harrison M. Characterization of prostaglandin production in tissue culture of rat renal medullary cells. Prostaglandins. 1976;12(1):37-49.
98. Hao CM, Breyer MD. Hypertension and cyclooxygenase-2 inhibitors: target: the renal medulla. Hypertension. 2004;44(4):396-7.
99. Wang CY, Mayo MW, Baldwin AS, Jr. TNF- and cancer therapy-induced apoptosis: potentiation by inhibition of NF-kappaB. Science. 1996;274(5288):784-7.
100. Mehlen P, Kretz-Remy C, Preville X, Arrigo AP. Human hsp27, Drosophila hsp27 and human alphaB-crystallin expression-mediated increase in glutathione is essential for the protective activity of these proteins against TNFalpha-induced cell death. EMBO J. 1996;15(11):2695-706.
101. Rao R, Hao CM, Breyer MD. Hypertonic stress activates glycogen synthase kinase 3beta-mediated apoptosis of renal medullary interstitial cells, suppressing an NFkappaB-driven cyclooxygenase-2-dependent survival pathway. J Biol Chem. 2004;279(6):3949-55.
102. Lopez-De Leon A, Rojkind M. A simple micromethod for collagen and total protein determination in formalin-fixed paraffin-embedded sections. J Histochem Cytochem. 1985;33(8):737-43.
103. McKim SE, Uesugi T, Raleigh JA, McClain CJ, Arteel GE. Chronic intragastric alcohol exposure causes hypoxia and oxidative stress in the rat pancreas. Arch Biochem Biophys. 2003;417(1):34-43.
104. Tazawa R, Xu XM, Wu KK, Wang LH. Characterization of the genomic structure, chromosomal location and promoter of human prostaglandin H synthase-2 gene. Biochem Biophys Res Commun. 1994;203(1):190-9.
105. Kim D, Nguyen MD, Dobbin MM, Fischer A, Sananbenesi F, Rodgers JT, et al. SIRT1 deacetylase protects against neurodegeneration in models for Alzheimer's disease and amyotrophic lateral sclerosis. EMBO J. 2007;26(13):3169-79.
106. Giovannini L, Migliori M, Longoni BM, Das DK, Bertelli AA, Panichi V, et al. Resveratrol, a polyphenol found in wine, reduces ischemia reperfusion injury in rat kidneys. J Cardiovasc Pharmacol. 2001;37(3):262-70.
107. Sener G, Tugtepe H, Yuksel M, Cetinel S, Gedik N, Yegen BC. Resveratrol improves ischemia/reperfusion-induced oxidative renal injury in rats. Arch Med Res. 2006;37(7):822-9.
108. Burg MB, Ferraris JD, Dmitrieva NI. Cellular response to hyperosmotic stresses. Physiol Rev. 2007;87(4):1441-74.
109. Harris RC. Cyclooxygenase-2 and the kidney: functional and pathophysiological implications. J Hypertens Suppl. 2002;20(6):S3-9.
110. Chevalier RL. Obstructive nephropathy: towards biomarker discovery and gene therapy. Nat Clin Pract Nephrol. 2006;2(3):157-68.
111. Chevalier RL, Forbes MS, Thornhill BA. Ureteral obstruction as a model of renal interstitial fibrosis and obstructive nephropathy. Kidney Int. 2009;75(11):1145-52.

112. Neuhofer W, Beck FX. Survival in hostile environments: strategies of renal medullary cells. Physiology (Bethesda). 2006;21:171-80.
113. Stern L, Backman KA, Hayslett JP. Effect of cortical-medullary gradient for ammonia on urinary excretion of ammonia. Kidney Int. 1985;27(4):652-61.
114. Hackbarth H, Harrison DE. Changes with age in renal function and morphology in C57BL/6, CBA/HT6, and B6CBAF1 mice. J Gerontol. 1982;37(5):540-7.
115. Davies I, Fotheringham AP, Faragher BE. Age-associated changes in the kidney of the laboratory mouse. Age Ageing. 1989;18(2):127-33.
116. Wood JG, Rogina B, Lavu S, Howitz K, Helfand SL, Tatar M, et al. Sirtuin activators mimic caloric restriction and delay ageing in metazoans. Nature. 2004;430(7000):686-9.
117. Bordone L, Guarente L. Calorie restriction, SIRT1 and metabolism: understanding longevity. Nat Rev Mol Cell Biol. 2005;6(4):298-305.
118. Yang Y, Fu W, Chen J, Olashaw N, Zhang X, Nicosia SV, et al. SIRT1 sumoylation regulates its deacetylase activity and cellular response to genotoxic stress. Nat Cell Biol. 2007;9(11):1253-62.
119. Sasaki T, Maier B, Koclega KD, Chruszcz M, Gluba W, Stukenberg PT, et al. Phosphorylation regulates SIRT1 function. PLoS One. 2008;3(12):e4020.
120. Aubin MC, Lajoie C, Clement R, Gosselin H, Calderone A, Perrault LP. Female rats fed a high-fat diet were associated with vascular dysfunction and cardiac fibrosis in the absence of overt obesity and hyperlipidemia: therapeutic potential of resveratrol. J Pharmacol Exp Ther. 2008;325(3):961-8.
121. Hashem MA, Jun KY, Lee E, Lim S, Choo HY, Kwon Y. A rapid and sensitive screening system for human type I collagen with the aim of discovering potent anti-aging or anti-fibrotic compounds. Mol Cells. 2008;26(6):625-30.
122. Inanaga K, Ichiki T, Matsuura H, Miyazaki R, Hashimoto T, Takeda K, et al. Resveratrol attenuates angiotensin II-induced interleukin-6 expression and perivascular fibrosis. Hypertens Res. 2009;32(6):466-71.
123. Brooks CL, Gu W. How does SIRT1 affect metabolism, senescence and cancer? Nat Rev Cancer. 2009;9(2):123-8.
124. Ruwart MJ, Rush BD, Friedle NM, Piper RC, Kolaja GJ. Protective effects of 16,16-dimethyl PGE2 on the liver and kidney. Prostaglandins. 1981;21 Suppl:97-102.
125. Rincon-Sanchez AR, Covarrubias A, Rivas-Estilla AM, Pedraza-Chaverri J, Cruz C, Islas-Carbajal MC, et al. PGE2 alleviates kidney and liver damage, decreases plasma renin activity and acute phase response in cirrhotic rats with acute liver damage. Exp Toxicol Pathol. 2005;56(4-5):291-303.
126. Hodges RJ, Jenkins RG, Wheeler-Jones CP, Copeman DM, Bottoms SE, Bellingan GJ, et al. Severity of lung injury in cyclooxygenase-2-deficient mice is dependent on reduced prostaglandin E(2) production. Am J Pathol. 2004;165(5):1663-76.
127. Osborne NN, Li GY, Ji D, Andrade da Costa BL, Fawcett RJ, Kang KD, et al. Expression of prostaglandin PGE2 receptors under conditions of aging and stress and the protective effect of the EP2 agonist butaprost on retinal ischemia. Invest Ophthalmol Vis Sci. 2009;50(7):3238-48.
128. Echeverria V, Clerman A, Dore S. Stimulation of PGE receptors EP2 and EP4 protects cultured neurons against oxidative stress and cell death following beta-amyloid exposure. Eur J Neurosci. 2005;22(9):2199-206.
129. Yang T, Schnermann JB, Briggs JP. Regulation of cyclooxygenase-2 expression in renal medulla by tonicity in vivo and in vitro. Am J Physiol. 1999;277(1 Pt 2):F1-9.

130. Chen J, Zhao M, Rao R, Inoue H, Hao CM. C/EBP{beta} and its binding element are required for NF{kappa}B-induced COX2 expression following hypertonic stress. J Biol Chem. 2005;280(16):16354-9.
131. Luo J, Nikolaev AY, Imai S, Chen D, Su F, Shiloh A, et al. Negative control of p53 by Sir2alpha promotes cell survival under stress. Cell. 2001;107(2):137-48.
132. Brunet A, Sweeney LB, Sturgill JF, Chua KF, Greer PL, Lin Y, et al. Stress-dependent regulation of FOXO transcription factors by the SIRT1 deacetylase. Science. 2004;303(5666):2011-5.
133. Kang YJ, Mbonye UR, DeLong CJ, Wada M, Smith WL. Regulation of intracellular cyclooxygenase levels by gene transcription and protein degradation. Prog Lipid Res. 2007;46(2):108-25.
134. Hoshino T, Tsutsumi S, Tomisato W, Hwang HJ, Tsuchiya T, Mizushima T. Prostaglandin E2 protects gastric mucosal cells from apoptosis via EP2 and EP4 receptor activation. J Biol Chem. 2003;278(15):12752-8.
135. Liou JY, Ellent DP, Lee S, Goldsby J, Ko BS, Matijevic N, et al. Cyclooxygenase-2-derived prostaglandin e2 protects mouse embryonic stem cells from apoptosis. Stem Cells. 2007;25(5):1096-103.
136. George RJ, Sturmoski MA, Anant S, Houchen CW. EP4 mediates PGE2 dependent cell survival through the PI3 kinase/AKT pathway. Prostaglandins Other Lipid Mediat. 2007;83(1-2):112-20.
137. Han JA, Kim JI, Ongusaha PP, Hwang DH, Ballou LR, Mahale A, et al. P53-mediated induction of Cox-2 counteracts p53- or genotoxic stress-induced apoptosis. EMBO J. 2002;21(21):5635-44. PMCID: 131088.
138. Cressey R, Pimpa S, Tontrong W, Watananupong O, Leartprasertsuke N. Expression of cyclooxygenase-2 in colorectal adenocarcinoma is associated with p53 accumulation and hdm2 overexpression. Cancer Lett. 2006;233(2):232-9.
139. Peterson DP, Murphy KM, Ursino R, Streeter K, Yancey PH. Effects of dietary protein and salt on rat renal osmolytes: covariation in urea and GPC contents. Am J Physiol. 1992;263(4 Pt 2):F594-600.
140. Nakanishi T, Uyama O, Nakahama H, Takamitsu Y, Sugita M. Determinants of relative amounts of medullary organic osmolytes: effects of NaCl and urea differ. Am J Physiol. 1993;264(3 Pt 2):F472-9.
141. Herrera M, Garvin JL. A high-salt diet stimulates thick ascending limb eNOS expression by raising medullary osmolality and increasing release of endothelin-1. Am J Physiol Renal Physiol. 2005;288(1):F58-64.
142. Bergstrom G, Evans RG. Mechanisms underlying the antihypertensive functions of the renal medulla. Acta Physiol Scand. 2004;181(4):475-86.
143. Herschman HR. Prostaglandin synthase 2. Biochim Biophys Acta. 1996;1299(1):125-40.
144. Zhuo J, Alcorn D, Allen AM, Mendelsohn FA. High resolution localization of angiotensin II receptors in rat renal medulla. Kidney Int. 1992;42(6):1372-80.
145. Wilkes BM, Ruston AS, Mento P, Girardi E, Hart D, Vander Molen M, et al. Characterization of endothelin 1 receptor and signal transduction mechanisms in rat medullary interstitial cells. Am J Physiol. 1991;260(4 Pt 2):F579-89.
146. Metzger D, Chambon P. Site- and time-specific gene targeting in the mouse. Methods. 2001;24(1):71-80.
147. Branda CS, Dymecki SM. Talking about a revolution: The impact of site-specific recombinases on genetic analyses in mice. Dev Cell. 2004;6(1):7-28.

148. Jones FS, Jones PL. The tenascin family of ECM glycoproteins: structure, function, and regulation during embryonic development and tissue remodeling. Dev Dyn. 2000;218(2):235-59.
149. Chiquet-Ehrismann R, Chiquet M. Tenascins: regulation and putative functions during pathological stress. J Pathol. 2003;200(4):488-99.
150. Chiquet-Ehrismann R. Tenascins. Int J Biochem Cell Biol. 2004;36(6):986-90.
151. Aufderheide E, Chiquet-Ehrismann R, Ekblom P. Epithelial-mesenchymal interactions in the developing kidney lead to expression of tenascin in the mesenchyme. J Cell Biol. 1987;105(1):599-608.
152. Natali PG, Nicotra MR, Bigotti A, Botti C, Castellani P, Risso AM, et al. Comparative analysis of the expression of the extracellular matrix protein tenascin in normal human fetal, adult and tumor tissues. Int J Cancer. 1991;47(6):811-6.
153. Truong LD, Foster SV, Barrios R, D'Agati V, Verani RR, Gonzalez JM, et al. Tenascin is an ubiquitous extracellular matrix protein of human renal interstitium in normal and pathologic conditions. Nephron. 1996;72(4):579-86.
154. Mackie EJ, Tucker RP. The tenascin-C knockout revisited. J Cell Sci. 1999;112 (Pt 22):3847-53.
155. Hsia HC, Schwarzbauer JE. Meet the tenascins: multifunctional and mysterious. J Biol Chem. 2005;280(29):26641-4.
156. Brellier F, Tucker RP, Chiquet-Ehrismann R. Tenascins and their implications in diseases and tissue mechanics. Scand J Med Sci Sports. 2009;19(4):511-9.
157. Eddy AA, Giachelli CM. Renal expression of genes that promote interstitial inflammation and fibrosis in rats with protein-overload proteinuria. Kidney Int. 1995;47(6):1546-57.
158. Blackwell TS, Yull FE, Chen CL, Venkatakrishnan A, Blackwell TR, Hicks DJ, et al. Multiorgan nuclear factor kappa B activation in a transgenic mouse model of systemic inflammation. Am J Respir Crit Care Med. 2000;162(3 Pt 1):1095-101.
159. van der Vos KE, Coffer PJ. FOXO-binding partners: it takes two to tango. Oncogene. 2008;27(16):2289-99.
160. Giannakou ME, Partridge L. The interaction between FOXO and SIRT1: tipping the balance towards survival. Trends Cell Biol. 2004;14(8):408-12.